



UNIVERSITY OF GENOVA

PHD PROGRAM IN BIOENGINEERING AND ROBOTICS

Green and Biodegradable Thermosets and Vitrimers: Sustainable and Environmental Friendly Alternatives to Conventional Plastics for Sustainable Packaging

by

Milad Safarpour

Thesis submitted for the degree of *Doctor of Philosophy* (36° cycle)

April 2024

Supervisor: Athanassia Athanassiou/ **Co-Supervisor:** Giovanni Perotto

Head of the PhD program: Paolo Massobrio

Thesis Jury:

MONTICELLI Orietta, *Università degli Studi di Genova*

Handwritten signature of Orietta Monticelli in black ink.

External

DORIGATO Andrea, *Università di Trento*

Handwritten signature of Andrea Dorigato in black ink.

External

Name, *University*

Internal

Dibris

Department of Informatics, Bioengineering, Robotics and Systems Engineering

Even though it will be quite impossible for me to thank them for their efforts, I am giving them this tiny token of appreciation.

Dedicated to my wife and my parents;

Without their help and encouragement, this accomplishment would not have been possible.

And dedicated to those with an interest in science and knowledge, I hope it will be the way for these loved ones.

Abstract

This thesis investigates the potential of sustainable and ecologically conscious materials as substitutes for traditional plastics. The primary emphasis is placed on examining biodegradable thermosets and vitrimers that are derived from renewable resources. The initial study examines the progression of naturally foamed composites derived from soybean oil, which incorporate substantial quantities of agricultural waste, as a sustainable alternative to Styrofoam™. The synthesis of these composites involves the utilization of bio-based thermosets and their curing at a low temperature in the presence of agricultural waste. This approach renders them not only ecologically sustainable but also economically advantageous. Furthermore, the aforementioned composites have been specifically engineered to possess biodegradability properties when exposed to marine settings, hence effectively mitigating the concern of prolonged accumulation of plastic waste. The second study presents a novel vitrimer material that possesses both flexibility and stretchability. This vitrimer is composed of renewable resources, including epoxidized soybean oil, vanillin, biobased diamine Priamine, and oleic acid, which aligns with the principles of green chemistry. Vitrimers present a viable and environmentally conscious substitute for plastics derived from fossil fuels, showcasing remarkable attributes in terms of recycling and reprocessing capabilities. Moreover, these materials demonstrate exceptional barrier characteristics and minimal migration into food simulants, rendering them highly favorable for utilization in flexible food packaging endeavors. Moreover, it should be noted that these vitrimers possess the ability to undergo biodegradation in seawater, hence ensuring a secure and environmentally sound end-of-life scenario in the absence of appropriate management practices. This thesis aims to establish a connection between the fields of material science and environmental sustainability by exploring the potential of biodegradable composites and vitrimers. These materials have the ability to reduce the environmental impact caused by plastic-based products while also providing practical alternatives for a range of applications, such as packaging and marine conservation.

key-words: Sustainability, Biodegradable thermosets, Renewable Resources, Vitrimers, Reversible crosslinker.

Table of Contents

| | |
|--|----------|
| List of Figures | vi |
| List of Tables..... | ix |
| List of Abbreviations..... | x |
| Acknowledgements | xiv |
| Chapter 1: Introduction | 1 |
| 1.1 overview..... | 1 |
| 1.2 Thermoplastic Polymers | 2 |
| 1.3 Thermosets Materials..... | 4 |
| 1.4 Curing Agents | 6 |
| 1.4.1 Amines:..... | 6 |
| 1.4.1.1 Aliphatic amines: | 8 |
| 1.4.2 Polyamide resin..... | 9 |
| 1.4.3 Anhydrides..... | 10 |
| 1.4.4 Cycloaliphatic | 13 |
| 1.4.5 Latent curing agents..... | 13 |
| 1.4.6 Polymercaptan | 14 |
| 1.5 Thermoset properties and application | 15 |
| 1.5.1 Brittleness and restricted design options..... | 16 |
| 1.5.2 Lengthy curing times | 16 |
| 1.5.3 Higher cost..... | 18 |
| 1.5.4 Challenges in repair | 19 |
| 1.5.5 Recycling thermoset | 20 |
| 1.6 Degradable and biobased Thermosets..... | 21 |
| 1.7 Problem of plastic pollution | 24 |
| 1.8 Life Cycle Assessment (LCA) | 26 |
| 1.9 Vitrimers | 27 |
| 1.9.1 Vitrimers properties | 29 |
| 1.9.1.1 Dynamic Bonds:..... | 29 |
| 1.10 Applications of vitrimers: | 35 |
| 1.10.1 Recyclable Plastics: | 35 |
| 1.10.2 Flexible Electronics: | 37 |
| 1.10.3 Biomedical Applications: | 38 |
| 1.10.4 Shape Memory Materials:..... | 40 |
| 1.11 Vitrimers limitations: | 41 |
| 1.12 activation energy (E_a) | 41 |
| 1.12.1 Transesterification: | 42 |
| 1.12.2 Dynamic Disulfide..... | 44 |
| 1.12.3 Dynamic covalent Diels-Alder: | 45 |
| 1.12.4 Dynamic Oxime bonds: | 48 |
| 1.12.5 Dynamic Thiol-Ene: | 49 |

| | |
|---|------------|
| Chapter 2: Biobased thermoset derived from epoxidized soybean oil and agri-waste as a sustainable alternative to Styrofoam..... | 53 |
| 2.1 Overview | 53 |
| 2.2 RESULTS AND DISCUSSION..... | 56 |
| 2.2.1 Synthesis..... | 56 |
| 2.2.2 Gel fraction:..... | 58 |
| 2.2.3 Environmentally Friendly Synthesis of composites: | 60 |
| 2.2.4 Mechanical Property: | 64 |
| 2.2.5 Biodegradability: | 69 |
| environments[347]..... | 69 |
| 2.3 CONCLUSIONS | 71 |
| styrofoam. One more benefit of the composites was their ability to biodegrade in seawater, where carrot pomace enhances the biodegradation kinetic. This material shows a promising blend of foaming, mechanical properties, thermal insulation, and safe biodegradation, positioning it as a strong biobased alternative to fossil materials. | 71 |
| 2.4 Experimental section | 72 |
| 2.4.1 Materials:..... | 72 |
| 2.4.2 Typical procedure for composites preparation: | 72 |
| 2.4.3 Measurements..... | 73 |
| Chapter 3: Biobased and biodegradable imine vitrimers from epoxidized soybean oil as packaging..... | 76 |
| 3.1 Overview | 76 |
| 3.2 RESULTS AND DISCUSSION..... | 80 |
| 3.2.1 Synthesis of vitrimer | 80 |
| 3.2.1.1 Gel fraction: | 82 |
| 3.2.2 Thermomechanical properties and adhesion tests | 85 |
| 3.2.3 Reprocessing of vitrimers..... | 92 |
| 3.2.4 Vitrimers for packaging..... | 100 |
| 3.3 CONCLUSIONS | 105 |
| 3.4 Experimental section | 107 |
| 3.4.1 Materials..... | 107 |
| 3.4.2 Preparation of VPI cross-linker (Vanillin- Priamine®)..... | 107 |
| 3.4.3 Typical Procedure for ESO cross-linking..... | 107 |
| 3.4.4 Measurements..... | 108 |
| Chapter 4: Conclusions | 113 |
| Bibliography | 117 |

List of Figures

| | |
|--|----|
| <i>Figure 1. Distribution of packaging materials [66].</i> | 4 |
| <i>Figure 2. Phases of the formation of thermosets.</i> | 6 |
| <i>Figure 3. Chemical structure of amine-based curing agents, a) schematic of typical reaction between NH₃ and alkyl or aryl groups b) aromatic amines: diamino-diphenylmethane (DDM), c) aliphatic amines: triethylenetetramine (TETA), and d) cycloaliphatic amines: isophorone diamine (IPDA).</i> | 7 |
| <i>Figure 4. Chemical structure of polyamide-based curing agents a) schematic of ...</i> | 10 |
| <i>Figure 5. a) Anhydride groups open to form half-esters and free carboxylic acids. This is usually caused by a hydroxyl group, such as an accelerator or the epoxy resin pendant hydroxyl. In Reaction b), the newly formed carboxylic acid group reacts with an epoxide to form an ester linkage and a new hydroxyl group, which reacts with another anhydride group as shown in Reaction a, and so on.</i> | 12 |
| <i>Figure 6. Chemical structure of Cycloaliphatic-based curing agents that reacts with epoxy group.</i> | 13 |
| <i>Figure 7. Chemical structure of Latent -based curing agents that reacts with epoxy group.</i> | 14 |
| <i>Figure 8. Chemical structure of polymercaptans-based curing agents that reacts with epoxy group.</i> | 14 |
| <i>Figure 9. Global epoxy polymer applications[142].</i> | 15 |
| <i>Figure 10. Synthesizing epoxidized soybean oil (ESO).</i> | 24 |
| <i>Figure 11. Phases of the formation of vitrimers.</i> | 29 |
| <i>Figure 12. Schematic image of dynamic covalent bonds utilized in vitrimer materials and the applications of these bond [259].</i> | 32 |
| <i>Figure 13. Using vitrimers in the production of recyclable plastics [279].</i> | 36 |
| <i>Figure 14. Using vitrimers in the flexible electronic [283].</i> | 38 |
| <i>Figure 15. Using vitrimers in the biomedical applications [290].</i> | 39 |
| <i>Figure 16. Using vitrimers in the shape memory Materials [294].</i> | 40 |
| <i>Figure 17 . Some examples of dynamic covalent bonds and activation energy (E_a) that are present in vitrimer [259].</i> | 42 |
| <i>Figure 18. Transesterification reactions of Vitrimers [308].</i> | 44 |
| <i>Figure 19 . Disulfide Exchanges reactions of Vitrimers [311].</i> | 45 |
| <i>Figure 20 . Dynamic covalent Diels-Alder reactions of Vitrimers [317].</i> | 47 |
| <i>Figure 21 . Dynamic Oxime bonds reactions of Vitrimers [320].</i> | 49 |
| <i>Figure 22. Dynamic Thiol-Ene reactions of Vitrimers [323].</i> | 51 |

| | |
|---|----|
| Figure 23. a) Schematic representation of the chemical synthesis of ESO & pripol via a thiol-epoxy coupling and a picture of a transparent thermoset Oil thermoset film, b) FT-IR spectra of ESO & pripol. | 58 |
| Figure 24 . Gel fraction of the oil thermoset was cured at 80 °C on various days using different catalysts, a) drying under the hood at 100°C. b) Representative gel fraction curves of the oil thermoset by the catalyst, N, N-1,1,3,3 Tetramethylguanidine (TMG) after the ethyl acetate was removed, c) Representative gel fraction curves of the oil thermoset by the catalyst, 1-Ethylimidazole (1-EI) after the ethyl acetate was removed. | 59 |
| Figure 25. a) Composition of the carrot powder, Carrot powder with 50µm mesh. b) Digital images of carrot powder, c) Magnified top view of carrot powder waste, d) Magnified top view of a single piece of carrot waste. | 63 |
| Figure 26. a) Carrot powder with 50µm mesh, b) Epoxidized Soybean Oil, c) Pripol, d) Synthesis of composites by several amounts of carrot powder (40-50-60 %) with ESO and Pripol (oil thermoset). | 63 |
| Figure 27. a) Kinetics of water absorption by carrot waste. b) Synthesis of composites containing different amounts of water absorption by 40% carrot waste with ESO and Pripol (Oil thermoset). | 64 |
| Figure 28. Density test curves of samples by 40% carrot waste with ESO and Pripol (Oil thermoset). | 66 |
| Figure 29. Thermal conductivity test curves of samples by 40% carrot waste with ESO and Pripol (Oil thermoset). | 67 |
| Figure 30. Representative tensile test curves of composite with several amounts of carrot powder (40-50-60 %) with ESO and Pripol (Oil thermoset). | 68 |
| Figure 31, a) Representative compression test curves of samples by 40% carrot waste with ESO and Pripol (Oil thermoset). b) Flexibility before and after compression tests. | 69 |
| Figure 32. Representative Biodegradation test curves of composite. | 70 |
| Figure 33. a) Schematic of synthesis of VPI crosslinker. b) ¹ H NMR (RT, 400 MHz) and c) ¹³ C (RT, 100 MHz) NMR spectra of VPI and the two reagents Priamine 1071 and Vanillin. | 81 |
| Figure 34. Gel fraction of the vitrimers cured at 180 °C for different days after the ethyl acetate was removed, a) drying under hood at 100°C, b) Representative gel fraction curves of composite with ESO, VPI, and OA. | 84 |
| Figure 35. TGA of vitrimers with ESO and VPI and different amount of OA. The TGA of LLDPE is also shown for comparison reasons. | 85 |
| Figure 36. a) DSC of vitrimers with ESO and VPI and different amount of OA, b) DSC second heating curve of PE. | 86 |
| Figure 37. DMA test curves of the vitrimers and LLDPE for comparison reasons. | 88 |

| | |
|--|-----|
| <i>Figure 38. a) Representative tensile test curves of the vitrimers, b) Representative tensile test curves of PE. c) Representative tensile test curves of vitrimers before and after being placed in water.</i> | 90 |
| <i>Figure 39. Creep test curves of vitrimers.</i> | 91 |
| <i>Figure 40. Representative T peel tests curves of the vitrimer1 and LLDPE for comparison.</i> | 92 |
| <i>Figure 41. Illustration that shows the three components of the vitrimer: ESO–VPI, OA and the exchange of imine that allows the vitrimer to rearrange its structure.</i> | 93 |
| <i>Figure 42. Arrhenius plot of relaxation times of vitrimers.</i> | 94 |
| <i>Figure 43. Comparison stress relaxation between vitrimers and PE at 100 °C.</i> | 96 |
| <i>Figure 44. a) ESO-VPI, 2.1 OA, 1.9 during the MFI measurement (190 °C/10 kg). b) Other vitrimers (1, 2, or 3).</i> | 97 |
| <i>Figure 45. a) Recycling of vitrimer 1 by steps of fragmentation and melt compression molding. b) Representative reprocessability test curves of Vitrimer 1.</i> | 98 |
| <i>Figure 46. Biodegradation of the vitrimer1 and its components in seawater.</i> | 99 |
| <i>Figure 47. SEM images of the vitrimers 1 before and after BOD.</i> | 100 |
| <i>Figure 48. Water vapor permeability of vitrimers and PE.</i> | 101 |
| <i>Figure 49. Oxygen permeability of vitrimer1 and PE.</i> | 102 |
| <i>Figure 50. Migration levels of vitrimers samples using Tenax® as food simulants</i> | 103 |
| <i>Figure 51. Water Contact Angle of vitrimers and PE.</i> | 104 |
| <i>Figure 52. Rectangular container (Pouch) make of vitrimer sealed at the edges. b) Paper box coated with vitrimer, and c) SEM images of the adhesion between the vitrimer and paper.</i> | 105 |

List of Tables

| | |
|--|----|
| <i>Table 1. Formulations of different samples</i> | 61 |
| <i>Table 2. Composition and Properties of ESO–VPI, OA Vitrimers and ESO–VPI Vitramer</i> | 82 |
| <i>Table 3. Gel fraction of the vitrimers before and after being placed in water.</i> | 83 |

List of Abbreviations

- ^1H NMR: proton nuclear magnetic resonance
- HDPE: high density polyethylene
- LLDPE: linear low density polyethylene
- LDPE: low density polyethylene
- SEM: scanning electron microscope
- FTIR: fourier transform infrared
- TGA: thermogravimetric analysis
- DSC: differential scanning calorimetry
- DMTA: dynamic mechanical thermal analysis
- BOD: biochemical oxygen demand
- ESO: epoxidized soybean oil
- mol%: molar percentage
- M_w : weight average molecular weight
- -OH: hydroxy group
- OP: oxygen permeability
- PE: polyethylene
- PP: polypropylene
- RH: relative humidity
- RT: room temperature
- T_m : melting temperature
- WVP: water vapor permeability
- UV: ultra violet
- Wt%: weight percentage
- OA: oleic acid
- VPI: vanillin- priamine[®]1071
- EtOH: ethanol
- EtOAc: ethyl acetate
- T_α : alpha transition(α -relaxtion) temperature
- T_g : glass transition temperature
- UHMWPE: ultra-high molecular weight polyethylene
- PS : polystyrene
- PET: polyethylene terephthalate
- PVC: polyvinyl chloride
- PLA: polylactic acid
- BADGE : bisphenol A diglycidyl ether
- BFDGE : bisphenol F diglycidyl ether
- NH_3 : ammonia
- DDM: diamino-diphenylmethane
- MDA: methylene-dianiline
- TETA: triethylenetetramine
- CHA: cyclohexylamine
- IPDA: isophorone diamine
- IPN: interpenetrating polymer network

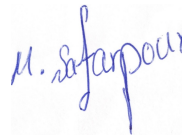
- TREN: tris(2-aminoethyl)amine
- DETA : diethylenetriamine
- EDA: ethylenediamine
- PADT: N,N,N',N', N''-penta(3-aminopropyl)-diethylenetriamine
- HDT: heat deflection temperature
- PMSO: polymercaptanized soybean oil
- BMI: bismaleimide
- MNA: methyl nadic anhydride
- HEMAP: 2-hydroxyethyl methacrylate phosphate
- TA: tannic acid
- FDCA: 2,5-furandicarboxylic acid
- DGEBA: diglycidyl ether of bisphenol-A
- GC-MS: Gas Chromatography-Mass Spectrometry
- BPA: bisphenol A
- DCAs: dicarboxylic acids
- PHA: polyhydroxyalkanoate
- PHB: polyhydroxy butyrate
- PHBV: polyhydroxy butyrate valerate
- PHV: polyhydroxy valerate
- PBS: polybutylene succinate
- PHAs: polyhydroxyalkanoates
- POE: poly(oxime-ester)
- Ea: activation energy
- T_v : topology-freezing transition temperature
- DA: diels-alder
- LCDAN: liquid crystalline Diels—Alder dynamic network
- LCN: liquid crystalline network
- POUs: poly(oxime-urethanes)
- HDI: hexamethylene diisocyanate
- NIL: nanoimprint lithography
- EAO: epoxidized algal oil
- PWF: treated pine wood fiber
- PMHS: polymethylhydrosiloxane
- AESO: acrylated epoxidized soybean oil
- EMT: epoxidized mangosteen tannin
- MTHPA: methyltetrahydrophthalic anhydride
- BDMA: N,N-Dimethylbenzylamine
- NaHCO_3 : sodium bicarbonate
- CFA: chemical foaming agent
- TMG: N, N-1,1,3,3 Tetramethylguanidine
- 1-EI: 1-Ethylimidazole
- DIPEA: N,N Diisopropylethylamine
- DBU: 1,8-Diazabicyclo(5.4.0)undec-7-ene
- VSB: vanillin-derived Schiff base
- DAM: 4,4-diaminodiphenyl methane
- DVA: divanillic acid
- CANs: covalent adaptive networks

- DMPA: 2,2-dimethoxy-2-phenylacetophenone
- MFI: melt flow index
- WCA: static water contact angle
- Ppm: parts per million
- TMS: tetramethylsilane
- ASTM: american Society for testing and materials

Statement of Original Authorship

I hereby declare that except where specific reference is made to the work of others, the contents of this dissertation are original and have not been submitted in whole or in part for consideration for any other degree or qualification in this, or any other university. This dissertation is my own work and contains nothing which is the outcome of work done in collaboration with others, except as specified in the text and Acknowledgements. This dissertation contains fewer than 65,000 words including appendices, bibliography, footnotes, tables and equations and has fewer than 150 figures.

Signature: Milad Safarpour



Date: 25/04/2024

Acknowledgements

First and foremost, I must express my wholehearted thanks to my parents, father and mother-in-law and family for their assistance and support. Without their patience and kindness, I am assured that this work would never have materialized.

I am grateful to my supervisor, Dr. Athanassia Athanassiou, who has always been generous during all phases of the research. I greatly appreciate the efforts made by supervisors Dr. Arkadiusz Zych and Dr. Giovanni Perotto. I am grateful to those who worked hard with me throughout the entire process of the current research.

I would like to express my gratitude to Dr. Martina Nardi for her assistance with ^1H and ^{13}C NMR measurements. I would like to acknowledge the help of Dr. Giacomo Tedeschi for Water vapor permeability (WVP) and Oxygen permeability (OP) measurements, I would like to extend my appreciation to Dr. Gabriele Intermite for Thermal conductivity measurements. I also want to thank Lara Marini and Giorgio Mancini for their valuable training and technical support at the Materials Characterization Facility (IIT). Additionally, I am grateful to Luca Ceseracciu for providing training and conducting mechanical property measurements at the Mechanical Facility (IIT). I would like to acknowledge Simone Lauciello for his contributions to the SEM measurements at the Electron Microscopy Facility (IIT).

I would like to take this opportunity to express my sincere gratitude to all of my dear friends for their unwavering support along the way in doing my Ph.D.

I also would like to give my sincere appreciation to Dr. Maedeh Najafi and Dr. Leyla Najafi for the kind assistance they gave me throughout my life, notably during the process of obtaining my Ph.D. Their unconditional love gave me the opportunity to finish this thesis.

Chapter 1: Introduction

1.1 OVERVIEW

Food packaging materials serve various purposes, such as protecting food from contamination, preserving freshness, and providing information to consumers [1]. The classification of packaging into different types, such as flexible Packaging [2]: This category includes materials that can adapt to the shape of the product, and are often used for materials like foil pouches, laminates, and vacuum-sealed bags [3]. They are used for products like chips, coffee, and frozen foods [4]. Hard packaging, includes materials that provide a sturdy and protective enclosure for the product. Common examples of hard packaging include plastic bottles, glass jars, and metal cans. Active and Smart Packaging [5]: These types of packaging incorporate features like oxygen scavengers, moisture control, and temperature indicators to extend shelf life and maintain freshness [6-8], reflecting the diverse functionalities and characteristics of packaging materials and designs. Different types of materials are used for food packaging, and they can be categorized into several main groups (**Figure1**): 1-Metal packaging[9] is commonly used for canned goods, such as canned fruits, vegetables, and beverages (e.g., canned soda) [10, 11]. Aluminium is also used for lightweight beverage cans [12]. 2-Paper and Cardboard [13]: These materials are often used for packaging dry goods, such as cereals, snacks, and bakery items [14]. They can be recycled and are generally considered more environmentally friendly compared to some plastics [15]. 3-Glass [16]: Glass is used for packaging foods such as jams, sauces, and beverages [17]. It is inert and doesn't interact with the contents, preserving the flavor and quality of the food [18]. 4-Thermoplastics: [19] Thermoplastics are a class of polymers that become pliable or moldable above a specific temperature and solidify upon cooling. They are widely used in packaging due to their versatility, lightweight nature, cost-effectiveness, ease of processing, and recyclability[20]. 5-Thermosetting plastics are a type of polymer that, once they have been cured or set, cannot be melted or reshaped. In packaging applications, where durability and heat resistance are essential, they are frequently used. Examples of these thermosets include phenolic resins and polyurethane resins.

1.2 THERMOPLASTIC POLYMERS

Common types of plastic packaging include a) Polyethylene (PE) [21] is a versatile and widely used type of plastic [22]. It is produced from ethylene monomers through a polymerization process [23]. PE is known for its strength, good solvent resistance, excellent flexibility, low cost and ease of processing, easy customization, durability, and resistance to moisture, chemicals impact [24]. However, its use is limited by low melting point, stress cracking, and poor wear resistance [22]. It is categorized into various types based on its density and branching, including High-Density Polyethylene (HDPE) and Low-Density Polyethylene (LDPE), linear low-density polyethylene (LLDPE) and ultra-high molecular weight polyethylene (UHMWPE) [25]. The worldwide polyethylene market, measured by output, reached 106.6 million tons in 2021 (34 % of the overall plastics market), and it is expected to grow to 124 million tons by 2027 [26]. Depending on the location, 35 to 45 % of all manufactured plastic is used for packaging, the majority of which is polyethylene [27, 28]. The wide use of polyethylene packaging is driven by the combination of the low price with excellent mechanical performance and high water vapor barrier [29]. In this case, LDPE exhibits a molecular arrangement that is more branched and less densely packed, leading to a lower density and increased flexibility. Because of this flexibility, LDPE is an excellent choice for applications such as plastic bags and wraps which require pliability to a significant degree [30]. The molecular structure of HDPE is more linear and tightly packed, which results in a higher density as well as greater strength and hardness [31]. Because of these characteristics, HDPE is the perfect material to use in the production of food containers, detergent bottles, and milk jugs, where robustness and durability are essential for keeping the contents contained [32]. The majority of polyethylene is produced from fossil-based resources [33], utilizing hydrocarbons extracted from crude oil and natural gas, and only a small amount (1%) is produced from renewable sources [34]. Regardless of the source of the monomer, PE is not able to biodegrade, and its fragmentation into smaller pieces over time due to UV oxidation or mechanical fragmentation are cause of environmental pollution [35]. b) One other material derived from petroleum-based materials is styrofoam, which is a commercial brand of polystyrene (PS)[36]. Polystyrene is a versatile plastic used in various applications, including packaging [37], food service containers [38], disposable cups and plates [39], insulation panels [40], consumer goods [41], hard plastic packaging

for items like yogurt cups [29] and more. It is also produced as a foamed material commercially called Styrofoam. Styrofoam is known for its low cost, insulation properties, and durability [42]. The exact quantity of petroleum-based products produced in the globe, such as styrofoam, can change from one year to the next depending on a variety of circumstances, including the state of the global economy and shifts in the level of demand from consumers [43]. On the other hand, it is anticipated that global plastics manufacturing will reach 450 million metric tons in the world, with around 14% of that amount comprising single-use plastic items like packaging and Styrofoam products [42, 44, 45]. However, if the trends that have been observed thus far continue, the production of plastics worldwide may reach over 1,100 million metric tons by the year 2050 [46], according to some estimates. Although materials derived from polystyrene (PS) have many benefits to offer, they also have significant drawbacks to their use, the fragmentation of styrofoam into smaller particles, often due to mechanical forces and weathering, can lead to microplastic pollution, which has raised concerns about its potential impact on ecosystems and wildlife [47]. This is one of the primary problems that they cause. When these substances make their way into oceans and other bodies of water, they can be harmful to marine life and cause changes in ecosystems due to their persistence [48, 49]. In addition, the usage of materials derived from petroleum has been linked to the chronic and low-level migration of styrene into food, which has the potential to have serious adverse effects on human health [32, 50].

c) Polypropylene (PP): PP is resistant to heat [51] and chemicals [21], making it suitable for microwave-safe containers, food storage containers, and bottle caps [52, 53].

d) Polyethylene Terephthalate (PET): PET is used for beverage bottles, food containers, and salad containers [54, 55]. It is lightweight [56] and transparent [57], making it suitable for showcasing products [58].

e) Polyvinyl Chloride (PVC): While PVC was once common in food packaging [59], its use has decreased due to environmental concerns [60]. It is still used in cling wrap and some bottle packaging [61].

f) Polylactic Acid (PLA): PLA is a bioplastic [62] made from renewable resources like corn starch or sugarcane [63]. It's used in packaging for items like salads, bakery goods, and snacks [64, 65].

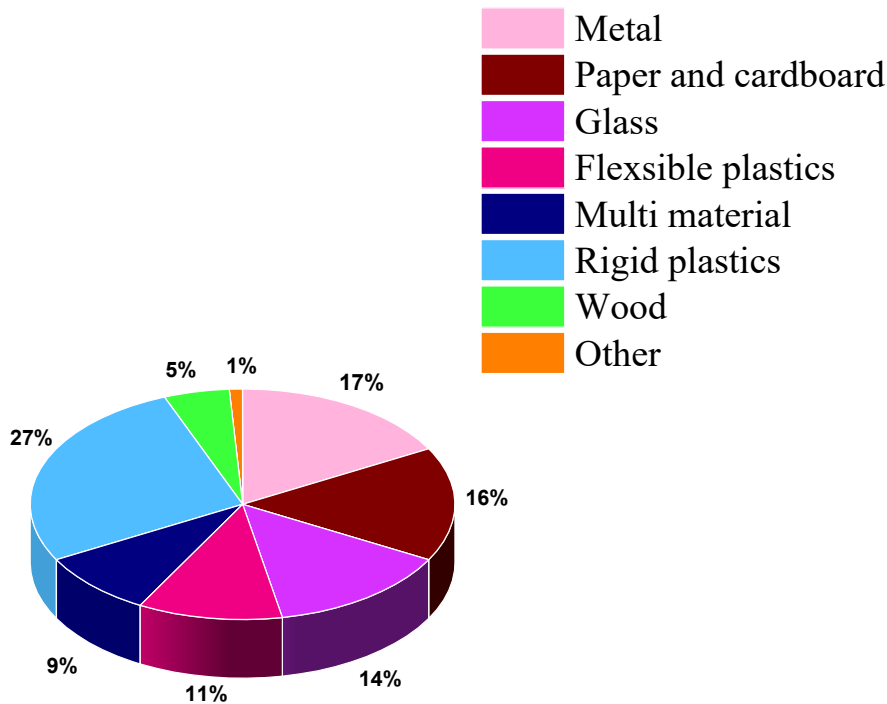


Figure 1. Distribution of packaging materials [66].

1.3 THERMOSETS MATERIALS

Thermosets are a type of polymer that have distinct characteristics and behaviours compared to thermoplastics [67, 68]. They get their name from the fact that they become permanently hard and insoluble after undergoing a chemical transformation during their processing or curing [69]. This chemical transformation, also known as curing or cross-linking, creates a three-dimensional network structure within the polymer matrix [70]. This means that thermosets cannot be remelted or reshaped once they have been set, unlike thermoplastics, which can be melted and reformed multiple times [71, 72]. These resins are usually in liquid or semi-liquid form before curing and are cast into a mold or onto a surface [73]. The mold is shaped to give the final product its required shape and size. Curing can be triggered by various methods, such as heat, chemical catalysts, or radiation (UV or electron beam) [74]. The curing process polymerizes the resin and forms the permanent network structure. For example, epoxy resin is a type of thermoset polymer that forms when epoxy monomers react with a curing agent or hardener [75]. Epoxy is a type of cyclic ether that consists of two carbon atoms and one oxygen atom in its structure. Epoxy rings can be found anywhere

inside the structure of a molecule, but more often than not, they are found as terminal groups that can be connected to a wide range of aliphatic or aromatic chemical compounds [76]. Because of the highly stressed character of the ring, the epoxy group is more reactive than the majority of other ethers, which makes it desirable for the processing of polymerization. Common examples include bisphenol A diglycidyl ether (BADGE), bisphenol F diglycidyl ether (BFDGE), and glyceryl ethers of novellas resins. The amalgamation of epoxy molecules and hardeners is a common practice in order to establish a lasting and robust interlocking system of chemical bonds [77]. When the molecules of epoxy are mixed with the curing agent, the curing agent provides active hydrogen atoms that can break the epoxide ring in the epoxy molecule, starting a chemical reaction [78]. Bi-functional reactants result in the formation of networks with a greater molecular weight between junction points, which means there is a lower degree of crosslinking [79, 80]. On the other hand, higher functionality prepolymers result in higher degrees of crosslinking [81]. This results in the formation of covalent bonds between different epoxy chains, creating a three-dimensional network structure. The network formation goes on until most of the epoxide groups have reacted with the curing agent, and the epoxy resin changes from a liquid or semi-liquid state to a solid material or until the desired level of network formation is reached [82]. Which gives epoxy its excellent mechanical and adhesive properties [83], which ultimately leads to exceptional mechanical characteristics [84], and remarkable stability [85]. This is usually done under specific temperature and time settings to ensure adequate curing. This solidification is irreversible, making epoxy resins highly durable and resistant to heat [86], and to chemicals and solvent resistance [87, 88]. As more covalent bonds are formed, the epoxy becomes increasingly rigid and thermosetting, resulting in a higher glass transition temperature (T_g), and a significant amount of energy is needed to initiate segmental motions within the epoxy [89]. After curing, the thermoset material is cooled and hardened further. Some thermosets may undergo post-curing treatments to improve their properties.

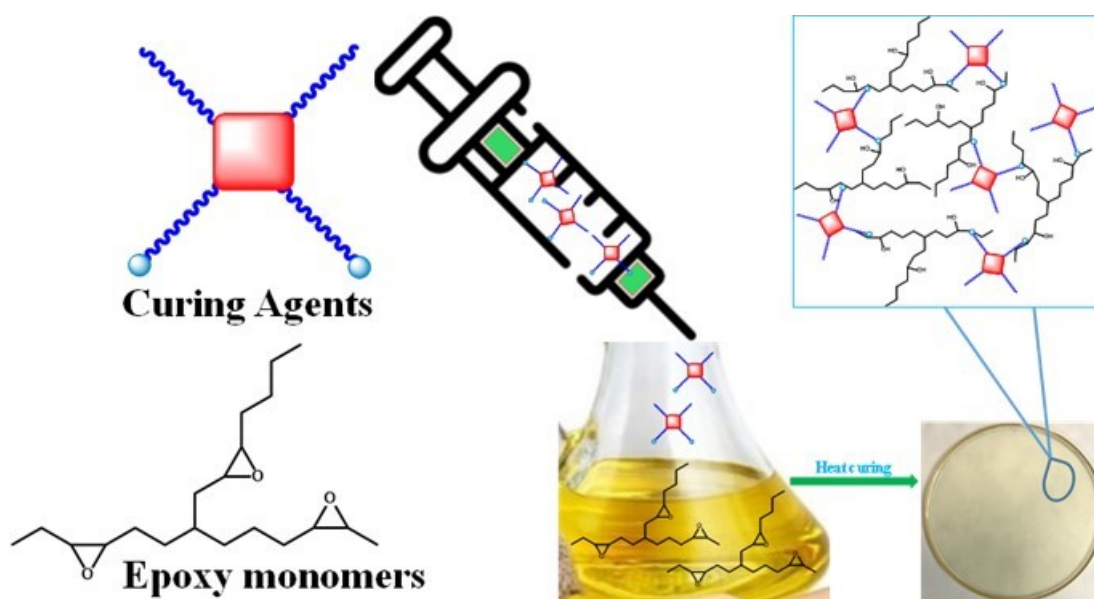


Figure 2. Phases of the formation of thermosets.

1.4 CURING AGENTS

Epoxy resins are frequently utilized in a wide variety of applications, and in order to change them from a liquid state into a solid, long-lasting material, they need to be cured with curing agents or hardeners. The choice of curing agent depends on factors such as the processing technique, intended curing conditions, desired physical and chemical qualities, environmental constraints, and cost. Each of these factors can significantly impact the characteristics of the cured epoxy. The following are some of the most commonly used curative agents:

1.4.1 Amines:

Amines are organic compounds that include one or more amine groups and are produced when ammonia (NH_3) loses some hydrogen atoms and obtains alkyl or aryl groups in their place [90]. The number of amine groups in the molecule determines whether they are monoamines, diamines, triamines, or polyamines. They can take the form of aromatic amines, such as diamino-diphenylmethane (DDM) and methylene dianiline (MDA) [91], aliphatic amines, such as triethylenetetramine (TETA), and cycloaliphatic amines, such as cyclohexylamine (CHA) and isophorone diamine (IPDA) (**Figure 3**)[92]. Amines of all varieties have been put to extensive use in epoxy resin systems despite the fact that the differences in the chemical structures of these

various types of amine lead to distinct characteristics in epoxy resins once they have cured [93]. For instance, the use of nonisocyanate polyurethanes has been reported to toughen epoxy resins through the formation of an Interpenetrating Polymer Network (IPN) structure, hydrogen bonding, and urethane linkage [94]. Furthermore, the study of the epoxy/amine equivalent ratio has been shown to impact the thermal properties, cryogenic mechanical properties, and liquid oxygen compatibility of bisphenol A epoxy resin containing phosphorus, highlighting the influence of amine composition on the performance of cured epoxy systems [95]. Additionally, the reinforcement of epoxy resin by additives of amine-functionalized graphene nanosheets has been explored, showcasing the potential for enhancing the properties of cured epoxy systems through the incorporation of amine-functionalized additives [96].

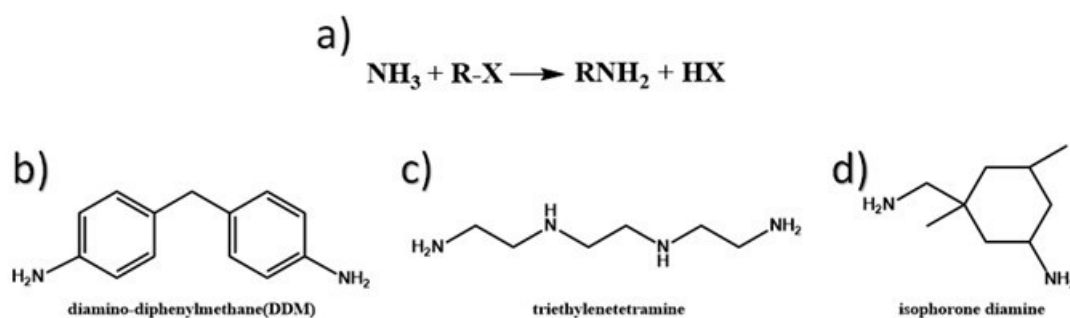


Figure 3. Chemical structure of amine-based curing agents, a) schematic of typical reaction between NH_3 and alkyl or aryl groups b) aromatic amines: diamino-diphenylmethane (DDM), c) aliphatic amines: triethylenetetramine (TETA), and d) cycloaliphatic amines: isophorone diamine (IPDA).

The curing speed of different amines is determined by the type of epoxy resin, the amount of loading of amine, and the type of amine [97]. In general, in order for the cured resin to transform into a crosslinker polymer, the curing agent must have active hydrogen atoms in a molecule and at least two amino groups. The initial reaction is the opening of the epoxy ring by a primary amine, which generates a secondary amine and a hydroxyl group. The secondary amine can then react further to create a tertiary amine, which can cause branching and crosslinking in systems with epoxy

prepolymers because primary amine addition would only produce linear polymers [98].

1.4.1.1 Aliphatic amines:

Aliphatic amines were one of the first materials to be widely accepted as curing agents for epoxy resins. Primary aliphatic amines that are poly-functional offer a quick (30 min to 4h) curing rate. This combined with their widespread availability, explains why they are commonly used in high-performance room-temperature curing epoxy coatings and adhesives [99]. Resins cured with aliphatic amines exhibit high strength and excellent bonding properties [100]. For instance, the use of 4 common aliphatic amines triethylenetetramine (TETA), Tris(2-aminoethyl)amine (TREN), diethylenetriamine (DETA), and ethylenediamine (EDA) with a varied quantity of amino groups and different molecular structures (linear vs. branched) were chosen as curing agents to investigating the physicochemical properties of the cured vanillin alcohol-based bio epoxies, to aid the optimization of the bio epoxy systems to promote industrial applications of these novel bio epoxy resins [101]. An additional illustration of this would be the utilization of the aliphatic-polyamine curing agent for epoxy resins, which is known as N,N,N',N', N''-penta(3-aminopropyl)-diethylenetriamine (PADT), that the isothermal reaction kinetics of DGEBA/PADT, dynamic mechanical properties, and thermal stability of its cured DGEBA system were the primary focuses of this piece of research [102]. Aliphatic amines also demonstrate resistance to alkalis and certain inorganic acids, water, and solvents [103]. However, they are not very resistant to many organic solvents. Aliphatic amine is a skin irritant and a toxic substance [104]. It is important to handle it with care, especially those that have low molecular weight and high vapor pressure. Epoxy resins cured with aliphatic amine usually have lower properties than those cured with an aromatic amine.

1.4.1.2 Aromatic amines:

Aromatic amines are composed of a stable phenyl group and one or more nitrogen atoms. They can cure epoxy resins with excellent heat resistance, with heat deflection temperature (HDT) values ranging from 150°C to 160°C, and have outstanding mechanical properties and high strength [105]. Moreover, the amine exhibits good electrical properties and exceptional chemical resistance, especially against alkalis [106]. As a result, it functions as a curing agent that is highly resistant to being dissolved by solvents. When utilized as a curing agent, the typical procedure involves

two sequential heating stages. The initial heating at a temperature of approximately 80°C is conducted to enhance the activation of the reaction and minimize heat production. This step enables for the gradual initiation of the desired chemical transformations without requiring excessive energy input, promoting controlled and efficient reaction initiation. It may also involve the activation of the aromatic amine followed by its involvement in a subsequent chemical transformation, leading to the formation of the desired product. Subsequently, the second heating at a higher temperature range of 150°C to 170°C aims to drive the reaction towards completion by providing the necessary energy for the desired chemical reactions to occur. This elevated temperature promotes the acceleration of reaction kinetics, facilitating the formation of the desired products and ensuring the completion of the chemical transformations [107, 108]. Aromatic amines have lower basicity compared to aliphatic amines, leading to a lower absorption capacity and rate due to their reduced Lewis basicity [109]. Additionally, the rate of reaction in aromatic systems is slower due to steric hindrance caused by the aromatic ring [110]. This steric hindrance also leads to a higher glass transition temperature (T_g), typically 40-60°C higher than that of a fully cured aliphatic resin [111]. As a result, the presence of steric hindrance and a higher T_g contribute to the improved thermal stability and mechanical properties of the cured epoxy resins, making aromatic amines highly suitable for high-temperature applications, particularly in the aerospace industry.

1.4.2 Polyamide resin

Polyamide resin is a type of curing agent for epoxy resin that is derived from the reaction of fatty acids with polyamines (**Figure 4a**). These curing agents are typically in the form of liquid or paste and contain reactive primary and secondary amines in its molecules. During curing, the amine groups in the polyamide react with the epoxy groups in the epoxy resin (**Figure 4b**) [112]. This reaction forms a three-dimensional network structure, transforming the liquid epoxy into a solid, cross-linked polymer, that can improve the excellent adhesion, chemical resistance, flexibility, toughness, low-temperature curing, and elongation of epoxy resin [113]. For example, in a study conducted by Zahra Baig et al. (2020), two different types of amide oligomers were synthesized through the reaction of isophthylol chloride with both aromatic and aliphatic amines individually. The synthesized oligomers were employed as additives and curing agents to assess the impact of their concentration and structure on the

thermal and mechanical properties of epoxy in comparison to a reference sample of DGEBA/4,40 oxydianiline cured material. The epoxy cured using this technique is commonly utilized in construction and coating applications [114].

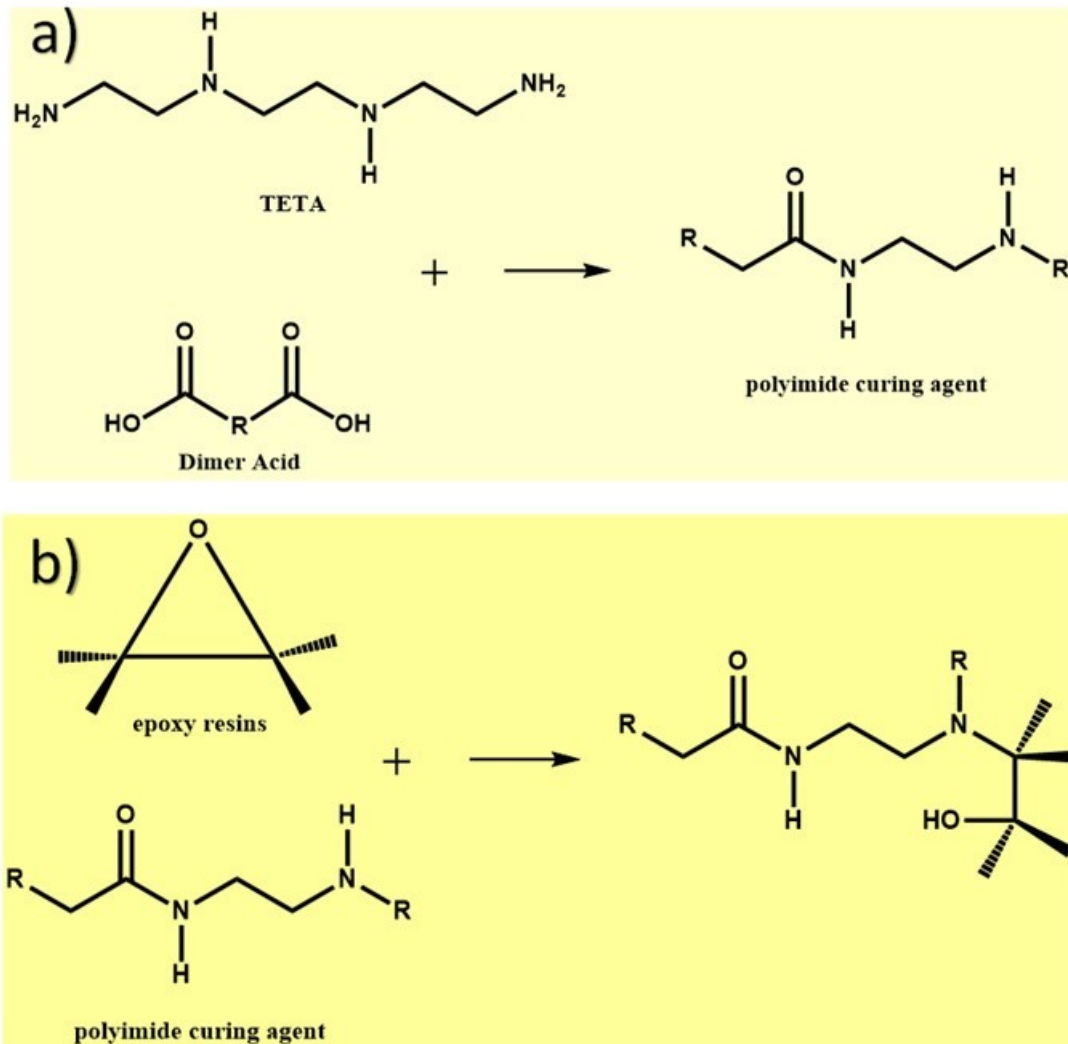


Figure 4. Chemical structure of polyamide-based curing agents a) schematic of Polyamide Synthesis derived from the reaction of fatty acids with polyamines Anhydrides b) schematic of epoxy resin cured with amide curing.

1.4.3 Anhydrides

Anhydrides are one of the most common types of curing agents used to harden epoxy resins through a chemical reaction called epoxy curing or crosslinking. This process involves the reaction of the epoxy groups in the resin with the anhydride groups in the curing agent and forms a three-dimensional network of cross-linked polymer chains[115]. The synthesis of acid anhydride curing agents by dehydrating diacids is

a widely studied chemical conversion. This process entails the transformation of diacids into acid anhydrides by eliminating water molecules, leading to the creation of cyclic anhydride structures. The reaction demonstrates the characteristic of reversibility, wherein, under specific circumstances, the anhydride ring can undergo hydrolysis to restore the initial diacid. The reversible nature of anhydride formation and hydrolysis is a crucial characteristic that influences their stability and reactivity in different applications, especially in the context of epoxy resin curing [116, 117]. The process of epoxy curing with anhydride hardeners is influenced by various competing mechanisms. First, due to the anhydride groups being unable to directly react with the epoxide groups, they ring-opened by a hydroxyl source. This hydroxyl source can originate from three possible sources: the hydroxyl group already present on the epoxy resin, a small amount of water present in the formulation, or the addition of a catalyst to form half-esters and free carboxylic acids (**Figure 5a**). Afterward, the newly formed carboxylic acid group reacts with an epoxide to form an ester linkage and a new hydroxyl group (**Figure 5b**), this process is referred to as an esterification reaction. Finally, the hydroxyl generated in the previous step reacts with another anhydride group as shown in the first reaction moreover simultaneously, the hydroxyl group has the ability to initiate the opening of the epoxy group's ring, resulting in the formation of a network of cross-linked bonds. This reaction is commonly referred to as homopolymerization [118, 119]. Anhydride curing agents have many advantages for epoxy resin curing, including a high ratio of anhydride to epoxy resin, which reduces resin viscosity and facilitates curing, excellent thermal and chemical resistance, high clarity, UV stability, high glass transition temperature, low cure exotherm, low cure shrinkage, long pot life, and tough and durable cured materials [117]. These properties make them suitable for many applications, such as being utilized in a variety of fiber-reinforced composite processes, such as filament winding, pultrusion, VARTM, and RTM [120]. In the aerospace industry for the purpose of manufacturing aircraft components like wings, fuselage, and landing gear [121]. Within the wind energy, is utilized in the manufacturing of blades for wind turbines [122]. In the electrical industry, there are manufacturing insulators, transformers, and other diverse electrical components [123]. However, there are certain limitations that they may encounter in certain situations. A key downside of untreated anhydrides is their swift reaction with water, rendering them uncured for procedures conducted in environments with elevated humidity levels [124]. Unlike epoxy systems cured with amines, epoxy

systems cured with anhydrides may continue to undergo reactions even after reaching the desired temperature for curing. This can make it difficult to achieve the theoretical vitrification point [119]. The reason for this is that epoxy systems cured with anhydrides have a higher cross-link density compared to those cured with amines. This results in a greater number of covalent bonds between the polymer chains. The presence of a high cross-link density can pose challenges in achieving the theoretical vitrification point, which signifies the transition of the epoxy system into a solid state with glass-like properties [125]. Additionally, in comparison to amine curing agents, it exhibits a weaker shrinkage effect during the curing process, and the product has superior heat resistance and insulation performance, making it extensively utilized in the electrical insulation field [119].

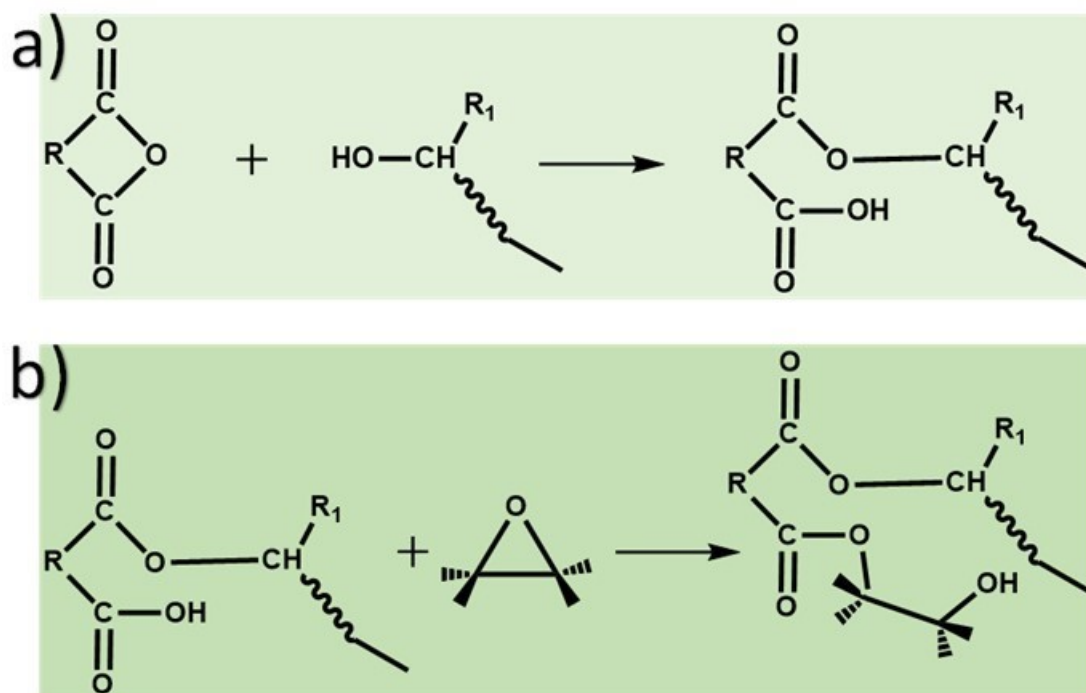


Figure 5. a) Anhydride groups open to form half-esters and free carboxylic acids. This is usually caused by a hydroxyl group, such as an accelerator or the epoxy resin pendant hydroxyl. In Reaction b), the newly formed carboxylic acid group reacts with an epoxide to form an ester linkage and a new hydroxyl group, which reacts with another anhydride group as shown in Reaction a, and so on.

1.4.4 Cycloaliphatic

Cycloaliphatic curing agents are a distinct type of curing agents that are utilized in epoxy resin systems. They have cyclic, non-aromatic molecules, often with cyclohexane or similar rings (**Figure 6**) [126]. These curing agents are selected for epoxy systems that need specific properties in the cured resin, such as high UV resistance, outdoor durability, chemical resistance, Temperature Resistance, and colour stability. They are commonly used for making electrical insulators, structural composites, and coatings [127].

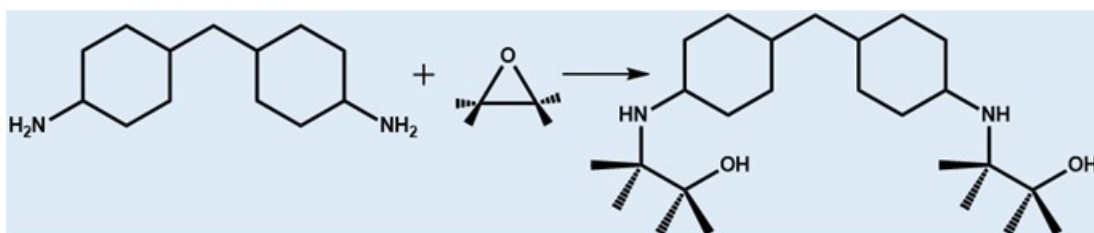


Figure 6. Chemical structure of Cycloaliphatic-based curing agents that reacts with epoxy group.

1.4.5 Latent curing agents

Latent curing agents also referred to as latent hardeners or latent catalysts are a specific type of curing agent utilized in epoxy resin systems (**Figure 7**). These agents remain inactive or dormant at room temperature and only become active when they are exposed to specific conditions, such as heat, radiation, moisture, or a combination of these factors [128]. Latent curing agents provide numerous benefits such as thermal stability, mechanical strength, and chemical resistance. They also allow for control over the curing process and extend the shelf life of epoxy formulations. These agents find applications in various fields including adhesives, coatings, composites, and potting compounds, where precise control over the curing process is crucial [129]. For example, in a study conducted by Jun Hyup Lee et al., highly adhesive epoxy-based sealing materials for LCDs were created by utilizing various types of dihydrazides as the thermal latent curing agent [130].

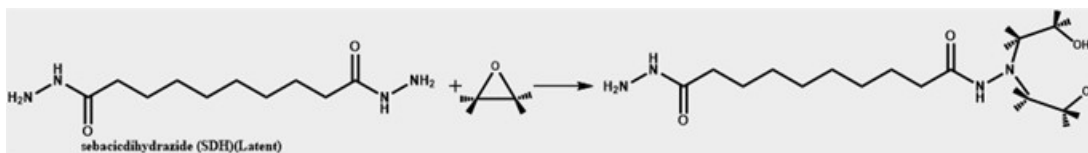


Figure 7. Chemical structure of Latent -based curing agents that reacts with epoxy group.

1.4.6 Polymercaptopan

Polymercaptopans are a type of liquid curing agent that can significantly accelerate the curing process of epoxy resins at room temperature (**Figure 8**). These agents possess thiol (sulfhydryl) functional groups that are capable of reacting with epoxy resins, thereby initiating the curing process [131]. In addition, they can also be utilized to expedite the curing process of other epoxy-curing agents, such as amines, polyamides, and amidoamines [132]. To prepare a typical polymercaptopan, you would need to mix an allyl ether of a polyoxypropylated pentaerythritol, a solvent, and an azo catalyst. For example, a study conducted by Grigor B. Bantchev et al. examined the effects of vegetable oil polymercaptopans. In order to explore the properties and applications of polymercaptopanized soybean oil (PMSO), the researchers conducted tests to examine its behavior when exposed to heat and UV light. Heating processes generate heat-bodied vegetable oils that find applications in various products such as gear oil, printing ink, and more. Understanding the impact of heat and UV radiation on PMSO can provide insights into the alterations observed in lubricants and polyurethane precursors containing PMSO [131]. Polymercaptopan curing agents are highly regarded for their flexibility, colour stability, toughness, moisture insensitivity, adhesion properties, and relatively low toxicity [133]. They are frequently utilized in a wide range of applications, including adhesives, sealants, and potting compounds, across various industries [134].

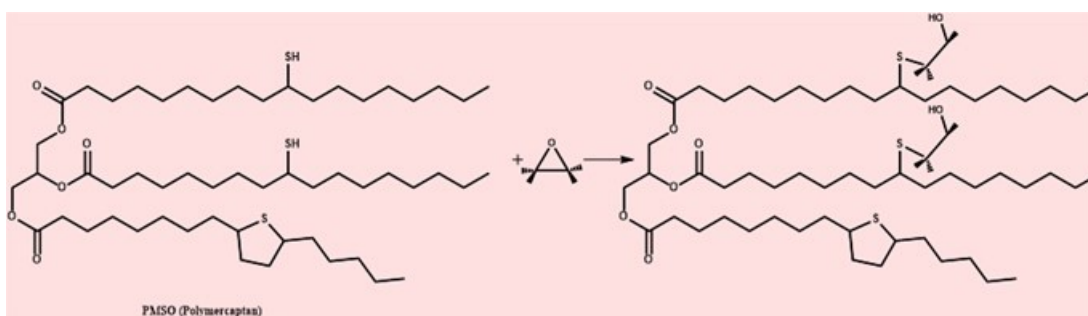


Figure 8. Chemical structure of polymercaptopans-based curing agents that reacts with epoxy group.

1.5 THERMOSET PROPERTIES AND APPLICATION

Thermosetting materials undergo a chemical change when they are cured, leading to a cross-linking or curing process. Covalent cross-links between polymer chains form a complex network that is insoluble and cannot be melted permanently and set their shape [135]. Thermosets are essential in industrial application such as electronic packaging [136], aerospace, mechanical, construction, automotive, marine, medical, and furniture industries, where strength, electrical insulation, durability, dimensional stability, chemical resistance, and high-temperature resistance are needed [84, 137]. Their irreversibility and ability to maintain their shape and properties under harsh conditions make them useful in applications ranging from aerospace and automotive parts to electrical, coatings [138], adhesives [139], composites [140], and construction [141] (**Figure 9**). However, it is important to acknowledge that they also have certain drawbacks and limitations that may render them less suitable situations. These include limited recyclability, brittleness, lengthy curing times, restricted design options, reduced flexibility, environmental impact, higher cost, and challenges in repair.

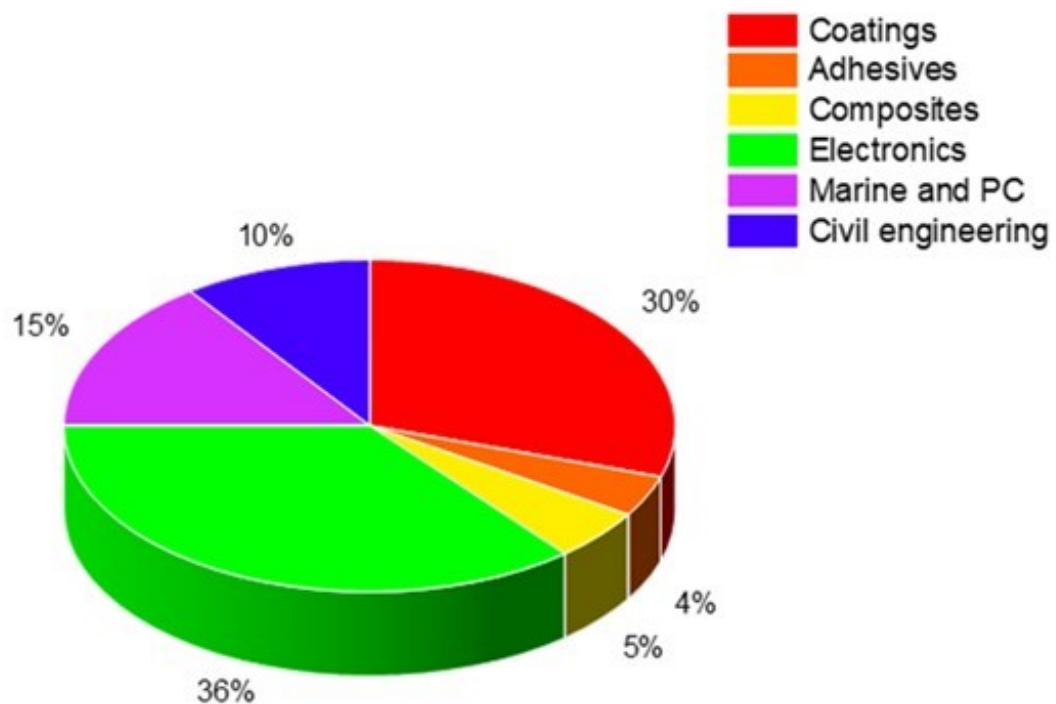


Figure 9. Global epoxy polymer applications[142].

1.5.1 Brittleness and restricted design options

Thermosets are a type of polymer that can withstand high temperatures while maintaining their rigidity. However, this rigidity can frequently result in brittleness and restricted design options, which makes them susceptible to cracking or breaking when subjected to stress [143]. Phenolic resin and phenolic-based composites, polyurethane elastomers, silicone elastomers, urea-formaldehyde resin, and melamine formaldehyde are some examples of thermosets that are known for their brittleness [144, 145]. It is important to note that the brittleness of thermosets can be managed or reduced, which in turn can provide greater design flexibility. This can be achieved through various techniques, including adjusting the formulation, optimizing curing conditions, or incorporating plasticizers [146]. The properties of a thermoset can vary based on its composition and the specific application it is intended for [147].

1.5.2 Lengthy curing times

Thermosetting materials require curing or cross-linking processes to set their structure and become solid. While some thermosets can cure relatively quickly, others have lengthy curing times due to the nature of their chemical reactions. Some examples of thermosets with lengthy curing times are phenolic resins, epoxy resins, polyimides, cyanate ester resins, and BMI (Bismaleimide) Resins [148]. For example, the curing time for phenolic resins: In a study conducted by Weisheng Yang et al. renewable phenolic resins were synthesized using lignin-derived monomers such as vanillin, methyl vanillate and syringaldehyde. The researchers directly polymerized these monomers to create the desired polymers, without the need for formaldehyde or other aldehydes. The reactions were carried out at a temperature of 110 °C for durations of 9 hours, 12 hours, 15 hours, and 18 hours, respectively [149]. An additional study was conducted by Marion Thébault et al. to illustrate this. They demonstrate the impregnation process of Kraft papers with a phenolic resin determines the quality of decorative laminate boards. These materials are used to manufacture the cores of the boards. This article presents the properties data of eight phenolic resins that were synthesized with different parameters of pH and reaction times at 60 °C and 90 °C. For example, at a pH range of 8 to 8.5, the reaction times typically range from 2 to 3 hours [150]. For example, the curing time for epoxy resins: Vaithilingam et al. (2020) described a method for obtaining epoxy composites using eugenol-benzoxazine monomer (EBUz) derived from thiourea and diglycidyl ether of bisphenol-A (epoxy),

along with amine functional carbon from cashew nut shells (f-CSC). The composite mixture was poured onto a glass plate and allowed to harden by following a specific temperature schedule (40 °C, 60 °C, 80 °C, 100 °C, 120 °C, 160 °C, and 180 °C for 1 hour at each temperature). This process resulted in the formation of films [151]. Alejandro Lerma-Canto and colleagues with the purpose of developing and optimizing an epoxy resin that is based on epoxidized hemp oil and utilized a different percentage of maleinized hemp oil as a potential substitute for the methyl nadic anhydride (MNA) that is derived from petroleum carried out a further investigation. The process of curing the samples was carried out at 90 °C for a duration of 3 hours, followed by post-curing at 120 °C for a duration of one hour [152]. For instance, the duration required for the curing process of polyimides: According to a study carried out by Valeri Ivanov Petkov et al. Two formulations of thermosetting polyimide based on 4,4-(hexafluoroisopropylidene) diphthalic anhydride were developed, with different levels of crosslinking sites to analysed to investigate the impact of crosslinking density on fracture toughness, glass transition temperature, and thermal oxidative stability. A two-step curing cycle was employed, with temperatures of 320 °C (for 30–60 min) and 370 °C (for 120–180 min) [153]. Furthermore, in a study conducted by Bo Mi Lee et al., polyimides were synthesized using a diamine that contained hydroxyl and cardo groups, along with a dianhydride. The gas permeation properties and various characteristics of hydroxyl polyimide are being compared to those of a commonly used polyimide. Furthermore, the hydroxyl polyimides exhibited remarkable solubility in commonly used organic solvents and displayed a high level of thermal stability. A curing cycle was employed at room temperature for a day after that using an IR ramp for two days [154]. According to a study conducted by Zhao-Xi Zhou et al., the curing process for cyanate ester resins consists of two distinct steps. Initially, the printed objects are subjected to a temperature of 100 °C in an oven for a duration of 2 hours, while being exposed to air. Subsequently, they are cleansed using ultrasonic waves in isopropyl alcohol to eliminate the E-CE residue resulting from thermal expansion. During the second step, the 3D-printed objects are subjected to a curing process in a programmable oven with a nitrogen atmosphere. The curing process involves exposing the objects to specific temperatures and durations: 90 °C for 1 hour, 120 °C for 1 hour, 150 °C for 1 hour, 180 °C for 2 hours, 200 °C for 1 hour, and 220 °C for 30 minutes. Ultimately, the specimens are allowed to cool down organically until they reach the ambient temperature. This study stands out by creating 3D-printed materials using

THEICTA, where the carbon-carbon double bonds are cured through radical polymerization. Through post-printing thermal treatment, the conversion of three cyanate groups into a triazine ring structure occurs. Furthermore, the two kinds of structures are interpenetrating. The high-performance 3D printing material holds promise in various industries, including space exploration, aviation, automotive, and electronics [155]. According to a study carried out by Mingzhen Xu et al., shows the preparation and characterization of DABA-Ph/BMI copolymers and their glass fiber-reinforced composites. The copolymers were synthesized via thermal curing in an air-circulation oven, involving a specific heating profile: 180 °C for 1 hour, 200 °C for 1 hour, 240 °C for 2 hours, 280 °C for 2 hours, and 320 °C for 2 hours. Then glass fabrics were impregnated with the DABA-Ph/BMI solution, dried at 160 °C for 10 minutes, and then hot-pressed under pressure in a stainless steel mold. The curing procedure for the composites followed a similar temperature profile as the copolymers. The thermal-mechanical properties of the resulting composites were investigated, revealing outstanding flexural strength, flexural modulus, and high glass-transition temperatures ($T_g > 450\text{ °C}$) [156]. These examples highlight that the curing time of thermosetting materials can be influenced by various factors, including temperature, curing agent, part geometry, and desired properties [157]. There are several strategies and techniques that can help mitigate or solve the problem of lengthy curing times in thermosetting materials. These include optimizing the curing process by carefully controlling temperature, time, and curing agent concentration [158], using catalysts and accelerators [159], preheating the mold or substrate before applying the thermosetting material [160], using alternative curing methods such as UV or electron beam curing [161], making formulation adjustments, performing pre-curing or partial curing, and parallel processing of multiple parts simultaneously to maximize production output [162].

1.5.3 Higher cost

Thermoset materials can sometimes have higher production costs compared to other materials due to factors such as specialized manufacturing processes, raw material costs, and quality requirements. Some examples of thermoset materials that are known for their higher cost are epoxy resin systems [147, 163, 164], Phenolic resins [164], Polyimide resins [165, 166], BMI resins [167]. It is noteworthy that although thermoset materials may have higher initial costs they are frequently selected [168],

for their exceptional performance characteristics in demanding applications, which can justify the investment [169]. Furthermore, the integration of various strategies focused on enhancing production processes [170], careful evaluation of material selection and designs [171], utilization of advanced manufacturing techniques [172], large-scale production [173], cost-benefit analysis [174], and lifecycle assessment [175] can facilitate the identification of potential avenues for cost reduction without compromising product quality and performance.

1.5.4 Challenges in repair

Repairing certain thermoset materials can be challenging due to their irreversible curing process, unique properties, and characteristics. These materials are often brittle and cannot be re-melted, making traditional repair methods such as remolding or reprocessing ineffective. Additionally, the chemical inertness of these materials, which is caused by the strong covalent bonds that they possess, makes it difficult for adhesives or solvents to effectively bond the materials together and specialized adhesives or specific curing conditions are required to successfully repair thermoset materials. Additionally, the high curing temperatures that are necessary during the manufacturing process might make it difficult to repair thermosetting materials. This is because exposing these materials to temperatures that are equivalent to those required for the manufacturing process may be either impracticable or detrimental to the components that are around them. In thermosetting materials that have been repaired, achieving homogeneity may be a challenging task. Furthermore, the repaired region may display differing mechanical and thermal characteristics in comparison to the original material, which might possibly result in performance issues. Maintaining the smooth and durable surface finish of thermosetting materials can pose challenges during repair processes, particularly when employing mechanical techniques such as grinding or sanding. The repair process may require specialized techniques, equipment, or materials, which could lead to increased issues and costs. Furthermore, it is imperative to prioritize the establishment of compatibility among various formulations of thermosetting polymers during the repair process in order to avoid any compromises in the overall performance. Some examples of thermosets that can be challenging to repair include carbon fiber-reinforced epoxy composites [176], fiber-reinforced phenolic laminates [177], polyester and vinyl ester resin-based structures [178], thermoset molding compounds [179], phenolic resin-based insulators [180], and

melamine formaldehyde-based kitchenware [178]. The resolution of difficulties encountered in the repair of thermosets necessitates careful consideration of the material's composition and the use of suitable repair techniques to guarantee the integrity of the repaired component.

1.5.5 Recycling thermoset

Thermoset plastics, such as phenolic resin, polyimides, phenolic composites, and melamine formaldehyde, are impossible to recycle through traditional melting and reshaping methods, unlike thermoplastics [181]. The challenges in thermoset recycling include the diversity of thermoset materials, the complex chemical structures involved, and the energy-intensive processes required for their recycling [171]. However, there are some emerging technologies and methods for recycling thermoset materials. Some thermoset materials can be mechanically recycled by grinding them into small particles, which can then be used as fillers in new thermoset materials. This process is limited in terms of the quality and range of products that can be produced [182]. Chemical recycling methods involve breaking down the chemical bonds of thermoset polymers to recover the constituent monomers, which can then be used to create new thermoset materials. For instance, a study conducted by Elisabetta Morici and colleagues. The objective of this review was to explore thermoset-recycling methods, specifically focusing on the recovery of valuable reinforcing fibres from commonly used thermoset composites. This was achieved through chemical recycling techniques that break down the 3D-links between polymer chains using solvents, both with and without catalysis systems and irradiation-assisted were examined, which aid in the recovery of mono-oligomers and fillers in the case of composites, as well as facilitate re-crosslink creation [182]. In addition, Okajima et al. employed supercritical methanol at a temperature of 270 °C and a pressure of 8 MPa to effectively cleave the ester bonds within the epoxy backbone and dissolve the matrix of the carbon fiber-reinforced sample. The authors have successfully demonstrated that the selective destruction of ester bonds can be achieved using supercritical fluid. Furthermore, they have shown that this process preserves both the C-C bond and the mechanical properties of the carbon fibers, ensuring their structural integrity. This presents an opportunity to utilize reclaimed mono-oligomers and carbon fibers in the development of innovative thermoset materials [183]. However, chemical recycling of thermosets is still in the experimental stage and faces several challenges [184]. Pyrolysis is a

thermal degradation process in which thermoset materials are heated in the absence of oxygen to break down their molecular structure. This can result in the production of oils, gases, and char, which can be used as feedstock for various industrial processes, including the production of new thermoset materials [185, 186]. For example, a study by presents a method for developing a flame-retardant and recyclable thermoset from epoxidized soybean oil (ESO) using 2-hydroxyethyl methacrylate phosphate (HEMAP) and tannic acid (TA) (Chen et al., 2023). This approach resulted in a thermoset with the highest UL-94 rating of V-0 and a limited oxygen index value of 26.7%, attributed to the synergistic flame-retardant effect of phosphate and TA. The incorporation of phosphate and TA effectively promoted the formation of dense carbon layers and delayed the pyrolysis of long aliphatic chains. Additionally, the ternary crosslinking of ESO, HEMAP, and TA resulted in a rigid network with superior mechanical properties. Moreover, the ESO-based thermoset exhibited a fast stress relaxation behavior due to the transesterification of dynamic β -hydroxyl phosphate esters, which enables the network with thermal-healing ability and recyclability [187].

and automotive. Recycling composites often involves separating the thermoset matrix from the reinforcing fibers. Various methods, such as mechanical, thermal, or chemical processes, can be used for this purpose. Upcycling thermoset materials involves converting them into higher-value products rather than simply recycling them into lower-value materials. This approach can be economically viable in some cases [188].

1.6 DEGRADABLE AND BIOBASED THERMOSETS

Common thermosets, such as phenolic resins, vinyl ester resins, polyester resin (Unsaturated Polyester Resin), melamine formaldehyde resins, and urea-formaldehyde matrix excellent resistance to environmental degradation caused by microorganisms, moisture, and other factors that typically cause the breakdown of organic materials [189]. Thermoset waste breaks down over time into small particles, which then accumulate in important ocean regions, freshwater environments, and terrestrial ecosystems [190]. Degradable thermosets are a specific type of polymer material like bioepoxy resins [191], epoxidized soybean oil (ESO) [192], starch-based thermosets [193], and lignin-based thermosetting polymers [194]. They have the ability to undergo controlled degradation or decomposition under certain conditions, such as hydrolysis, photo degradation, enzymatic degradation, or chemical treatment [195].

Despite this degradation process, they are able to maintain their original structural integrity and functionality until the trigger for degradation occurs, for instance according to a recent study conducted by Xianchao Chen et al., the researchers have presented the design of a thermoset hyperbranched epoxy resin (EFTH-n) that is both degradable and recyclable. This resin is synthesized using bio-based 2,5-furandicarboxylic acid (FDCA). The resin exhibited exceptional performance when tested with the common diglycidyl ether of bisphenol-A (DGEBA). Notably, it demonstrated significant enhancements in impact strength, tensile strength, flexural strength, storage modulus, and elongation, with improvements of up to 181.84%, 60.22%, 24.08%, 32%, and 58.0% respectively. The researchers have reached the conclusion that the resin has the potential to greatly enhance the degradation of the cured composites under gentle conditions, without the need for organic solvents. Additionally, the recycling yield of FDCA was found to be 56.8 wt%. The degradation mechanism was investigated using Gas Chromatography-Mass Spectrometry (GC-MS)[191]. In addition, according to the findings of research that was carried out by Binbo Wang and colleagues, they were able to create a bio-sourced building block for high-performance degradable plastics by using the bio resources vanillin (a derivative of lignin) and glycerol through solvent-free acetalization with high conversion rate and high selectivity. The building block demonstrates rapid degradation into nontoxic vanillin and glycerol within a short span of 3 minutes under mild acidic conditions. This degradation occurs even when exposed to pH and temperature levels similar to that of gastric juice in the human stomach, this leads to the exceptional chemical degradability of the epoxy thermosets, which is advantageous for recycling purposes. The degradable thermosetting plastic showed much higher mechanical properties (stronger and tougher) and comparable thermal properties relative to a commercial high-performance counterpart based on bisphenol A (BPA) due to the benzene ring, heterocycle, and methoxyl group-related hydrogen bond [196]. As mentioned, these materials possess the same durability and performance as traditional thermosetting plastics and they have the added advantage of being able to break down into non-toxic components, which helps in reducing plastic waste and pollution [197]. This enables the reduction of the long-term environmental impact caused by plastics. Degradable thermosets are utilized in a wide range of applications, including packaging materials, composite materials, adhesives, coatings, biomedical devices, as well as within the automotive and aerospace industries [198]. One of the notable resins utilized in the

production of biodegradable materials is commonly referred to as epoxidized soybean oil. Epoxidized soybean oil (ESO) has emerged as a promising bio-derived material for the production of environmentally friendly epoxy resins that make use of curing agents such as diamines, dicarboxylic acids, or anhydrides. [199]. The process of synthesizing epoxidized soybean oil (ESO) entails a chemical transformation that occurs between soybean oil, hydrogen peroxide, and either acetic or formic acid. This process results in the conversion of the double bonds present in the oil into epoxy groups (**Figure 10**) [200]. Epoxidized soybean oil (ESO) has several valuable properties, such as due to its high chemical reactivity, the epoxy groups present in ESO exhibit significant chemical reactivity, rendering it valuable for engaging in reactions with various chemicals and polymers [199]. Efficiency in terms of cost, compared to several synthetic plasticizers and stabilizers, ESO is frequently seen as a more economical choice [201], due to the fact that it is non-toxic, ESO is a preferred choice for applications that include the possibility of coming into contact with people, animals, or food. These properties are particularly significant in sectors like as the packaging of food and the manufacturing of medical equipment [202], large worldwide [203], and derived from a natural source (soybean oil), and is considered biodegradable production [204]. These characteristics make ESO a desirable alternative for deployment in industrial operations when compared to some synthetic plasticizers and stabilizers. In the study presented by (Fadda, 2024), the researchers investigated the use of epoxidized soybean oil (ESO) and fatty acid-derived Pripol as sustainable alternatives to fluorine chemistry and nanoparticles for imparting hydrophobicity to fish leather made from salmon skin. The aim was to meet the waterproofing requirements of the fashion industry while utilizing discarded biomass from the food industry. The combination of Pripol and ESO was utilized to create a crosslinked material that was applied as a coating to enhance the wettability properties of the fish leather, addressing its fast water absorption issue [205]. The article by Zeng et al. (2017) investigate the curing of epoxidized soybean oil with biobased dicarboxylic acids (DCAs) with different carbon chain lengths to create entirely sustainable polymers. The curing rate, activation energy, and glass transition temperature of cured ESO/DCA decreased with increasing chain length of DCAs, the tensile strength and Young's modulus increased, and elongation at break decreased due to the decreased crosslinking density caused by the increased chain length between crosslinking sites [206]. Additionally, Ma & Webster (2015) mention the use of a citric acid solution as

a curing agent for epoxidized soybean oil, indicating the potential of naturally occurring acids as cross-linkers for bio-based thermosets [207].

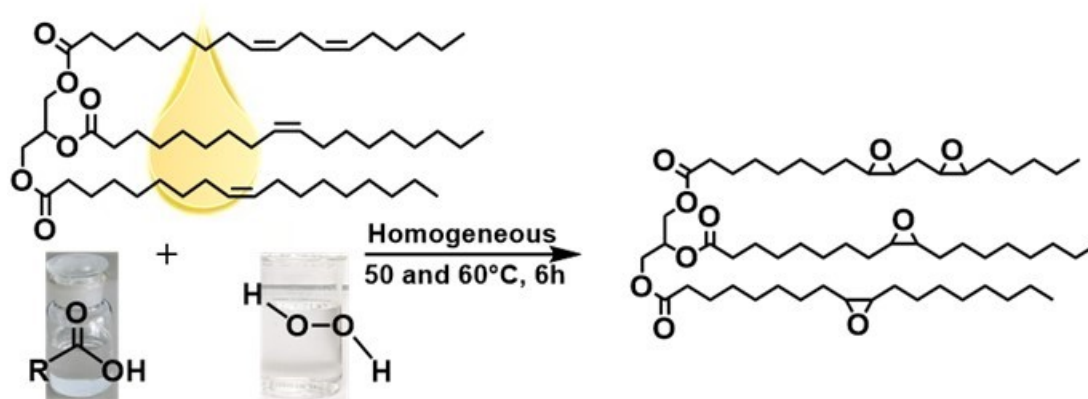


Figure 10. Synthesizing epoxidized soybean oil (ESO).

1.7 PROBLEM OF PLASTIC POLLUTION

Nowadays, more than 450 million tonnes of plastics are produced annually in the world [208]. If the trends that have been observed thus far continue, the production of plastics worldwide may reach over 1,100 million metric tons by the year 2050 [46], according to some estimates. Depending on the location, 35 to 45 % of all manufactured plastic is used for packaging [27, 28], a sector that has the lowest mean product lifetime, of less than 6 months. This makes packaging the industrial sector that contributes most in the global plastic waste generation, with more than 140 million tonnes yearly. Mismanagement of packaging waste, which accounts for a great portion of municipal solid waste (almost 40 %), is one of the main sources of plastic environmental pollution [209]. Even though the bulk of packaging polymers might potentially be recycled, the collection, cleaning and separation process is expensive and time-consuming, and for this reason plastic garbage is typically incinerated or buried in landfills [210]. The majority of plastics are produced from fossil-based resources [33], utilizing hydrocarbons extracted from crude oil and natural gas, and only a small amount (1%) is produced from renewable sources [34]. Regardless of the source of the monomer, plastic is not able to biodegrade, and its fragmentation into smaller pieces over time due to UV oxidation or mechanical fragmentation are cause of

environmental pollution [35]. Additionally, it has been estimated that 0.1 % of the total worldwide production of plastic, which is equivalent to more than 8.3 billion metric tons, has made its way into the oceans and seas of the world in the form of plastic marine debris [211]. If current trends continue, this percentage will more than double by 2040 [212], and by 2025, some estimates suggest that there will be one ton of plastic for every three tons of fish in the world's oceans [213, 214]. Moreover, giant plastic islands are floating on the ocean's surface, and beaches all over the world are filling up with plastic trash [215, 216], which has caused serious environmental concerns, particularly for marine life, because plastic debris can easily be ingested and cause choking, injury, poisoning, or starvation in marine animals [217, 218]. In order to find solutions to these issues, a large number of scientists are focusing their efforts on the creation of alternatives to materials derived from petroleum. Plant-based materials [219], natural fibers [220], bioplastics [221], which are manufactured from renewable resources such as corn starch or sugarcane, and mycelium-based materials [222, 223], which are developed from mushrooms and other fungi, are some of the promising choices that are currently available.

The development of biodegradable plastics that can be designed to break down naturally in the environment, typically through the action of microorganisms such as bacteria, fungi, and microbes, into water, carbon dioxide, and biomass [224, 225]. They are commonly produced from renewable biomass sources like lignin, cellulose, soy, starch, and bioethanol and are currently a subject of great interest [226, 227]. The capacity for bioplastic production varies depending on the specific type of bioplastic and the region of the world in question. However, It is expected that the capacity for the manufacturing of bioplastics will more than double from its current level of around 1.81 million metric tons in 2022 to approximately 6.3 million metric tons in 2027 [228]. Strach blends, polylactic acid (PLA) and polyhydroxyalkanoate (PHA) are examples of commercially available biodegradable plastics that make up slightly more than 48 % of the world's total capacity for biodegradable polymers [229]. There are also other examples, such as polyhydroxy butyrate (PHB), polyhydroxy butyrate valerate (PHBV), and polyhydroxy valerate (PHV) [230]. Biodegradable plastics are often marketed as more environmentally friendly because they have the potential to reduce plastic waste and the associated environmental problems and can, in principle, be biodegraded without any harmful effects [226, 231]. However, the biodegradation of bioplastics is dependent on a variety of environmental factors, including

temperature, humidity, the availability of oxygen, and the activity of microorganisms [232]. For example, PLA (polylactic acid) requires a temperature range of around 60-70 °C for optimal biodegradation [233], polybutylene succinate (PBS) must be heated to temperatures between 50 and 60 degrees Celsius [234], whereas PHAs (polyhydroxyalkanoates), which can biodegrade at somewhat lower temperatures of around 30-40 °C [235]. In the oceans, the temperature is usually much lower, which significantly slows down the biodegradation of those materials to the point that some of them (e.g. PLA) can't practically biodegrade. Therefore, alternative materials capable of biodegradation in the marine environment are highly desirable.

1.8 LIFE CYCLE ASSESSMENT (LCA)

Life Cycle Assessment (LCA) is an essential instrument that is utilized for the purpose of analyzing the environmental consequences that are linked with items and processes throughout the entirety of their life cycles. It entails evaluating a variety of environmental characteristics, including acidification, ecotoxicity, eutrophication, global warming, ozone depletion, and resource depletion, in addition to evaluating human health implications, such as carcinogenic and non-carcinogenic substances [236]. In the articles by (Li et al. (2023), Romeiko et al. (2020), Riazi et al. (2019)), the importance of conducting life cycle assessments to evaluate the environmental impacts of soybean oil production, particularly concerning greenhouse gas emissions and other environmental factors [237-239]. The study by Xin Huang explores the utilization of bio-based epoxidized soybean oil (ESO) vitrimer in combination with reclaimed glass fiber fabric (RGFF) to create a uniform and compact cartilage-like interwoven structure. The life-cycle assessment (LCA) of ESO/RGFF composites-based triboelectric nanogenerators (TENG) demonstrates a 44%–49% decrease in carbon footprint when compared to fully petrochemical-based materials, highlighting the environmental benefits of this upcycling approach that combines plastic wastes with biomass [240]. The article by Arias et al. (2020) provides a detailed analysis of bio-adhesives in the wood panel industry using a life cycle assessment (LCA) approach. Through a cradle-to-gate LCA, perspective of bio-adhesives such as soy, Kraft lignin, Organosolv, and tannin. These bio-adhesives have the potential to serve as alternatives to the most conventional fossil resins in the manufacturing of wood panels. Furthermore, the researchers came to the conclusion that there is a wide range of opportunities for the production of adhesives that are more environmentally friendly

than conventional fossil resins, and even for the development of formaldehyde-free adhesive alternatives. Lignin-based adhesives, on the other hand, were found to have a greater influence on the environment than fossil-based adhesives, but soy- and tannin-based bio-adhesives demonstrated a superior environmental performance in comparison to fossil oils [241]. The life cycle assessment (LCA) study conducted on ESS resin and ESS-based biocomposites compared to BPA-based composites revealed significant insights into the environmental impacts of these materials (Ghasemi et al., 2020). The study identified hotspots in the production process, highlighting the contributions of vegetable oil methyl ester and hydrogen peroxide to various environmental impact categories. The bio-based resin demonstrated an overall reduction in environmental footprint compared to petroleum-based resin, except in eutrophication and carcinogenics impact categories [242].

1.9 VITRIMERS

Vitrimers are a unique type of polymeric material that possess characteristics and properties that fall between those of thermoplastic and thermoset materials [243]. Vitrimers and thermoset polymers both possess covalently cross-linked networks, which contribute to their exceptional thermal stability, mechanical strength, and chemical resistance [244]. Unlike conventional thermoset materials, which form permanent bonds through cross-linking during the curing process and have no reprocessing or recycling capabilities after their intended use, consequently, these thermosets are usually either disposed of in landfills or incinerated, causing significant environmental problems and a noticeable rise in material expenses [245], vitrimers have the ability to exchange two or more of their crosslinking bonds with each other when sufficient energy is supplied. Because of this interaction, molecules are able to move in relation to each other. This movement allows the material to flow, be recycled, and undergo reprocessing at a macroscopic level (**Figure 11**)[192, 244]. Based on a study conducted by Changfei He et al., it has been demonstrated that Poly(oxime-ester) (POE) vitrimers can be successfully synthesized through thiol-ene click chemistry reactions carried out at room temperature. POE networks exhibit characteristics akin to thermosets, as they possess insolubility in typical organic solvents and demonstrate commendable structural stability. However, under elevated temperatures, POE networks demonstrate exceptional malleability and

reprocessability due to the occurrence of oxime transesterification. The recently discovered dynamic network has demonstrated a remarkable ability to undergo multiple reprocessing and recycling cycles without any noticeable degradation in its chemical, physical, and mechanical properties [246]. A similar example is vitreous silica, also known as quartz glass, which has the ability to flow and whose behaviour can be described using the Arrhenius law [247]. They act like permanently cross-linked polymers at service temperatures, but at elevated temperatures, the exchange reactions within their network speed up, which makes flow possible while maintaining the same number of chemical bonds and cross-links [192]. Vitrimers, similar to thermoplastics, possess the unique ability to alter their topology. For example, according to a study that was carried out by Zhenyu Lyu and colleagues, the metathesis of dioxaborolanes has been shown to be a method that is both quick and thermally stable for the preparation of vitrimers from a variety of commodity thermoplastics, including poly(methyl methacrylate), polystyrene, and high-density polyethylene. Despite the fact that they are irreversibly cross-linked, these vitrimers have the remarkable ability to be treated several times through the processes of extrusion or injection molding. During the process of dioxaborolanes metathesis, molecules are able to exchange fragments that are linked together by the strong B–O bonds of the boronic ester groups. This process allows for changes in the molecular topology without reducing connectivity, as a result of exchange reactions that keep the number of chemical bonds and cross-links constant [248]. This characteristic makes them highly appealing for a wide range of applications [249]. Additionally, they can be easily reheated, remolded, and cooled as needed, all without undergoing any changes to their chemical composition.

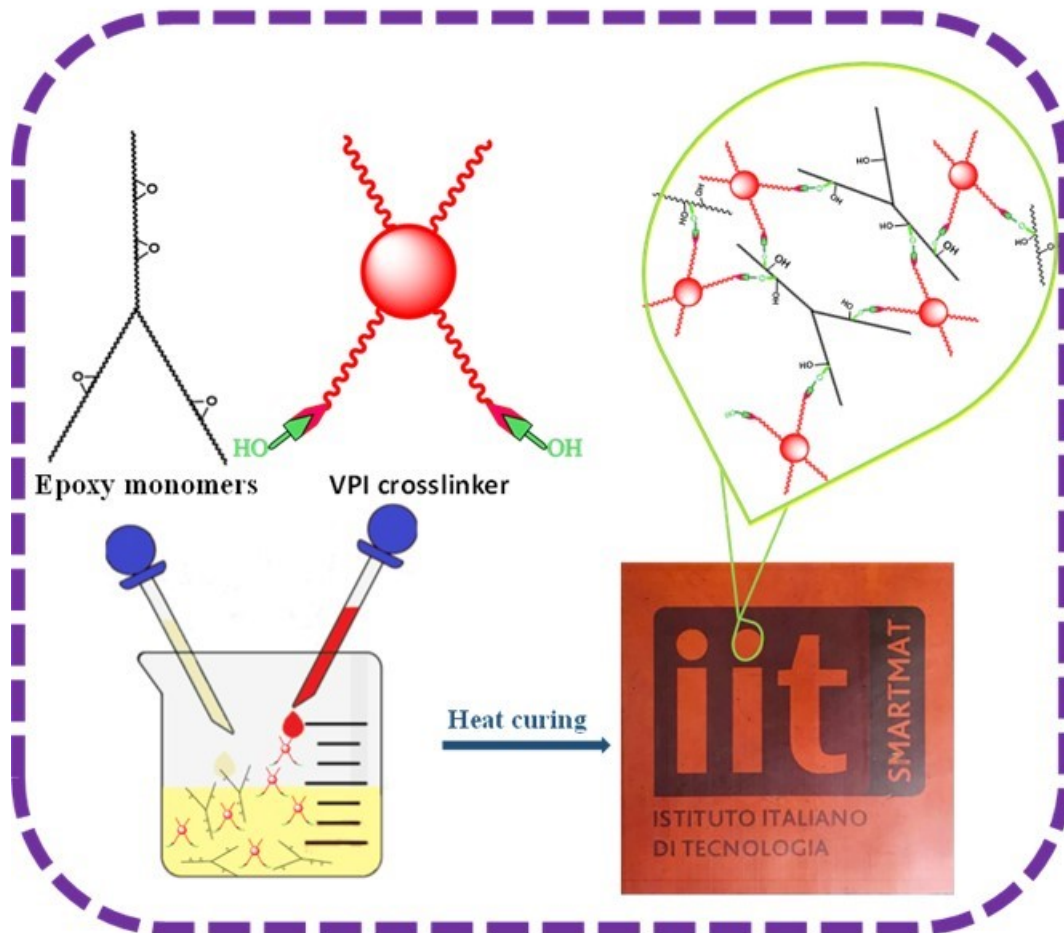


Figure 11. Phases of the formation of vitrimers.

1.9.1 Vitrimers properties

1.9.1.1 Dynamic Bonds:

The presence of dynamic covalent bonds within the polymer network of a vitrimer is what distinguishes it from other types of molecules (**Figure 12**)[250]. Under certain circumstances, these bonds are able to disassemble and reassemble themselves without causing any damage to the material. The disulfide, imine, transamination of vinylogous urethanes, transalkylation, and transesterification bonds are all examples of common types of dynamic bonds in vitrimers. For example, Obadia et al. provided evidence of the reprocessing and recycling of highly cross-linked ion-conducting networks by utilizing transalkylation exchanges of C-N bonds. This study emphasized the efficiency of dynamic covalent bonds in vitrimers [251]. Hendriks et al. showcased the development of poly(thioether) vitrimers via transalkylation of trialkylsulfonium salts, emphasizing the permanent cross-linking and recyclability of vitrimers [252].

Additionally, Neal et al. conducted a study on improving the mechanical properties of a covalent self-healing material by incorporating sacrificial hydrogen-bonding amide. Their research showcased the possibility of enhancing that contain static covalent bonds go through an irreversible crosslinking process during the curing phase. This results in the production of a polymer network that is stiff and long-lasting, and it also prevents the thermosets from being reprocessed or reshaped after the curing process has been completed [253].

1.9.1.2 Self-Healing:

Due to the dynamic nature of their bonds, vitrimers can exhibit self-healing properties, when vitrimers are exposed to certain conditions, such as heat or pressure, they have the ability to perform some degree of self-healing [250]. This characteristic renders them appropriate for applications in which materials are subject to potential wear or damage over a period of time [254]. For instance, according to a recent study conducted by Arkadiusz Zych et al., presents a novel method for producing a biobased reprocessable vitrimer. This material is created by coupling epoxidized soybean oil acrylate with a diboronic ester dithiol dynamic cross-linker using thiol acrylate. The resulting vitrimer material exhibits the unique property of being reprocessable multiple times, similar to a thermoplastic, without compromising its mechanical properties. Additionally, it can be conveniently recycled through reversible hydrolysis in 90% ethanol and subsequent solvent evaporation, thereby regenerating the original vitrimer. One of the key advantages of this developed material is its ability to self-repair mechanical abrasion-related defects, such as scratches and cuts, at room temperature. This self-healing capability is attributed to the material's low glass transition temperature and rapid boronic ester exchange. As a result, the vitrimer demonstrates great potential as a self-healing coating, offering promising applications in various industries. Furthermore, the study highlights the environmental benefits of the vitrimer material. In the event of unintended environmental release, the substance possesses the ability to undergo biodegradation, effectively addressing the issue of waste accumulation. This property aligns with the growing emphasis on sustainable and environmentally friendly materials, making the vitrimer a promising candidate for addressing both performance and environmental concerns [192]. one the other hand, the lack of inherent self-healing capabilities in traditional thermosets has been a significant limitation in their application. The crosslinking mechanisms in traditional

thermosets, such as epoxy resins and phenolic resins, result in irreversible networks that do not possess the ability to autonomously repair damage [255].

1.9.1.3 Recyclability:

The fact that vitrimer bonds are dynamic in nature makes it possible for the material to be recycled in an easy manner. Through the process of breaking and subsequently reforming chemical bonds, the polymer exhibits the ability to undergo reshaping, remolding, or even depolymerisation, followed by depolymerised[256]. This characteristic not only minimizes waste but also makes a significant contribution to the overall sustainability of the material. For instance, in a study conducted by Liu et al., epoxy vitrimers were utilized as a matrix material for the production of carbon fiber-reinforced composites. The findings of the study demonstrated the remarkable recyclability of these composites, highlighting the potential of vitrimers in waste reduction and the promotion of sustainability [257].

Furthermore, Chen et al. have developed a method to create elastomeric vitrimers that are mechanically strong, capable of self-healing, and recyclable. This is achieved by incorporating dynamic dual cross-links consisting of boronic ester bonds and Zn^{2+} -O coordination. These vitrimers have been successfully integrated into rubber materials, enabling them to be repaired and reused. This research highlights the potential of vitrimers in reducing waste and promoting sustainability [258]. The lack of recyclability for conventional thermosetting plastics has resulted in a significant accumulation of waste throughout the manufacturing process and at the end of their useful life. This has raised considerable concerns regarding their environmental implications and long-term viability. In addition, the presence of covalent intermolecular cross-linkages in thermosetting plastics contributes to their enhanced strength and stiffness, which imparts resistance to damage. However, this characteristic also presents challenges in terms of recyclability. Consequently, the disposal of conventional thermosetting polymers frequently results in down cycling, incineration, or landfilling, thereby contributing to environmental pollution and the inefficient use of resources [179].

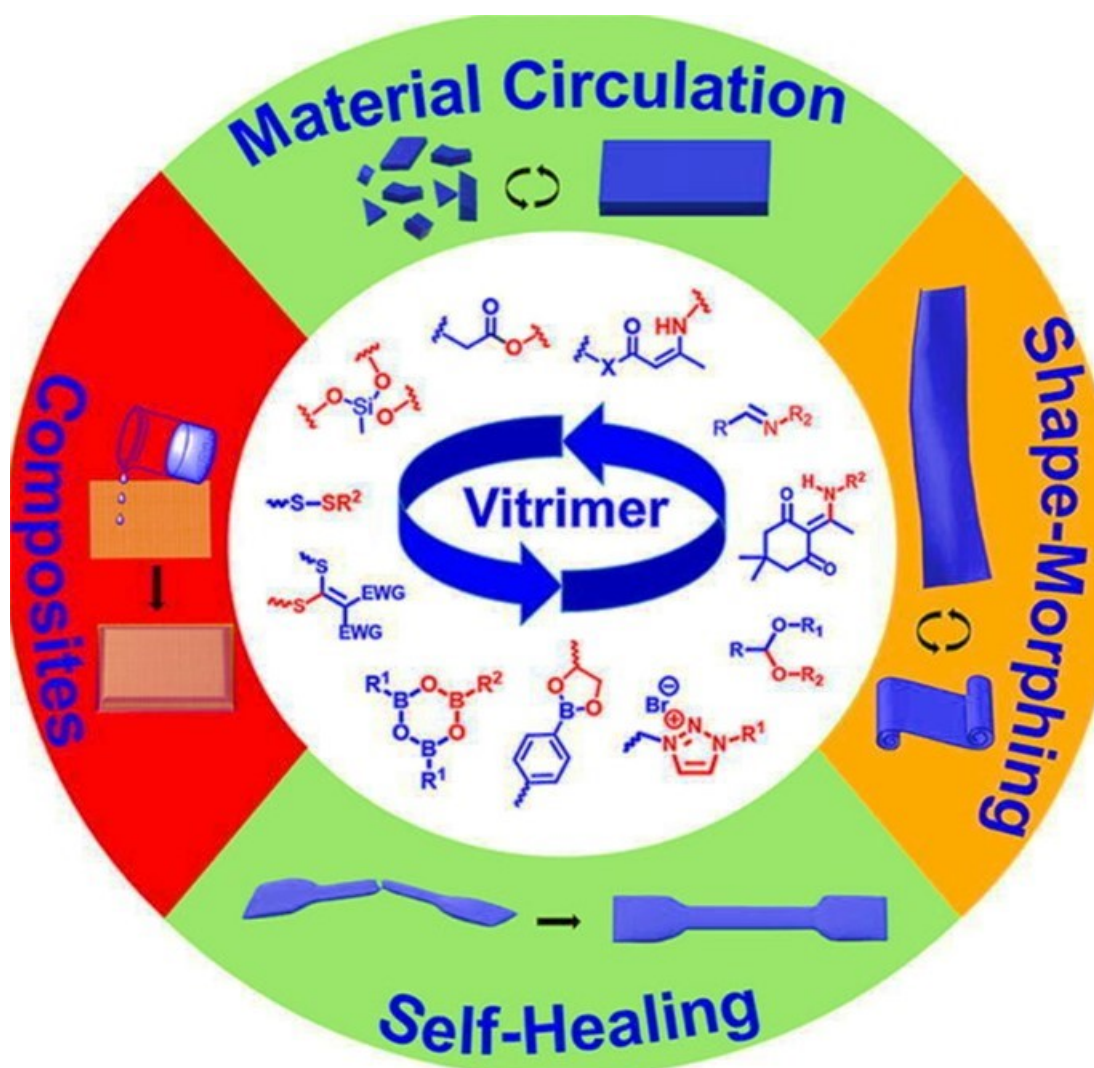


Figure 12. Schematic image of dynamic covalent bonds utilized in vitrimer materials and the applications of these bond [259].

1.9.1.4 Thermal Stability:

Vitrimers frequently demonstrate favourable thermal stability, characterized by elevated glass transition temperatures (T_g). Due to the presence of this property, they are suitable for use in applications involving high temperatures [260]. Additionally, vitrimers have the ability to undergo reversible transitions between a glassy state and a rubbery state in response to temperature changes. The thermal reversibility of this material enables it to be processed and shaped [261]. In their study, Legrand and Soulié-Ziakovic (2018) conducted a thorough investigation into the thermal behaviour of vitrimers. They were able to identify two specific transition temperatures that effectively demonstrate the unique thermal properties exhibited by these materials. The glass-transition temperature (T_g) is the first transition temperature that indicates

the shift from the glassy state to the rubbery state in vitrimers. The transition is linked to the alteration in molecular mobility and the initiation of segmental motion within the material. Legrand and Soulié-Ziakovic have identified a second transition temperature, referred to as T_v . This temperature is associated with exchange reactions and signifies the shift from the viscoelastic solid state to the liquid state in vitrimers. The transition is crucial because it indicates the moment when the material changes from behaving like a solid to behaving like a liquid. This change occurs because of the exchange reactions happening within the network [262]. For example, Zhou et al. conducted a study that showed polyimine vitrimers have remarkable thermal stability. The researchers synthesized polyimine vitrimers using vanillin and found that they exhibited minimal weight loss when exposed to high temperatures. Additionally, the study demonstrated that these vitrimers had excellent reprocessability, fast chemical degradability, and adhesion properties. This reference provides support for the claim regarding the thermal stability of polyimine vitrimers and their potential suitability for high-temperature applications [263]. However, traditional thermosets are non-reprocess able due to their cross-linked molecular structure, which lacks thermal reversibility. This constraint leads to the practice of down cycling or incinerating the materials once they have reached the end of their useful life [264].

1.9.1.5 Chemical Stability:

Vitrimers are able to maintain their chemical stability while undergoing bond exchange, which effectively prevents any degradation of the material. These materials exhibit various behaviours, such as stress relaxation and thermal reprocessability, while still maintaining their chemical stability. This is possible because of the reversible nature of their bonds. They offer the unique combination of reprocessability and chemical stability during the bond exchange [248]. A study conducted by Mao Chen et al. demonstrates the synthesis of epoxy vitrimers through the utilization of a curing agent containing disulfide-containing carboxylic acid. These vitrimers demonstrate fast stress relaxation and have relaxation times that range from 1.5 seconds at 200 °C to 5500 seconds at 60 °C. Additionally, they exhibit malleability at a relatively low temperature of 65°C. Furthermore, this epoxy vitrimer can be effectively reprocessed at a temperature of 100 °C within a time frame of 1 hour. It is worth noting that no significant decrease in mechanical strength was observed even after undergoing four cycles. It has potential applications in the electronics industry, particularly in situations where high temperatures are not permissible. These epoxy

vitrimers are well-suited for self-healing and recyclable electronic encapsulation due to their moderate T_m . In such applications, stress and cracking can arise from variations in the thermal index of expansion, leading to a decline in the performance of integrated circuits at higher temperatures (with an upper limit of approximately 125 °C) [265]. Conversely, conventional thermosets, by virtue of their intrinsic chemical composition, may experience chemical deterioration as time passes. The presence of static covalent cross-links in conventional thermosets renders them vulnerable to chemical breakdown, hence restricting their ability to be reprocessed and recycled. The limited chemical stability during bond exchange poses a barrier to their potential for long-term use and disposal choices [266].

1.9.1.6 Biodegradability:

vitrimers can be made more biodegradable by incorporating biodegradable fillers, reinforcing agents, or additives into the material [267]. Including these additives can improve the overall sustainability of vitrimer materials by facilitating biodegradation in natural environments when disposed of. It is possible to create vitrimers that exhibit the capacity to undergo degradation over a period upon exposure to particular environmental circumstances. This implies that, over a period, these materials have the capability to undergo decomposition by microorganisms and other natural mechanisms, resulting in the production of substances that do not pose any detrimental effects on the environment. An example is a study conducted by Philipp Haida et al. In this study, the researchers focused on the development of starch-reinforced vinylogous urethane vitrimer composites. The results of their research showed significant improvements in biodegradability, reprocessability, and sustainability in addressing the environmental impact associated with thermosetting polymers [268]. An example is a study conducted by Philipp Haida et al. In this study, Additionally, in a study conducted by Jie Li et al. the synthesis of soft, fully bio-based poly-hydroxyl thermosets through catalyst-free transesterification has shown decent re-processability and biodegradability, further contributing to the advancement of sustainable materials [269]. In addition, a study conducted by Wei Zhao et al. has investigated the use of vitrimer-cellulose paper composites. This research has introduced a novel category of materials that are strong, intelligent, environmentally friendly, and sustainable. It emphasizes the potential of vitrimers in addressing the environmental issues linked to conventional thermosets [270]. This characteristic renders them well-suited for applications that aid sustainability and to minimize environmental impact [271].

Unlike vitrimers, the traditional thermosets, which are derived from nonrenewable fossil resources, which known for their permanent covalent cross-links. This property makes them challenging to reprocess, recycle, and reshape [272, 273]. In addition, the widespread use of traditional thermosets leads to the fast depletion of fossil-based resources and the buildup of persistent plastic waste in the environment[192].

This characteristic makes them highly appealing for a wide range of applications.

1.10 APPLICATIONS OF VITRIMERS:

1.10.1 Recyclable Plastics:

Vitrimers, which belong to a class of polymers containing dynamic covalent bonds, have garnered significant interest due to their potential in the production of recyclable plastics (**Figure 13**) [259]. These materials have the ability to be recycled multiple times without significant degradation in their material properties. This is made possible by breaking and reforming their dynamic bonds during the recycling process. According to Zhao et al. [270], vitrimers offer a novel approach to material design at the molecular level by combining the characteristics of traditional thermosets and thermoplastics. Vitrimers possess dynamic covalent bonds that allow for reprocessing, reshaping, and the ability to self-heal. These properties make vitrimers suitable for a wide range of applications, such as adhesives, elastomers, coatings, and composite materials (Chen et al.,[274]; Yang et al., [275]; Okubo & Yao, [276]). Furthermore, researchers have investigated the use of vitrimers in sustainable materials. These studies have shown that vitrimers have the potential for closed-loop recyclability and can be used to produce fully bio-based epoxy vitrimers that exhibit similar mechanical properties and thermal stability as the original vitrimers (Zhong et al., [277]; Hubbard et al., [278]). In addition, researchers have found that incorporating specific bonds, like dithioacetal bonds, has resulted in significant advancements in vitrimer technology. This discovery has broadened the possibilities for using vitrimers in the production of recyclable plastics (Sungjin Kim [279]; Jie Zheng et al. [259]). The use of vitrimers in recyclable plastics is in line with the increasing interest in sustainable materials and the concept of a circular economy. With the significant increase in plastic production over the years, there is an urgent requirement for efficient recycling technologies and materials that can help achieve carbon neutrality in the plastic industry (Sun et al., [280]; Kwesiga, [281]). In addition, regulations promote the use

of recycled plastics to support the concept of a circular economy. This highlights the significance of recycling plastics derived from petroleum-based sources (Revest, [282]). Furthermore, the use of vitrimers as recyclable plastics is in line with the objective of reducing plastic waste and increasing recycling rates. This is especially relevant in the context of electronic waste, where there are both challenges and opportunities to improve the recycling rate of plastics.

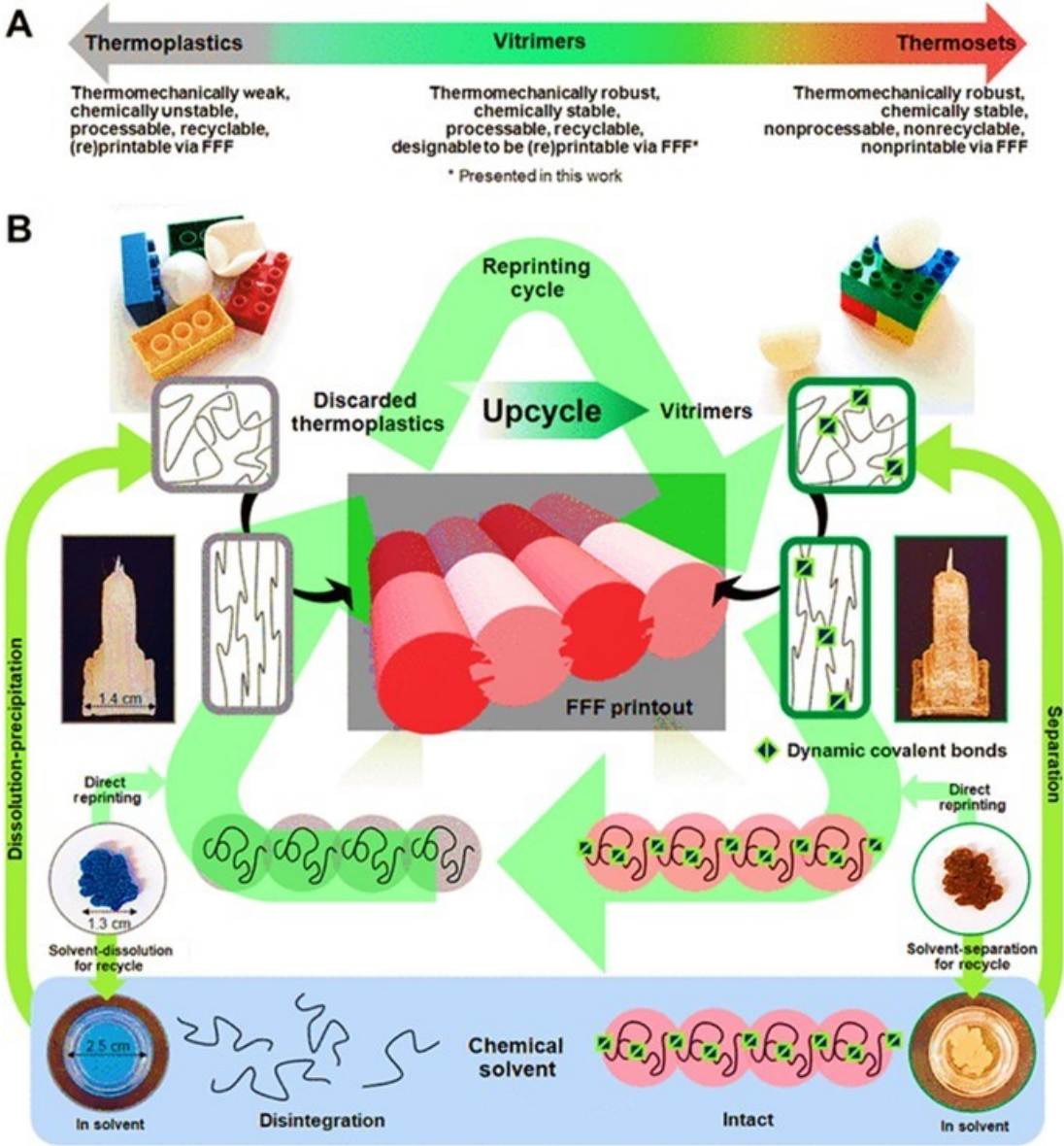


Figure 13. Using vitrimers in the production of recyclable plastics [279].

1.10.2 Flexible Electronics:

Vitrimers offer mechanical robustness and resilience in the realm of flexible electronic substrates, enabling the creation of electronic devices that can be bent and stretched. Vitrimers possess a dynamic nature that allows them to endure mechanical deformation without compromising their structural integrity. This characteristic is crucial for their use in flexible electronic applications (**Figure 14**)[283]. Moreover, the self-healing properties of vitrimers can enhance the durability and dependability of flexible electronic substrates by automatically repairing any damage resulting from mechanical strain [274, 284]. Vitrimers possess dynamic covalent bonds that allow them to respond effectively to mechanical stress and deformation. This unique characteristic makes them highly suitable for various applications such as flexible electronic substrates, interconnects, and encapsulation materials [285-287].

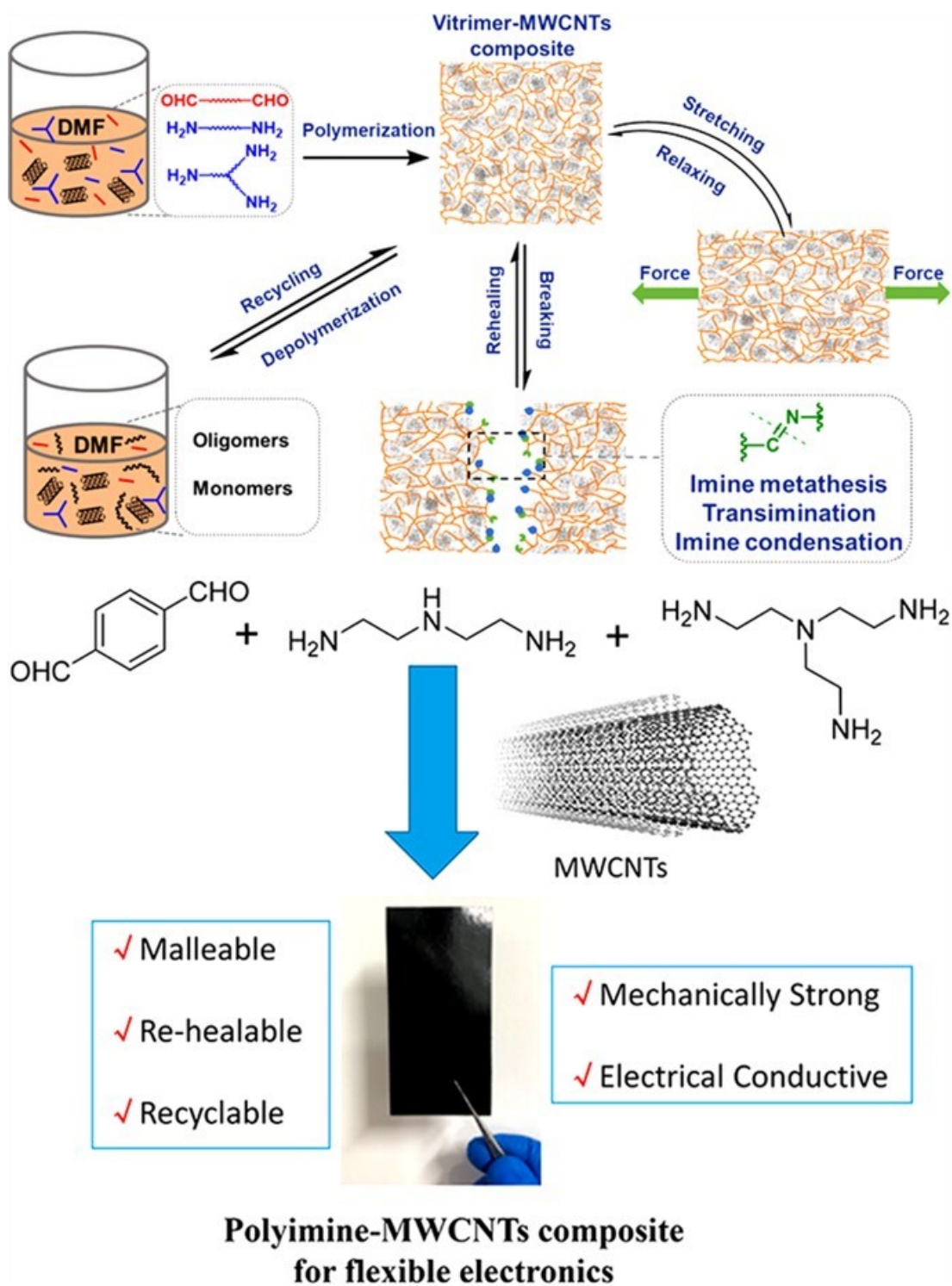


Figure 14. Using vitrimers in the flexible electronic [283].

1.10.3 Biomedical Applications:

Certain vitrimers possess biocompatibility and can be effectively utilized in various applications, such as medical devices and drug delivery systems (**Figure 15**) [288].

The selection of materials for biomedical applications heavily relies on the crucial factor of biocompatibility. Vitrimers have demonstrated biocompatible properties, making them appropriate for use in contact with biological systems without any harmful effects. A study conducted by Kim et al. assessed the biocompatibility of vitrimers through in vitro cell culture experiments. This study supports the idea that vitrimers are biocompatible. The results of the study showed that vitrimers have the ability to support cell adhesion and proliferation, suggesting that they could be used in various biomedical applications [289, 290]. The dynamic nature of medical devices allows for the presence of self-healing properties, which can be advantageous in enhancing the longevity and strength of these devices [291]. In addition, vitrimers have the ability to be molded into intricate shapes and structures, which makes them highly suitable for various applications including tissue scaffolds, implants, and prosthetics. The versatility of vitrimers in medical device development has been demonstrated by Zhao and colleagues, who successfully fabricated vitrimer-based scaffolds for tissue engineering applications. This provides corroboration for the aforementioned statement [270].

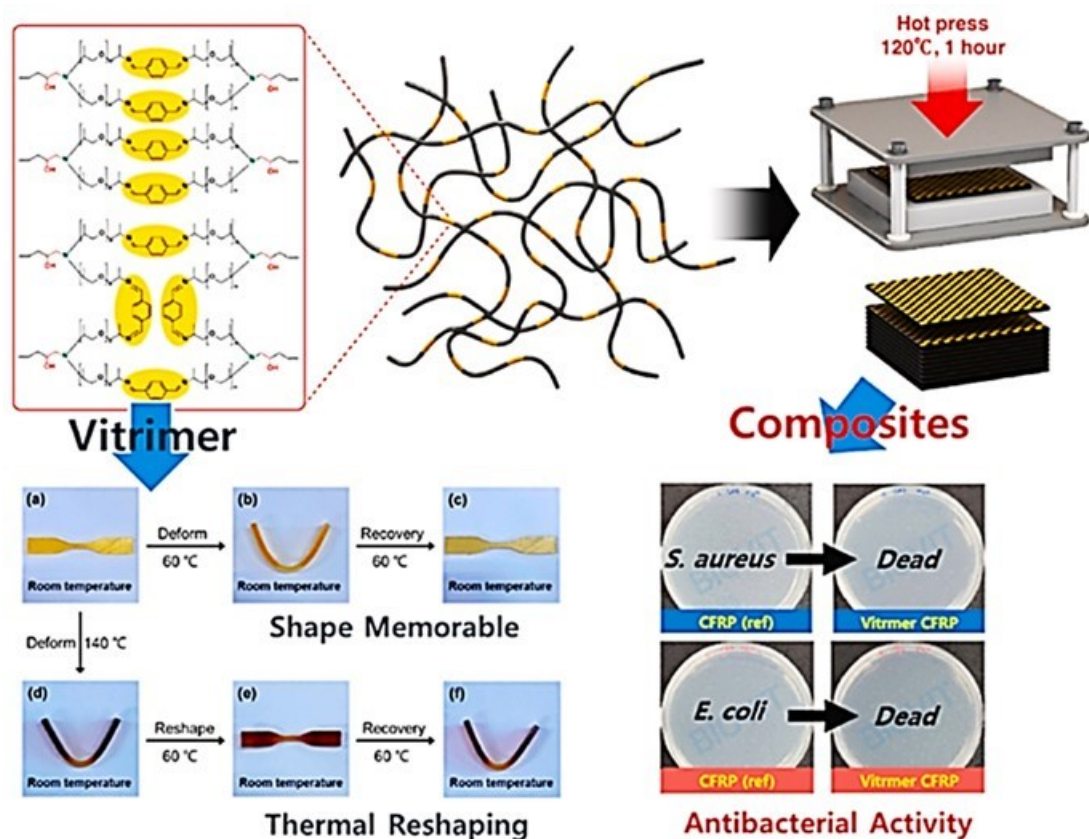


Figure 15. Using vitrimers in the biomedical applications [290].

1.10.4 Shape Memory Materials:

Vitrimers exhibiting shape memory characteristics have been widely employed in various domains, including robotics, smart textiles, and biomedical devices (**Figure 16**)[292-294]. In the work conducted by Yang et al., the research primarily aimed at creating dual-triggered and thermally reconfigurable form memory graphene-vitrimers. These materials are anticipated to streamline the manufacturing of intricate structures and expand the potential uses of shape memory polymers [295]. Furthermore, the research conducted by Liang et al. demonstrates the potential of developing depolymerizable δ -lactone based vitrimers with shape memory as an environmentally friendly alternative to traditional soft elastomers. These vitrimers exhibit promising characteristics for various applications, including lenses, mold materials, soft robots, and microfluidic devices [296]. Tailoring the electromechanical properties of natural rubber vitrimers has shown increased actuation capabilities at lower electrical fields, offering the potential to be applied in smart textiles. This was demonstrated in the research conducted by Bui and colleagues [297]. In the study conducted by Choi et al., they have successfully created weldable and reprocessable shape memory epoxy vitrimers. These vitrimers have been specifically designed for extrusion-based 4D printing applications, taking advantage of their inherent cross-linked structure to enhance shape memory capabilities [298].

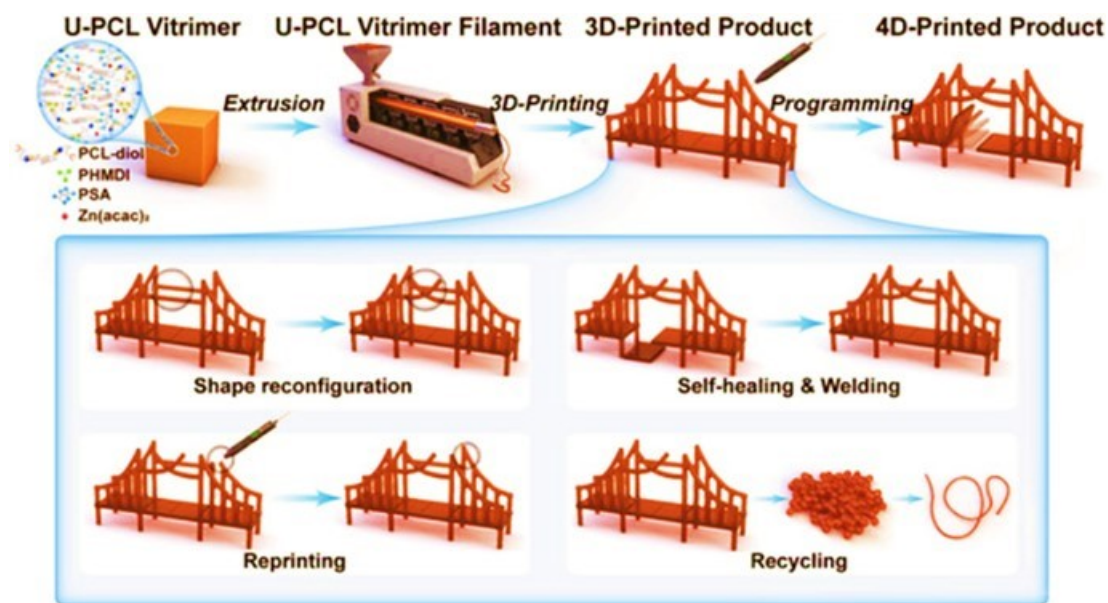


Figure 16. Using vitrimers in the shape memory Materials [294].

1.11 VITRIMERS LIMITATIONS:

The strength of vitrimers is a significant concern when compared to traditional thermosetting polymers. Although vitrimers possess properties of both thermosets and thermoplastics, they do not possess the same level of strength as conventional thermosetting polymers. Thermosetting polymers are renowned for their exceptional mechanical properties and resistance to solvents, which can be attributed to their permanently cross-linked networks. However, vitrimers, despite their advantageous properties such as heat process ability, recyclability, and weld ability, do not possess the same level of mechanical strength as traditional thermosetting polymers [299]. Another limitation of vitrimers is their susceptibility to creep, which results in poor dimensional stability. This limitation restricts their potential applications (Wang et al. [300]). Furthermore, it is noted that a significant number of vitrimers necessitate the use of high catalyst loadings, which gives rise to concerns regarding their durability and potential applications (Cuminet et al. [301]). Additionally, it is important to note that if the catalyst loading is not sufficient, the vitrimer properties will be restricted. This highlights the need for a careful and precise formulation of the catalyst (Liu et al. [302]). These limitations emphasize the difficulties in attaining the desired mechanical properties and stability in vitrimers, which are essential for their extensive use.

1.12 ACTIVATION ENERGY (EA)

The activation energy (E_a) is a critical factor in determining the rate at which dynamic covalent bonds can undergo exchange or rearrangement in vitrimers (**Figure 17**)[303, 304]. Increasing the activation energy barriers can result in a decrease in the speed of dynamic bond exchange processes. This, in turn, enhances the stability of the material and reduces its susceptibility to quick deformation or self-healing. On the other hand, reducing activation energy barriers can enhance the speed of bond exchange, thereby increasing the material's sensitivity to external factors such as heat or pressure. Here is a list of various chemical reactions that can occur in vitrimers, resulting in alterations to a wide range of bond types:

| Dynamic Bond | Scheme | $E_a / \text{kJ mol}^{-1}$ | $T_g / ^\circ\text{C}$ |
|--------------------------------|--------|----------------------------|------------------------|
| Ester (3.1.1) | | 60-150 | 80 |
| Carbamate (3.1.2) | | 90-140 | 54 |
| Carbonate (3.1.2) | | 80-120 | 15 - 35 |
| Carbamide (3.1.3) | | 70-80 | - 70 |
| Acetal (3.2.1) | | 55-140 | 66 - 71 |
| Imine (3.2.2) | | 10-130 | 55 - 135 |
| Vinylogous Urethane (3.3.1) | | 30-80 | 87 |
| Diketo-enamine (3.3.1) | | 30-50 | 125 |
| Thioether (3.3.2) | | 55-70 | - 110 |
| Triazolium (3.4.1) | | 140-150 | - 8 - 23 |
| Pyridinium (3.4.1) | | 45 | - 22 |
| Anilinium (3.4.1) | | 50-60 | 11 - 15 |
| Sulfonium (3.4.2) | | 113 | 30 - 60 † |
| Dioxaborolane (3.5.1) | | 40-80 | 98 |
| Boroxine (3.5.1) | | 80 | 68 |
| Silyl Ether (3.5.2) | | 80-180 | 125 |
| Disulfide (3.5.3) | | 50-60 | 127 |

Figure 17. Some examples of dynamic covalent bonds and activation energy (E_a) that are present in vitrimer [259].

1.12.1 Transesterification:

Transesterification is a chemical process in which ester bonds (C-O-C) undergo exchange reactions (Figure 18) [305]. Vitrimers have the ability to undergo transesterification reactions, which enables the material to be reprocessed and

recycled. The activation energy (E_a) for these vitrimers is usually moderate. This implies that these materials need a specific amount of thermal energy to undergo bond exchange, resulting in their stability at normal room temperatures, when necessary, they can be reprocessed at higher temperatures [261, 306]. For example, the study conducted by Jiawei (Li et al., 2022) focuses on synthesizing and characterizing hydroxyl-terminated polybutadiene-based polyurethane vitrimer (HTPB-PU_v) networks with dynamic boronic ester bonds. The research showcases the successful creation of HTPB-PU_v networks using a one-pot reaction method. This involved incorporating a cross-linker called 2,2'-(1,4-phenylene)-bis(4-mercaptan-1,3,2-dioxaborolane (BDB)). The 55% HTPB-PU_v network demonstrates excellent malleability due to the rapid dioxaborolane metathesis reaction of boronic ester bonds. This reaction has an activation energy (E_a) of 25 kJ/mol (The value is in the range of 7.7–76.7 kJ/mol for the vitrimer with boronic ester bonds) and a glass transition temperature (T_g) of -105 °C. The networks of HTPB-PU_v exhibit distinct capabilities in reprocessing, self-healing, welding, and shape memory. The recycled samples exhibit excellent reprocessability due to the incorporation of dynamic boronic ester bonds into PU networks, achieved through hot pressing at a temperature of 130 °C for a duration of 3 hours [307]. The article authored by Dimitri Berne et al. introduces a new epoxy vitrimer system that does not require a catalyst. This system utilizes α -CF₃-substituted ester functions to internally activate the transesterification reaction. The study expands on the concept of fluorine neighboring group activation, which has recently emerged as a novel approach to enhance acid-epoxy reactions and transesterification in vitrimer materials. It has been demonstrated that the inclusion of fluorine atoms in the α - or β -position can increase the reactivity of ester functions, resulting in accelerated transesterification reaction rates. The stress-relaxation analyses showed that the relaxation time was relatively fast. Specifically, for VD, the relaxation time was 708 seconds at a temperature of 190°C, while for VB, the relaxation time was 1400 seconds at a temperature of 150°C. Materials based on DGEBA and BDGE exhibited an Arrhenius behavior, with activation energies of 67 and 71 kJ mol⁻¹, respectively, being determined for these materials. The presence of the CF₃ group in the α position of the carbonyl group greatly accelerated both the epoxy-acid ring-opening reaction and the transesterification reactions [308].



Figure 18. Transesterification reactions of Vitrimers [308].

1.12.2 Dynamic Disulfide

Disulfide Exchanges are chemical reactions in which sulfur-sulfur (S-S) bonds are exchanged with one another (**Figure 19**)[309]. vitrimers have the ability to be reshaped or healed through disulfide exchange reactions when they are subjected to heat or other triggers. Disulfide-based vitrimers can undergo rapid bond exchange at lower temperatures due to their low E_a values [310]. These properties make them well-suited for self-healing applications, as they have the ability to repair damage at room temperature or with gentle heating. These properties make them well-suited for self-healing applications, as they have the ability to repair damage at room temperature or with gentle heating. For instance, The article, written by Luzuriaga et al., discusses the development of epoxy resin that incorporates exchangeable disulfide crosslinks. The goal is to create fiber-reinforced thermoset composites that can be easily reprocessed, repaired, and recycled. By incorporating disulfide bonds into the epoxy resin, it becomes possible to facilitate rapid bond exchange at lower temperatures. This, in turn, enables easier reprocessing, repair, and recycling of the resulting thermoset composites. This is in line with the overall objective of improving the sustainability and lifespan of fiber-reinforced thermoset composites. It aims to tackle the difficulties related to recycling traditional thermoset materials. The relaxation

times (τ^*) were observed to vary from 3 hours at 130 °C to 20 seconds at 200 °C. The relationship between the relaxation time τ^* and temperature can be described by Arrhenius' law, which yielded an activation energy (E_a) of 55 kJ mol⁻¹ for the dynamic epoxy network. The low activation energy can be attributed to the fact that aromatic disulfide exchange does not require heat. This aligns with the observed rapid relaxation times at elevated temperatures [189]. Furthermore, the article, authored by Kim et al., discusses the development of polymers that are robust, transparent, and easy to process, while also possessing intrinsic self-healing capabilities at room temperature. The study highlights the importance of using aromatic disulfide and hydrogen bonds in elastomers to achieve effective self-healing under normal conditions. This represents a significant breakthrough in the field of self-healing materials. This study examined the use of epoxy-based catalyst-free elastomers for self-healing purposes. The elastomers were designed to heal themselves using aromatic disulfide and hydrogen bonds, without the need for solvents, pressure, or heat. The research emphasized the potential of these materials to achieve self-healing at room temperature. The inclusion of these dynamic bonds in the elastomers showcases their capacity to attain self-healing properties without relying on external interventions. This further bolsters the advancement of materials with inherent self-healing capabilities [311].

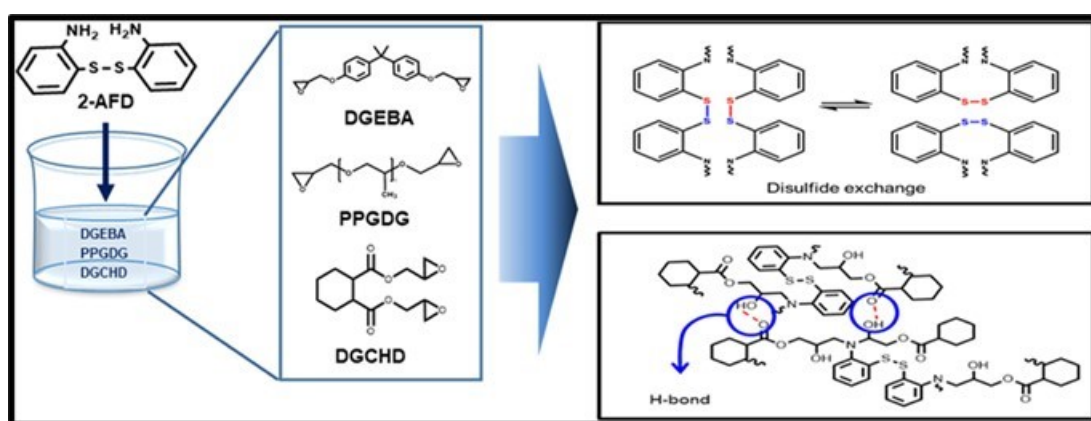


Figure 19 . Disulfide Exchanges reactions of Vitrimers [311].

1.12.3 Dynamic covalent Diels-Alder:

Dynamic covalent Diels-Alder cycloaddition reactions take place between diene groups and dienophile groups (**Figure 20**)[312, 313]. biobased Vitrimers that

incorporate Diels-Alder reactions can be reshaped and reprocessed by using heating or other methods to break and reform covalent bonds. This allows for the Vitrimers to be reprocessed multiple times. The activation energy for Diels-Alder reactions changes depending on the diene and dienophile that are used in the reaction [314]. The adjustment of the activation energy (E_a) for these reactions enables the customization of the vitrimer's thermal responsiveness. Lower activation energy (E_a) values facilitate more rapid reshaping processes, whereas higher E_a values provide enhanced stability when exposed to elevated temperatures [315]. Wudl et al. reported one of the earliest examples of self-healing materials based on thermoreversible DA reactions. The materials were synthesized by performing a Diels-Alder (DA) reaction between tetrafunctional furan and trifunctional maleimide monomers. It is important to note that the resulting DA adduct can be reversed at high temperatures. The materials exhibited a mending efficiency of approximately 50% and 40% when heated for 2 hours at temperatures of 150°C and 120°C, respectively [316]. The researchers, Jiang et al., have successfully developed a liquid crystalline Diels-Alder dynamic network actuator that possesses the unique ability to self-lock. This actuator demonstrates programmability at room temperature and can be processed in solution. The novel main-chain liquid crystalline Diels—Alder dynamic network (LCDAN) demonstrates remarkable simplicity in actuator programming and reprocessing when compared to existing liquid crystalline network (LCN) systems. The actuator utilizes a dual functional azobenzene-based chemical that serves as both mesogens and photochromic groups. These are connected to the polysiloxane backbone to create the network. The system enables reversible bending motions when exposed to light irradiation. By modifying the initial macroscopic shape, one can effectively adjust the function, motion, and other performances of the system. Furthermore, the Liquid Crystal Elastomer with a Disordered-to-Ordered Phase Transition (LCDAN) exhibits the remarkable ability to undergo reversible transformations between ordered and disordered phases. This unique characteristic presents the potential for the LCDAN to be reshaped into intricate three-dimensional structured actuators. In addition, the actuator demonstrates remarkable capability in generating photoinduced mechanical force, thereby facilitating the movement or rolling of sizable 3D actuators with adjustable direction and velocity. This study showcases the potential of developing materials that exhibit nonreciprocal and reprogrammable movements, thereby expanding the opportunities for actuator programming and reprocessing [317].

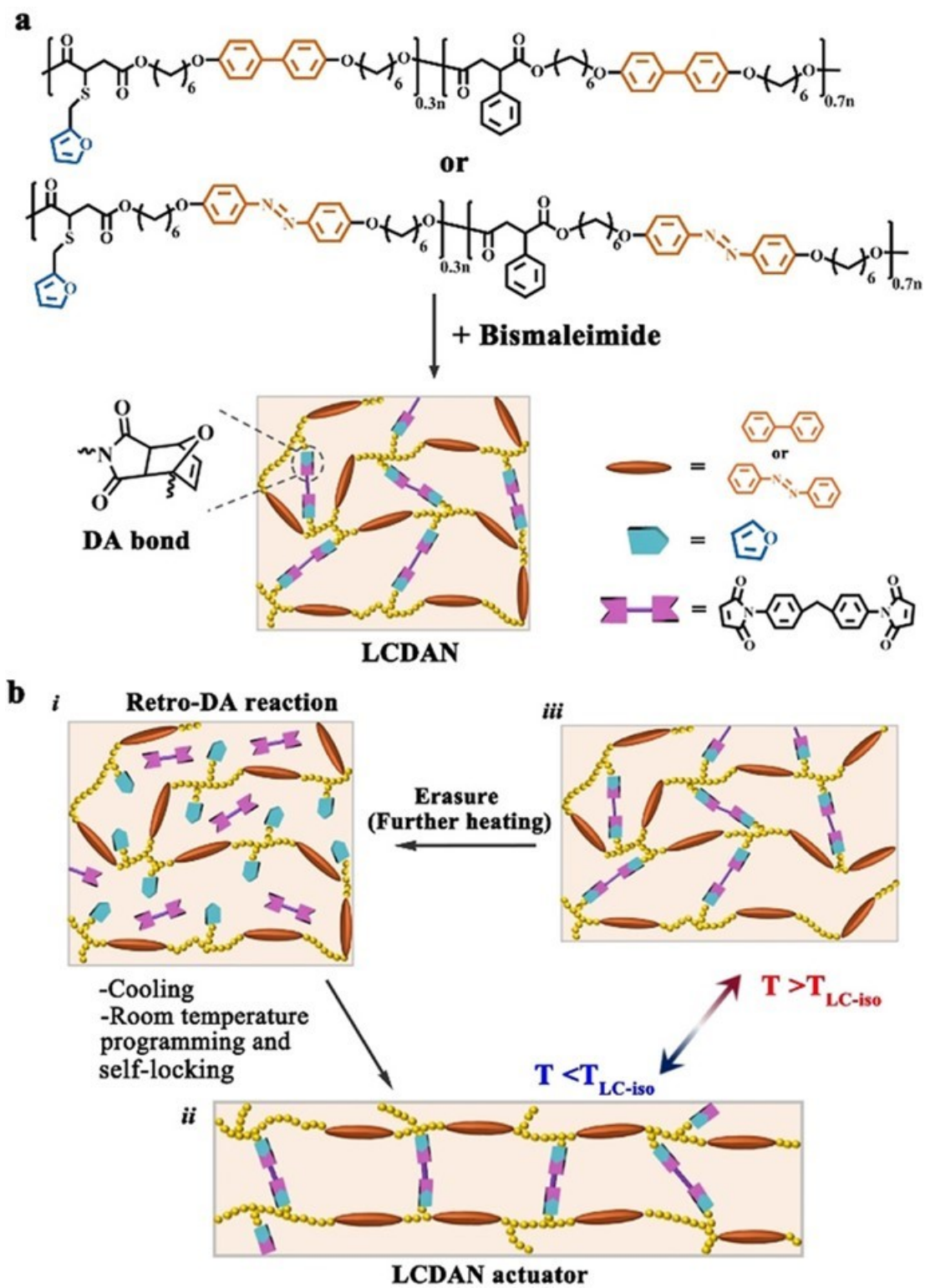


Figure 20 . Dynamic covalent Diels-Alder reactions of Vitrimers [317].

1.12.4 Dynamic Oxime bonds:

Oxime bonds can both form and be broken during the process (**Figure 21**)[318]. Vitrimers that have oxime bonds can be repaired or reshaped using reversible oxime formation reactions, which are typically set off by heat or moisture. The activation energy needed for the production or breakdown of oxime and imine can be adjusted by selecting the appropriate reactants. Vitrimers that have lower activation energies (E_a) are more sensitive to external stimuli, such as heat or wetness. An increase in activation energy levels leads to improved stability and requires a higher amount of energy for the processes of reshaping or mending. The process of reversible imine formation involves the formation and breakage of imine bonds (C-N). For instance, vitrimers that contain imine bonds are able to go through reversible reactions, which make them reshape or heal when exposed to specific conditions [319]. The article authored by Changfei He et al. presents a noteworthy breakthrough in the field of vitrimer materials. The authors have successfully designed and synthesized a new class of catalyst-free poly(oxime-ester) (POE) vitrimers through photo-initiated "thio-ene" reactions at room temperature. This innovative approach enables the UV-polymerization of vitrimers, offering a variety of processing techniques for creating a networked architecture that is both easy to work with and efficient. The POE networks that are formed exhibit properties that are similar to thermosets. They are insoluble in typical organic solvents and possess excellent structural stability. However, when exposed to high temperatures, the oxime transesterification process enhances the flexibility and ability to be reprocessed of the POE networks. It is worth noting that this dynamic network can be easily processed and recycled multiple times without any degradation of its chemical and physical properties. The synthesis process is highly effective and efficient, allowing for the creation of POE vitrimers with a wide range of adjustable properties. This is made possible by the use of tunable monomers. In addition, the analysis that was carried out on the model reaction by utilizing the Arrhenius method resulted in an activation energy (E_a) of $63.5 \pm 7.8 \text{ kJ mol}^{-1}$. This value is lower than the activation energy (E_a) of a standard epoxy ester system that contains catalysts, which is around 88 kJ mol^{-1} . It was decided to add an excessive amount of free oxime into the polymer in order to facilitate the associative exchange process. As a result of increasing the quantity of free oximes, vitrimers were produced that had lower T_v (from 43 to 12 degrees Celsius) and faster relaxing durations (from

5102 to 2725 seconds at 100 degrees Celsius). [246]. Another article authored by Liu et al. introduces a novel category of dynamic covalent polymers called poly(oxime-urethanes) (POUs). These polymers are synthesized through the uncatalyzed polyaddition of multifunctional oximes and hexamethylene diisocyanate (HDI) at room temperature. The resulting POUs display stress relaxation behavior similar to that described by the Arrhenius equation. This behavior is attributed to the oxime-promoted trans carbamoylation process, which occurs through a dissociative mechanism. As a result, reversible oxime-carbamate bonds are formed at temperatures around 100 °C. The re-processability condition of this material is advantageous when compared to conventional PU materials that usually require higher temperatures, typically exceeding 200 °C. The characteristic oxime-nitrone tautomerization mediates the mild temperature needed for bond reversibility. POUs have significant potential in various applications because of their excellent mechanical performance, easy preparation, and dynamic properties, all achieved without the need for catalysts. The Arrhenius analysis of the model reaction yielded an activation energy (E_a , t) for trans carbamoylation of $28.2 \text{ kcal}\cdot\text{mol}^{-1}$ [320].

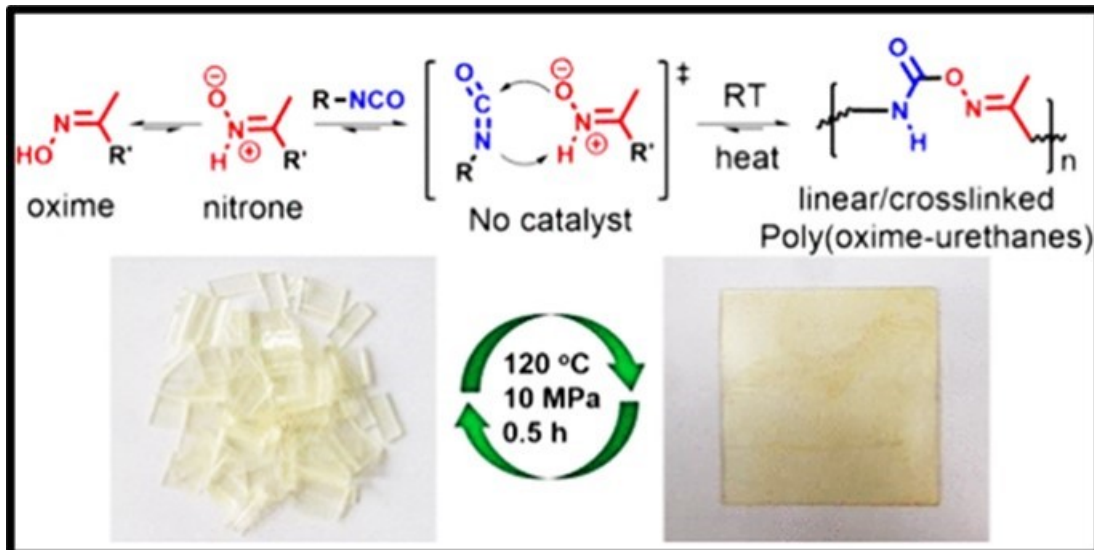


Figure 21 . Dynamic Oxime bonds reactions of Vitrimers [320].

1.12.5 Dynamic Thiol-Ene:

Thiol-Ene reactions are chemical reactions that involve the interaction between thiol (-SH) and alkene (-C=C-) groups (**Figure 22**)[321]. Vitrimers that utilize thiol-ene

chemistry have the ability to be reshaped, and repaired by undergoing thiol-ene reactions. The activation energy (E_a) values of thiol-ene reactions can vary depending on the specific thiol and alkene employed [322]. Adjusting the activation energy (E_a) provides the ability to regulate the vitrimers sensitivity to either light or heat. Lower activation energy values facilitate quicker reshaping and enhance the ability to self-heal. The article authored by Gayla Berg Lyon et al. delves into the application of thiol-ene vitrimers in nanoimprint lithography (NIL) to produce surface features. The thiol-ene reaction was employed to produce photocurable vitrimers that demonstrate stress relaxation and flow behavior at elevated temperatures. TBD, known for its excellent transesterification catalytic properties, has also been discovered to be highly compatible with thiol-ene formulations. It has been observed that TBD does not induce premature gelation in the absence of light and does not hinder the reaction from achieving complete conversion rapidly upon exposure to light. The stress relaxation behavior of TBD follows an Arrhenius dependence within the temperature range of 145 to 175 °C. The analysis of $\ln(\tau^*)$ versus inverse temperature relationship data shows a consistent linear trend (with an average R_2 value of 0.999), indicating an apparent activation energy of 51 ± 3 kJ/mol. It is evident that the relaxation was influenced by the rate of bond reshuffling reactions [323]. The study conducted by Breuillac et al. focused on polybutadiene vitrimers that utilize dioxaborolane chemistry and dual networks comprising both static and dynamic cross-links. The objective of the research was to develop reprocessable elastomers with enhanced creep resistance through the incorporation of dual networks that consist of both dynamic and static cross-links. The initial relaxation process observed in vitrimers pertains to the relaxation of unattached chains and chain segments located between cross-links. Subsequently, the second relaxation process, which enables comprehensive stress relaxation, takes place via the exchange of covalent bonds between the dioxaborolane cross-links. The relaxation times demonstrated a temperature dependence similar to Arrhenius behavior, where higher temperatures led to faster relaxation and a lower activation energy. This resulted in relaxation times of 815 and 142 seconds at 100 and 160 degrees Celsius, respectively. Furthermore, the zero-shear viscosities of the vitrimers were determined, revealing a positive correlation with the degree of cross-linking and a measured viscosity activation energy of 32.5 kJ/mol [324].

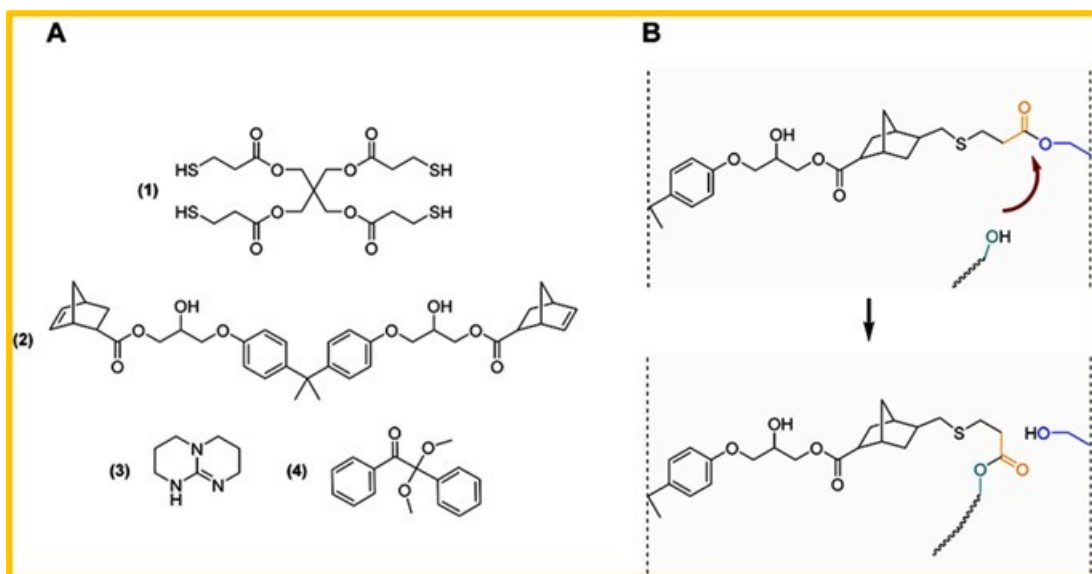


Figure 22. Dynamic Thiol-Ene reactions of Vitrimers [323].

1.13 RESEARCH QUESTION OF YOUR THESIS

How can the utilization of biodegradable thermosets and vitrimers, which are derived from renewable resources, contribute to a sustainable and environmentally conscious transition away from conventional plastics?

Chapter 2 of this thesis focuses on the synthesis and characteristics of naturally foamed composites derived from soybean oil and agricultural waste. The main aim is to offer an environmentally friendly substitute for Styrofoam™. The study involves the utilization of significant amounts of agricultural waste and the curing of bio-based thermosets at low temperatures, with the aim of investigating the ecological and economic benefits associated with this method. Furthermore, there is a strong emphasis on the engineered biodegradability of these composites in marine environments in order to address concerns regarding the long-term accumulation of plastic waste.

Chapter 3 of this thesis introduces a novel vitrimer material that is composed of renewable resources, including epoxidized soybean oil, vanillin, biobased diamine Priamine, and oleic acid. In accordance with the principles of green chemistry, this vitrimer demonstrates notable attributes of flexibility and stretchability, thereby highlighting its potential as a viable and environmentally conscious alternative to plastics derived from fossil fuels. The examination of vitrimers' recycling and reprocessing capabilities, as well as their remarkable barrier characteristics and limited

migration into food simulants, underscores their appropriateness for use in flexible food packaging. Additionally, the study acknowledges the end-of-life scenario of vitrimers, emphasizing their capacity to undergo biodegradation in seawater.

In essence, this thesis aims to develop a thorough comprehension of the potential of biodegradable composites and vitrimers in mitigating the environmental consequences linked to plastic-based products. The objective of this research is to establish connections between the fields of material science and environmental sustainability by examining the properties, synthesis methods, and applications of various materials. The ultimate goal is to offer viable alternatives for a range of applications, such as packaging and marine conservation.

Chapter 2: Biobased thermoset derived from epoxidized soybean oil and agri-waste as a sustainable alternative to Styrofoam

Abstract

Styrofoam™ is a commonly used petroleum-based material that is widely employed in lightweight and protective packaging systems. On the other hand, Styrofoam™ is manufactured using petroleum resources that are not renewable. It is also non-biodegradable and cannot be recycled in most existing recycling facilities. Additionally, it has the potential to cause chronic, low-level migration of styrene into food. To deal with the environmental pollution concerns, to move away from fossil resources, we propose a fully biobased, biodegradable, and naturally foamed soybean oil-based composites containing high amounts of agri-waste.

Bio-based thermosets were synthesized by cross-linking epoxidized soybean oil (ESO) with pripol 1040, a fatty acid trimer. Thanks to the liquid cross-linker, curing of the composites can be performed at relatively low temperature of 80 °C, in the presence of agri-waste, like carrot residue after juice extraction, without degrading them. To give a second life to agri-waste in added-value products, up to 50 % by wt. of vegetable powder was incorporated into the ESO-Pripol Oil thermoset, which in addition improved tensile and compression strength as well. Moreover, moisture present in the agri-waste evaporates during the curing process creating gas bubbles and providing a natural way of foaming. Fully biobased foams could provide a good level of a good level of thermal insulation and mechanical resistance. Finally, the composites are biodegradable in marine environments preventing their long-term bioaccumulation in the ecosystem.

2.1 OVERVIEW

The use of fossil materials, particularly plastics derived from petroleum, has led to significant environmental issues due to their non-biodegradability and contribution to pollution [47]. It is estimated that the production of plastics may reach over 1,100

million metric tons by 2050 [49], exacerbating the problem of plastic waste in the environment and oceans [325]. In response to these challenges, there is a growing interest in developing biobased materials as alternatives to fossil plastics [326]. Bioplastics, derived from renewable biological sources, have gained attention for their potential to reduce reliance on non-renewable resources and mitigate plastic pollution. The capacity for bioplastic production is expected to increase significantly in the coming years, with several commercially available bioplastics offering advantages such as biodegradability and lower carbon footprint [231]. However, the biodegradation of bioplastics is influenced by environmental factors, and there is a need for materials that can biodegrade in natural environments.

There were no articles that directly performed the life cycle assessment (LCA) analysis on the manufactured materials that were investigated in this study or on their usage as foam. Therefore, it is crucial to prioritize studying the LCA analysis on these materials in the future. Nevertheless, the study conducted by Xin Huang explores the utilization of bio-based epoxidized soybean oil (ESO) vitrimer in combination with reclaimed glass fiber fabric (RGFF) to create a uniform and compact cartilage-like interwoven structure. The life-cycle assessment (LCA) of ESO/RGFF composites-based triboelectric nanogenerators (TENG) demonstrates a 44%–49% decrease in carbon footprint when compared to fully petrochemical-based materials, highlighting the environmental benefits of this upcycling approach that combines plastic wastes with biomass [240]. Furthermore, the life cycle assessment (LCA) study conducted on ESS resin and ESS-based biocomposites compared to BPA-based composites revealed significant insights into the environmental impacts of these materials (Ghasemi et al., 2020). The study identified hotspots in the production process, highlighting the contributions of vegetable oil methyl ester and hydrogen peroxide to various environmental impact categories. The bio-based resin demonstrated an overall reduction in environmental footprint compared to petroleum-based resin, except in the eutrophication and carcinogenic impact categories [242]. Overall, these studies illustrate the importance of conducting LCAs to guide sustainable material development and decision-making processes by providing insights into the environmental impacts of various materials and processes. This suggests that there's a good chance that if similar analyses were conducted for materials in this study, we might also observe a reduction in carbon footprint.

Epoxy resins, widely used in various applications, are non-biodegradable and non-recyclable, posing challenges for their end-of-life disposal. To address this issue, there is a growing interest in developing environmentally-friendly epoxy resins using biobased building blocks. Epoxidized soybean oil (ESO) has emerged as a promising bio-derived material for producing eco-friendly epoxy resins due to its high reactivity, cost-effectiveness, and non-toxic nature [326]. In our work we will show how the use of a biobased crosslinker allowed the synthesis of a 100% biobased thermoset that can be cured at a relatively low temperature, 80 °C, requiring less energy for its processing. Additionally, in this work, we will show that it is possible to create a composite of the crosslinked oils capable of incorporating a significant proportion (up to 50%) of agri-waste powders. This biobased composite showed higher mechanical properties than the pure oil samples. The resulting the composites are designed to be biodegradable in marine environments, which prevents them from accumulating in the ecosystem over the long term. Finally in this work we explored a new possibility given by the incorporation of vegetable biomass: the possibility to induce a degree of foaming into the material. This new option emerges from the combination of having a low temperature for crosslinking and the possibility to leverage moisture absorption given by vegetable biomass. The foaming reduces the overall density of the composite by an order of magnitude, opening new possibilities for their use as sustainable replacements of fossil foam packaging. The article "New bio-based epoxy materials and foams from microalgal oil" by Négrell et al. (2016) explores the utilization of epoxidized algal oil (EAO) with priamine® as the hardener. Although they produce bio-based epoxy materials and foams but they use Poly(methylhydrogenosiloxane) or MH15 as a blowing agent [327]. The study by Altuna et al. (2015) focuses on the mechanical and thermal characterization of biobased thermosetting epoxy foams. The researchers created foams from epoxidized soybean oil with varying amounts of sodium bicarbonate foaming agent, leading to foam densities between 0.16 to 0.55 g/cm³ [328]. Pradeep et al. (2022) investigated the influence of silane-treated pine wood fiber (PWF) on the thermal and mechanical properties of partially biobased composite foams. To prepare the PWF-filled, epoxy foam and epoxidized pine oil were mixed with polyacrylates-modified polyamines as a hardener and Polymethylhydrosiloxane (PMHS) as a foaming agent [329]. The study by Bonnaillie & Wool (2007) introduces a resilient thermosetting foam system with a high bio-based content derived from acrylated epoxidized soybean oil (AESO) and utilized carbon dioxide as a foaming

agent. Finally, the researchers were able to obtain cell sizes that were greater than 1 mm [330]. The study by Mazzon et al. (2015) specifically addresses the development of lightweight, rigid foams for automotive applications by utilizing highly reactive epoxy resins made from vegetable oil-based epoxy foam and incorporating sodium bicarbonate as a reactive foaming agent [331]. Khundamri et al. (2019) present the synthesis of foam from epoxidized soybean oil-based epoxy foam and epoxidized mangosteen tannin (EMT) with methyltetrahydrophthalic anhydride (MTHPA) as a hardener. In addition, azodicarbonamide and zinc oxide were used as a blowing agent and an activator, respectively. All epoxy foam samples showed subzero T_g (-6.5 to -5.4 °C) and semi-closed cells with irregular shapes [332]. In the study conducted by (Huang et al., 2019), the researchers focused on the development of bio-based thermosetting epoxy foams utilizing epoxidized soybean oil (ESO) and fumaropimaric acid (FPA) as the curing agent. The formulation was further compounded with N,N-Dimethylbenzylamine (BDMA) as the catalyst and sodium bicarbonate (NaHCO₃) as the foaming agent. The mixture was heated in an oven at 140 °C to facilitate the foaming process. The resulting materials exhibit a balance of rigidity and flexibility, making them suitable for diverse applications where both strength and resilience are required [333]. As these studies have shown, the majority of bio-sourced epoxies foams require a chemical foaming agent (CFA). In contrast, our bio-based thermosets with vegetable powder (40, 50, and 60%) do not require CFA because the moisture in the agri-waste evaporates during the curing process, generating gas bubbles and providing a natural method of foaming.

Overall, this approach offers several benefits, such as low-temperature curing, improved mechanical properties, and biodegradability in marine environments, making it an environmentally friendly and sustainable solution.

2.2 RESULTS AND DISCUSSION

2.2.1 Synthesis

The primary objective of this work is to develop biobased alternatives to thermosets that are in accordance with the principles of green chemistry. To achieve this objective, we have combined epoxidized soybean oil (ESO) with Pripol 1040, which is a biobased building block obtained through the condensation of fatty acids. Pripol 1040 acted as the cross-linker or curing agent by reacting with the epoxy rings, resulting in

the effective crosslinking of ESO and transforming it into a fully biobased thermoset material (as shown in **Figure 23a**). Due to the liquid state of both ESO and Pripol 1040 at room temperature, one advantage of using them is the simple nature of mixing the two substances to form a homogeneous reaction mixture without requiring any extra solvents. Curing could be achieved by heating the solution of the two oils at 80°C for 10 days. This process ensured thorough cross-linking, which strengthened the overall structure of the thermoset material. The crosslinking occurs because of the reaction between the carboxyl groups of Pripol and the epoxy groups of ESO, resulting in the opening of the epoxy ring and the formation of a new ester bond. We used Fourier-transform infrared spectroscopy (FTIR) to confirm the success of the cross-linking process and evaluate the degree of conversion. The FTIR analysis showed that the reaction results in a decrease of the intensity of the peaks at 822 cm^{-1} related to the epoxy rings, in ESO, and at 1705 cm^{-1} related to carboxylic groups, in Pripol 1040, consequently, the intensity of the peak at 1738 cm^{-1} , associated with the ester groups, increased as reported in (**Figure 23b**).

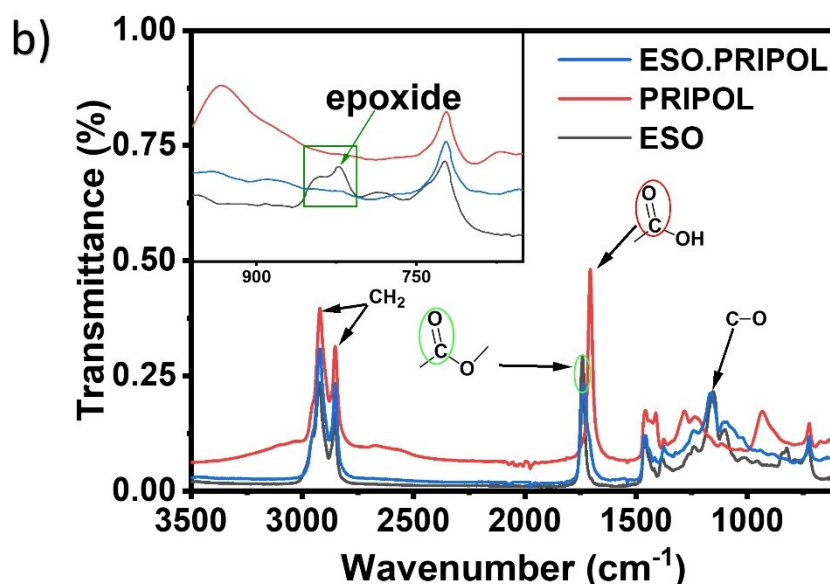
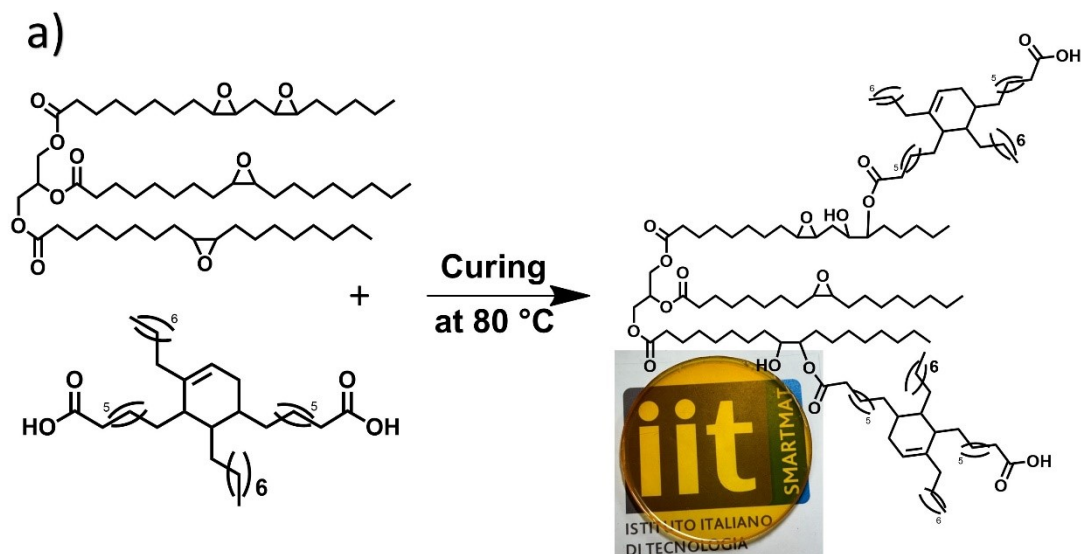


Figure 23. a) Schematic representation of the chemical synthesis of ESO & pripol via a thiol-epoxy coupling and a picture of a transparent thermoset Oil thermoset film, b) FT-IR spectra of ESO & pripol.

2.2.2 Gel fraction:

During the material synthesis, two catalysts were examined in order to decrease the curing time while maintaining a substantial degree of crosslinking. The two catalysts N, N-1,1,3,3 Tetramethylguanidine (TMG) and 1-Ethylimidazole (1-EI) were chosen for their ability to speed up the opening of the epoxy ring, they exhibit a high selectivity in reducing by products and side reactions [334, 335]. and have lower toxicity profiles compared to N,N Diisopropylethylamine (DIPEA) and 1,8-Diazabicyclo(5.4.0)undec-

7-ene (DBU) [336]. Furthermore, TMG and 1-EI stand out for their cost-effectiveness when compared to other catalysts. For instance, the price of 100ml of TMG is 61€, whereas 100g of N,N Diisopropylethylamine (DIPEA) costs 150, 00 €. Additionally, their stability and long-lasting properties facilitate convenient storage and handling. In order to determine the ideal curing time, various samples consisting of the oil mixture with 0.5%,1%,1.5%,2% of TMG or 1-EI catalysts, as well as a control sample in which no catalyst was added, were cured at 80 degrees Celsius for varying amounts of time, ranging from 1 day to 3 days (**Figure 24a**). During each curing time that was evaluated, the control sample remained liquid, whereas the samples that included TMG and 1-EI transformed into solid materials. The gel fraction of the material was utilized to evaluate the crosslinking kinetics. Throughout all the time points, the sample that was cured without a catalyst dissolved completely in ethyl acetate (gel fraction close to 0%), suggesting minimal cross-linking. Contrastingly, the samples treated with 1-EI and TMG exhibited significant levels of crosslinking, with gel fractions reaching an impressive 95% and 96%, respectively after 24 hours (**Figure 24b-c**).

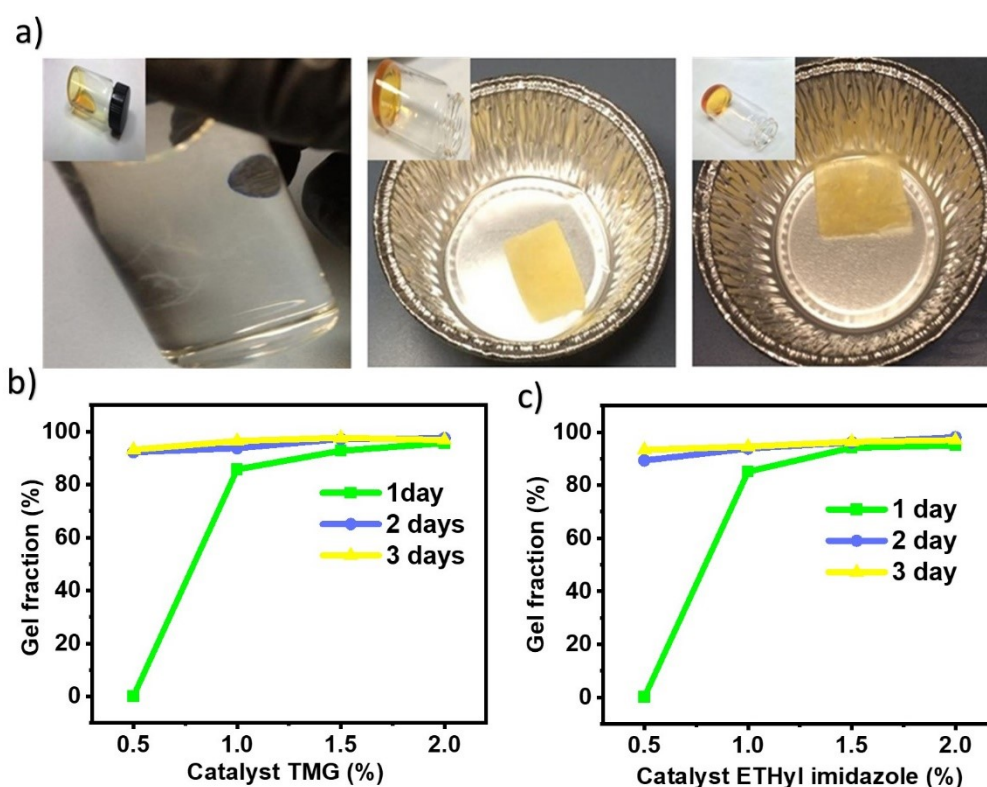


Figure 24 . Gel fraction of the oil thermoset was cured at 80 °C on various days using different catalysts, a) drying under the hood at 100°C. b) Representative gel fraction curves of the oil thermoset by the catalyst, N, N-1,1,3,3

Tetramethylguanidine (TMG) after the ethyl acetate was removed, c) Representative gel fraction curves of the oil thermoset by the catalyst, 1-Ethylimidazole (1-EI) after the ethyl acetate was removed.

2.2.3 Environmentally Friendly Synthesis of composites:

In order to reduce the overall cost and potentially enhance biodegradability, we conducted experiments in which we incorporated varying quantities of vegetable by products into the material. We selected a powder of carrot because carrot powder contains various bioactive compounds such as phenolics, carotenoids, polyacetylenes, and ascorbic acid [337] with different functional groups on its surface, including carboxyl and hydroxyl, that can participate in crosslinking reactions with the matrix material. These groups can undergo condensation reactions with functional groups in the matrix, such as hydroxyl or amino groups, leading to the formation of covalent bonds. This enhances the interfacial adhesion between the carrot powder and the matrix, improving the composite's oxidative stability, mechanical strength, and durability. The composition of the carrot powder was analyzed by Giovanni Perotto, et al in paper titled "Bioplastics from vegetable waste via an eco-friendly water-based process." The results of the composition in this study align with their findings [338] (**Figure 25a**). Powder of carrot pomace that was ground and had been sieved using a sieve with a 50-micron (**Figure 25 b,c,d**). Different amounts of powder (40-50-60% in comparison to the final weight ratios of the composite) were combined with ESO and Pripol Prior to curing (**Table 1**). In the end, the composite material was poured into a Teflon mold and then cured in an oven at 80 °C for a duration of 10 days, without the use of a catalyst. As mentioned, the curing time for the sample with the vegetable powder was the same as the sample without it. The scanning electron microscopy (SEM) images demonstrate that the oil thermoset and carrot powder were blended together seamlessly, creating a homogeneous reaction mixture without the need for any solvents. Additionally, there were no signs of powder aggregation within the composites. However, it is important to mention that increasing the amount of carrot powder in the composite resulted in a significantly rougher surface of the samples. Furthermore, the analysis of the cross-section confirms that the vegetable has been uniformly incorporated into the material. (**Figure 26**).

Table 1. Formulations of different samples

| Sample name | Epoxidize soybean oil [g] | Pripol 1040 [g] | Carrot powder [g] | ESO –Pripol [%] | Carrot powder [%] | Curing temperature [°C] |
|-----------------------|---------------------------|-----------------|-------------------|-----------------|-------------------|-------------------------|
| ESO-Pripol-Carrot 0% | 4.53 | 5.47 | 0 | 100 | 0 | 80 |
| ESO-Pripol-Carrot 40% | 2.66 | 3.34 | 4 | 60 | 40 | 80 |
| ESO-Pripol-Carrot 50% | 2.21 | 2.79 | 5 | 50 | 50 | 80 |
| ESO-Pripol-Carrot 60% | 1.77 | 2.23 | 6 | 40 | 60 | 80 |

a)

| | Cellulose (mol%) | Pectin (mol%) | Hemicellulose (mol%) | Aliphatic polyesters (C16) (mol%) |
|-------------|---------------------|------------------|-------------------------|--|
| Carrot | 61 | 28 | 8 | 3 |
| Parsley | 48 | 31 | 15 | 6 |
| Radicchio | 44 | 34 | 4 | 18 |
| Cauliflower | 46 | 24 | 9 | 21 |

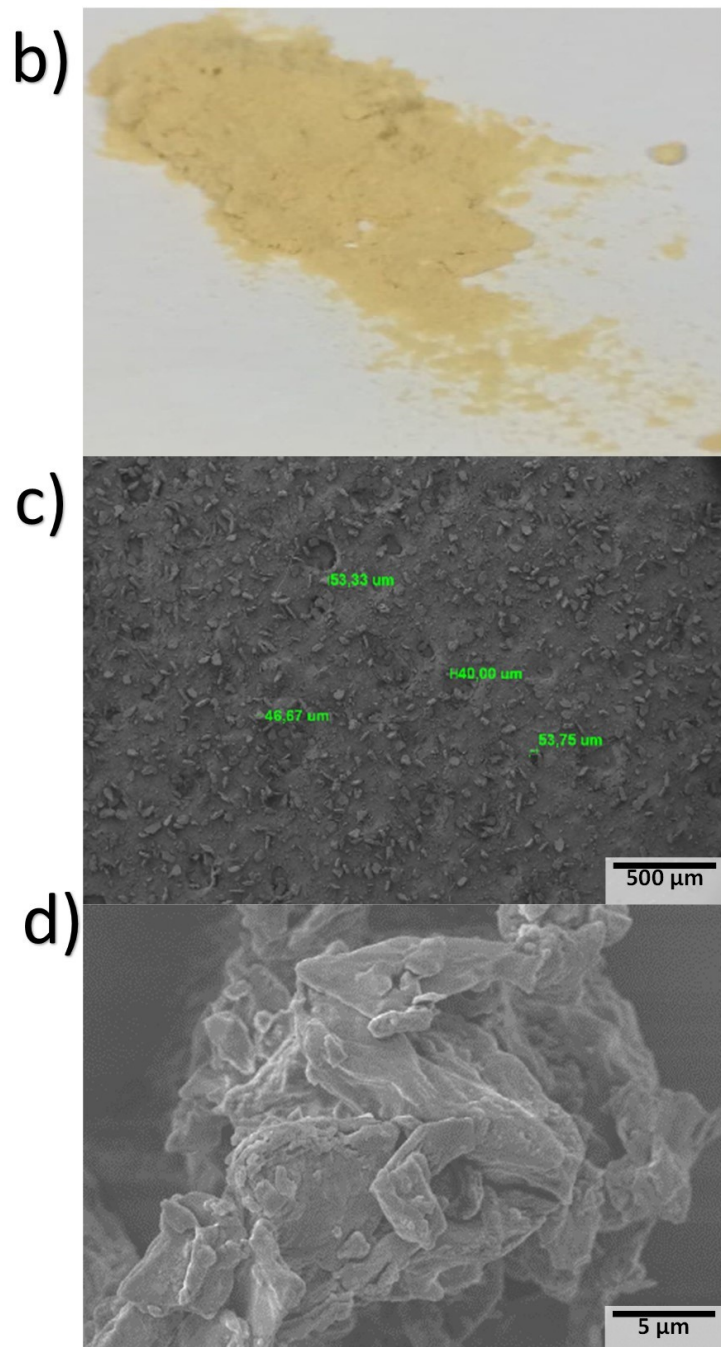


Figure 25. a) Composition of the carrot powder, Carrot powder with 50 η m mesh. b) Digital images of carrot powder, c) Magnified top view of carrot powder waste, d) Magnified top view of a single piece of carrot waste.

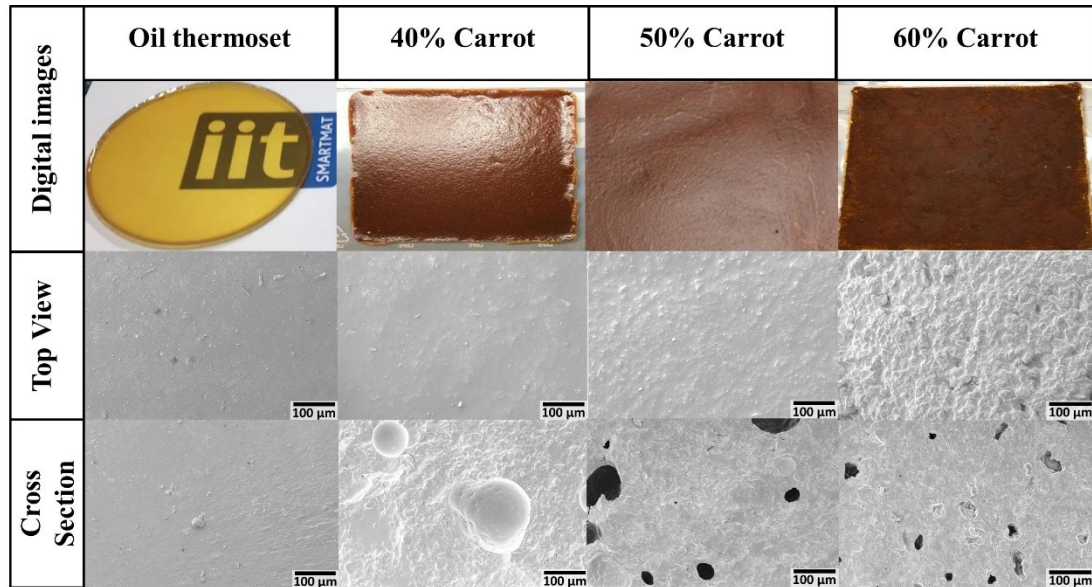


Figure 26. a) Carrot powder with 50 η m mesh, b) Epoxidized Soybean Oil, c) Pripol, d) Synthesis of composites by several amounts of carrot powder (40-50-60 %) with ESO and Pripol (oil thermoset).

The addition of vegetable powder provides a new opportunity for this material: the potential to generate foam in the composite by utilizing the moisture absorbed in the vegetable powder, which can be released as vapor during the curing process and form bubbles within the solid material. The moisture absorption of carrot powder was measured by subjecting it to a controlled environment with 100% humidity for a period of 14 days. Carrot pomace experienced a 13.5% increase in water absorption after one day, which further increased to approximately 40% after 10 days (**Figure 27a**). **Figure 27b** displays oil thermoset and oil-based thermosets that were synthesized with 40% carrot powder. These samples were tested without conditioning in high humidity (oil-vegetables composite) and after being conditioned for 1 day and 10 days (oil-vegetable foam). The samples were cured at 80 ° C for 10 days. The water absorption results in an increase in the porosity of the sample, as evident from both the macroscopic morphology and microstructure. The SEM images provide a clear visual representation

of the water absorption by the vegetable powder. This absorption leads to the formation of voids within the materials, as seen in (Figure 27b).

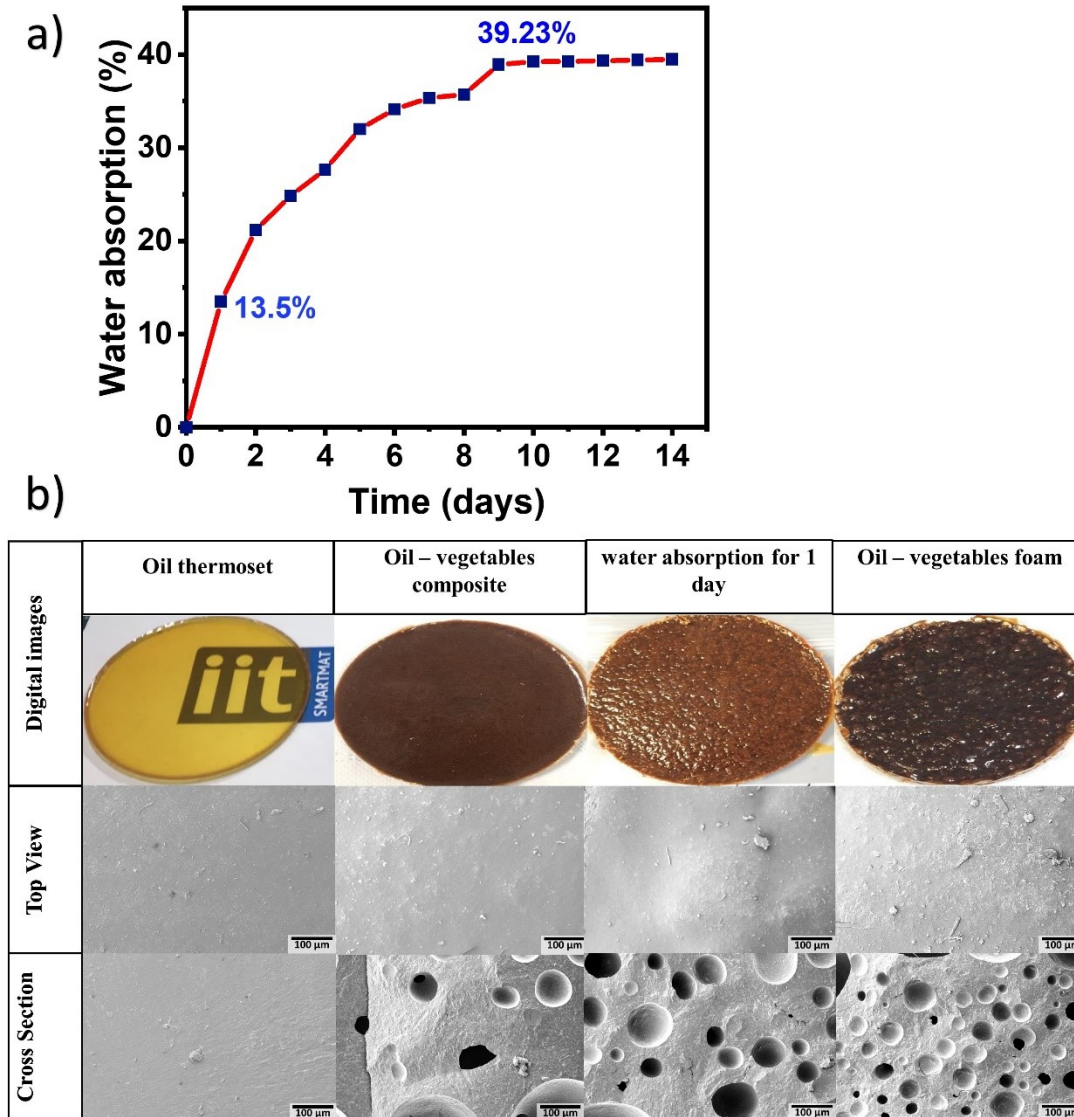


Figure 27. a) Kinetics of water absorption by carrot waste. b) Synthesis of composites containing different amounts of water absorption by 40% carrot waste with ESO and Pripol (Oil thermoset).

2.2.4 Mechanical Property:

Density is a measure of the overall density of a substance, expressed as the ratio of mass to volume. As shown in the data reported in (Figure 28), the oil thermoset showed a density of $0.985 \pm 0.010 \text{ g/cm}^3$, testifying the homogeneous and dense nature

of the material (density of epoxidized soybean oil equal 0.994 g/cm^3 and density of Pripol™ 1040 equal 1.0 g/cm^3). The incorporation of carrot powder slightly reduced the density to $0.965 \pm 0.012 \text{ g/cm}^3$. Foaming of the sample, taking advantage of the water absorption, significantly decreased the density of the material down to $0.664 \pm 0.012 \text{ g/cm}^3$. Compared to the density of styrofoam, that was measured to be $0.031 \pm 0.002 \text{ g/cm}^3$, and that of PU foams (0.015 g/cm^3) [339], the density of our material is higher, probably because of the poorer foaming effect of water in these conditions or the reduced retention of water vapor during the initial phases of crosslinking. The skeletal density measurements revealed that the oil thermoset has a density of $0.9925 \pm 0.0002 \text{ g/cm}^3$, while the oil-vegetable composite exhibited a density of $1.0226 \pm 0.0002 \text{ g/cm}^3$ (carrot powder: $1.5024 \pm 0.0005 \text{ g/cm}^3$), and the oil-vegetable foam had a density of $0.9512 \pm 0.0003 \text{ g/cm}^3$. The discrepancy in density measurements for the oil thermoset and oil-vegetable composite samples can be explained. The distinction between the absolute and skeletal density of the oil-vegetable foam can be elucidated by considering the permeability of helium within the material, which is influenced by the presence of open pores, resulting in a higher overall density. During the measurement of skeletal density, it is important to consider the presence of open pores. These pores can be filled with helium, resulting in a decrease in the effective volume of the skeletal structure. Consequently, the skeletal density is boosted as the mass remains steady while the volume decreases due to the presence of helium in the voids. For instance, the skeletal density of the styrofoam is $0.134 \pm 0.005 \text{ g/cm}^3$.

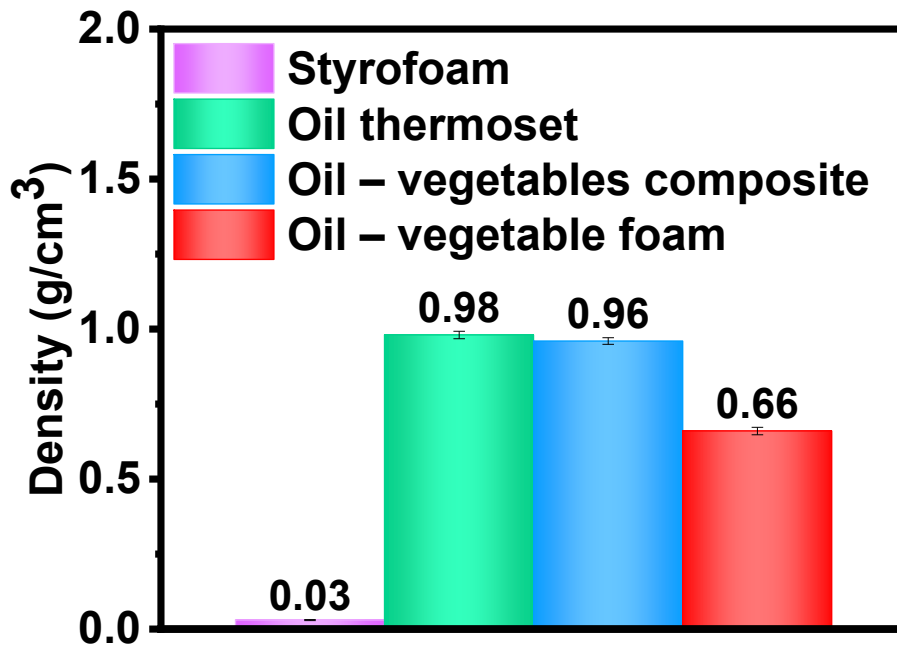


Figure 28. Density test curves of samples by 40% carrot waste with ESO and Pripol (Oil thermoset).

The foam generated as a result of water absorption and desorption has the potential to offer a certain level of thermal insulation. According to the data presented in (Figure 29), the thermal conductivity of the sample was reduced according to the foaming: The sample that was exposed to moisture for a period of ten days showed notable improvements in foaming, reduced density, and enhanced thermal insulation. The thermal conductivity of the sample with the highest porosity was 0.12 (W/m K), which is one order of magnitude lower than the bulk sample's thermal conductivity of 1.2 (W/m K). Although the thermal conductivity of oil-vegetable foams remains four times higher than that of Styrofoam (0.033 W/m K), the method demonstrated in this study presents a hopeful and sustainable alternative to a completely biobased thermal insulation material. Oil-vegetable foam has superior thermal conductivity than perlite-based insulation materials, with values ranging from 0.25 W/m K to 0.42 W/m.K[340, 341] and cellulose 0.15 W/m K to 0.25 W/m K [342]. Despite the fact that oil-vegetable foam is not preferable to polyurethane, it is important to note that PU foams are not made from biobased materials [342]. Another advantage of this method is its simplicity, as it does not involve the use of high-temperature or supercritical CO₂, which is employed in bioplastics such as PLA [343].

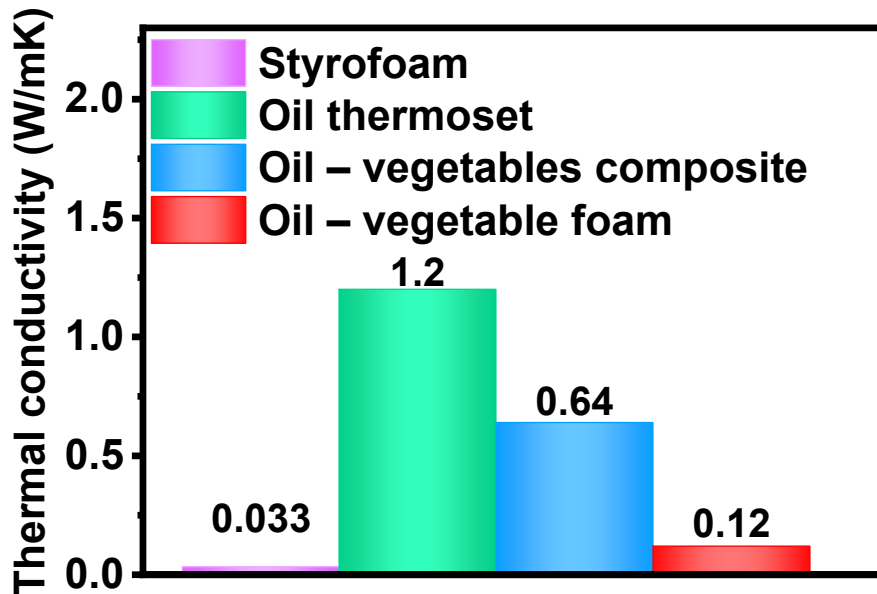


Figure 29. Thermal conductivity test curves of samples by 40% carrot waste with ESO and Pripol (Oil thermoset).

Figure 30 illustrates the outcomes of a tensile test conducted on oil-vegetable samples with varying quantities of vegetable powder. The thermoset, when not mixed with any vegetable material, exhibited a low rigidity of 0.14 ± 0.07 MPa and a significant elongation at break of $40.46 \pm 4\%$. An appreciable enhancement in tensile stress was seen when carrot powder was added to the oil thermoset. The improvement can be attributed to the effective interaction between the Oil thermoset and filler, likely due to the presence of different functional groups on the surface of the carrots, such as carboxyl and hydroxyl groups. These groups actively interact with the Oil thermoset and enhance its reinforcing properties. It is possible to hypothesize that these functionalities located on the surface of the filler material can contribute to the formation of the network. When there is no interaction between the Oil thermoset and the filler, incorporating a high percentage of filler results in a drop in elongation at break without an increase in stiffness. The findings of our study on the oil-vegetable thermoset indicate that the thermoset composite may accommodate a maximum of 50% carrot powder without compromising its strong mechanical capabilities. It is worth mentioning that the material exhibits excellent performance under such a high concentration of vegetable powder. This phenomenon is typically not observed in

thermoplastics, but it has been demonstrated in non-biobased thermosets such as silicone-starch and silicone-beetroot bio elastomer composites. This behaviour is attributed to a strong interaction between the silicone and the functional groups present in biomass [344, 345].

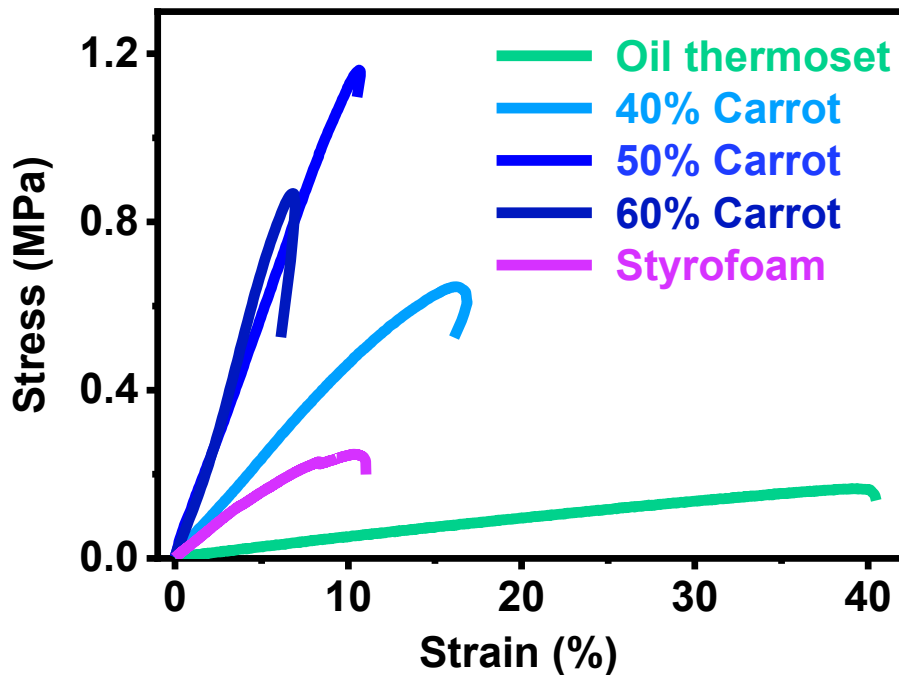


Figure 30. Representative tensile test curves of composite with several amounts of carrot powder (40-50-60 %) with ESO and Pripol (Oil thermoset).

The findings of compression tests that were carried out on oil thermosets, thermosets that contained forty percent carrot pomace, and biobased foam that was created with forty percent carrot pomace and was subjected to an atmosphere with one hundred percent humidity for ten days (Foam Composite) are displayed in (Figure 31a). In the same manner as what was observed in the tensile test, the oil thermoset exhibited a lesser compression modulus in comparison to the oil-vegetable thermoset, which demonstrated the greatest compression modulus of 0.99 ± 0.06 MPa. As anticipated, the oil-vegetable foam demonstrated a superior level of flexibility, and it is worth mentioning that it effortlessly returned to its initial state once the pressure was released. This was not observed in the other samples, including styrofoam (Figure 31b), which suffered permanent damage during testing and did not recover their

original form. These findings emphasize the benefits of incorporating carrot powder into thermoset composites, improving their foaming properties and flexibility.

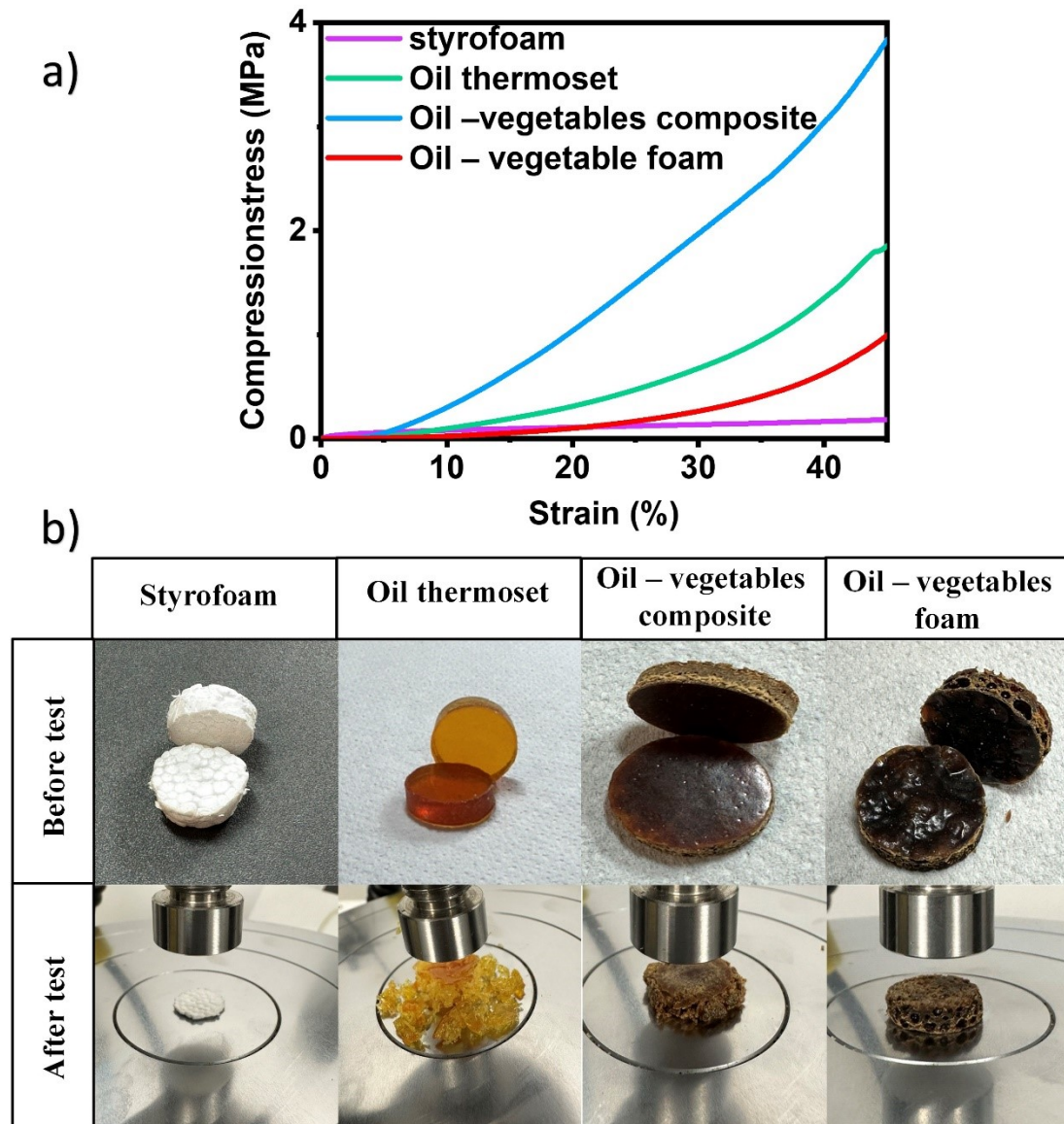


Figure 31, a) Representative compression test curves of samples by 40% carrot waste with ESO and Pripol (Oil thermoset). b) Flexibility before and after compression tests.

2.2.5 Biodegradability:

The composite prepared in this project underwent testing to determine its biodegradability in marine environments. This environment is characterized by a slow biodegradation kinetic, primarily due to the limited amount of mechanical stress and the presence of microorganisms[346]. The biodegradability of the oil-vegetable composites material exhibited a faster rate compared to the oil-thermoset. It displayed

a kinetic profile similar to that of microcrystalline cellulose. This outcome can be attributed to the inclusion of carrot powder, which undergoes biodegradation at a more rapid rate. Interestingly, both the carrot powder and oil – vegetables composite showed rapid biodegradation within a short span of 2-3 days, whereas the Oil thermoset took approximately 30 days to show signs of biodegradation. After a period of 30 days, the BOD values for the oil-vegetable thermoset and carrot powder were 33.05 mg O₂/100 mg material and 63 mg O₂/100 mg material, respectively, compared to those of the oil thermoset and microcrystalline cellulose. Despite having a slower degradation kinetic, the oil thermoset, which includes the oil-vegetable composite, exhibited a gradual indication of biodegradation. In contrast, several biodegradable bioplastics, such as PLA, are known to be non-biodegradable in marine environments[347].

This discovery displays the feasibility of producing biodegradable thermosets using vegetable oils as the biobased source. Additionally, the incorporation of prepolymer dynamic cross-links greatly enhances the material's biodegradability in comparison to conventional Styrofoam (Figure 32).

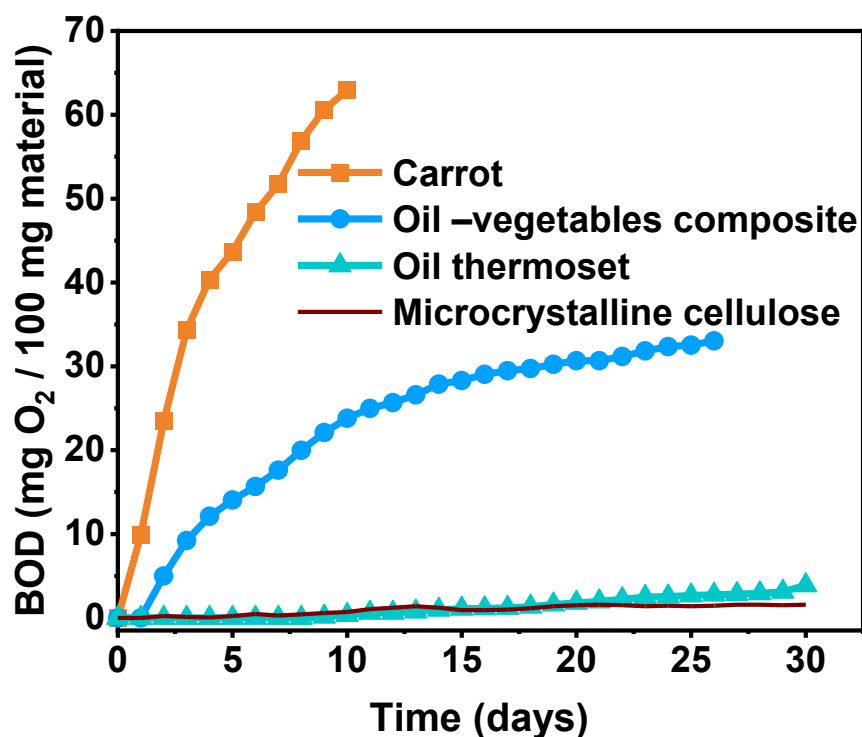


Figure 32. Representative Biodegradation test curves of composite.

2.3 CONCLUSIONS

This study presents the synthesis of a newly produced thermoset material that was exclusively derived from bio-based constituents, and that can be foamed using only moisture as the foaming agent. Therefore, in order to achieve this goal, soybean oil (ESO) was cross-linked with the oil-based building block Pripol by taking advantage of the reaction that occurred between the epoxy group of ESO and the carboxyl groups of Pripol. Several amounts of carrot powder, up to 60%, were effectively integrated into the material. All synthesis can be conducted in bulk without the requirement for extra solvents, following the principles of green chemistry. Significant quantities of carrot pomace could be added without changing the material's properties and improving the mechanical characteristics of the final product. Compared to the previous literature reported, the "New bio-based epoxy materials and foams from microalgal oil" by Négrell et al. (2016) uses Poly(methyl hydrogen siloxane) or MH15 as a blowing agent [327]. The study by Bonnaillie & Wool (2007) introduces a resilient thermosetting foam system with a high bio-based content derived from acrylated epoxidized soybean oil (AESO) and utilized carbon dioxide as a foaming agent and mechanical properties displayed promise, with a compressive strength of approximately 1 MPa.[330]. Khundamri et al. (2019) present the synthesis of foam from epoxidized soybean oil-based epoxy foam and epoxidized mangosteen tannin (EMT) with methyltetrahydrophthalic anhydride (MTHPA) as a hardener. Also azodicarbonamide and zinc oxide were used as a blowing agent and an activator, respectively [332]. In the study conducted by (Huang et al., 2019), the researchers focused on the development of bio-based thermosetting epoxy foams utilizing epoxidized soybean oil (ESO) and fumaropimaric acid (FPA) as the curing agent. The formulation was further compounded with N,N-Dimethylbenzylamine (BDMA) as the catalyst and sodium bicarbonate (NaHCO₃) as the foaming agent. The results indicate that the presence of rosin hydrogen phenanthrene ring structure has a positive impact on enhancing the glass transition temperature and mechanical properties of thermosets and the thermosetting epoxy foams demonstrated remarkable thermal stability, exhibiting a density ranging from 361 to 231 kg.m⁻³.[333]. Altuna et al. described the synthesis of syntactic foams using epoxy copolymers derived from ESO, which exhibited satisfactory compressive and flexural properties [348]. In addition, there have been reports on the production of thermosetting epoxy foams with varying

apparent density, utilizing ESO and methyl tetrahydrophthalic anhydride (MTHPA) as the main components [328]. As these studies have shown, the majority of bio-sourced epoxies foams require a chemical foaming agent (CFA) and includes a mix of non-renewable resources. In this study, by utilizing the vegetable biomass's moisture absorption capability, it is possible to create fully biobased foams without requiring post-processing or the use of supercritical CO₂. Despite the fact that the new biobased materials have a higher density than fossil PS foams, the thermal conductivity of the new biobased materials presented here was in a similar order of magnitude, which is in line with the state-of-the-art biobased alternatives, but at the same time with significantly more benign biodegradation profile. Another noteworthy observation was made regarding the foam composite's ability to exhibit elastic behavior following compression testing, with the foam composite having the ability to return to its original state once the pressure was relieved, a property that was absent in both the control specimens and styrofoam. One more benefit of the composites was their ability to biodegrade in seawater, where carrot pomace enhances the biodegradation kinetic. This material shows a promising blend of foaming, mechanical properties, thermal insulation, and safe biodegradation, positioning it as a strong biobased alternative to fossil materials.

2.4 EXPERIMENTAL SECTION

2.4.1 Materials:

Epoxidized Soybean Oil (ESO) with an average molecular weight of 950 g/mol and 4 epoxide groups per molecule was kindly provided by ATP r&d SRL (Italy), Pripol 1040 – trimer acid obtained by trimerization of unsaturated fatty acids from vegetable oils with an average molecular weight of 830 g/mol and 2.78 carboxylic acid groups per molecule was provided by CRODA (United Kingdom). Carrot powder was provided by HARMS FOOD GMBH (Zeven, Germany). N, N-1, 1, 3, 3 Tetramethylguanidine (TMG), 1-Ethylimidazole (1-EI) and ethyl acetate were purchased from Merck, and all of which were utilized in the form in which they were obtained.

2.4.2 Typical procedure for composites preparation:

To make composites, the process entails mixing an ESO and Pripol cross-linker in a glass vial connected with a magnetic stirrer. The ratio of ESO to Pripol cross-linker

used is 4:2.78. Due to the liquid state of both ESO and Pripol at room temperature, they can be readily blended to create a uniform reaction mixture without the need for solvents. Approximately 50% of carrot powder was added to the ESO-PRIPOL oil thermoset. The vegetable waste was initially pulverized using a blender for a duration of 20 minutes, followed by the process of sieving using a 50- μ m mesh sieve shaker to gather the resulting powder. The resultant powder is used with the ESO-Pripol combination to create the composite. Subsequently, the composite is poured into a Teflon mold and subjected to a curing process in an oven at a temperature of 80 °C for a duration of 10 days. In order to decrease the duration of the curing process, two distinct catalysts, specifically N, N-1,1,3,3-Tetramethylguanidine (TMG) and 1-Ethylimidazole (1-EI), were subjected to testing. The catalyst is introduced into the blend of the two oils, and the substance is subjected to thermal treatment in the oven at a temperature of 80°C.

2.4.3 Measurements

FTIR

Infrared spectra were collected by using a single reflection attenuated total reflection (ATR) accessory (MIRacle ATR, PIKE Technologies) that was coupled to a Fourier transform infrared (FTIR) spectrometer (Bruker Vertex 70 V). All of the spectra were captured in a vacuum in the range of 4000–500 cm^{-1} with a resolution of 4 cm^{-1} , and a total of 64 scans were accumulated.

Mechanical properties

The mechanical properties of sample films were analysed using a dual-column Instron 3365 universal testing machine with a 10 N load cell and pneumatic clamps at room temperature. The samples used for the test were taken directly from cured materials and shaped like dumbbells, following the ISO 527-2 type 5A standard (dimensions of 2.5 mm x 3 mm x 2.5 mm). The experiment was conducted five times, with at least three measurements taken for each sample, and the data were averaged to determine the mean value. The samples were subjected to a tensile rate of 10 mm/min during testing.

Gel fraction

A 200 mg sample of the resultant substance was placed in a vial and combined with roughly 20 ml of ethyl acetate. The solution was allowed to stand for a duration of 24 hours, after which the ethyl acetate was extracted. The undissolved portion of the

substance was subjected to additional washing with ethyl acetate and subsequently dried in a fume hood at a temperature of 100°C for a duration of three days. Subsequently, the mass of the desiccated substance was determined. The gel fraction was determined using the following formula:

$$(W_2 / W_1) \times 100\% = \text{Gel fraction (or Cross-linked Material)}$$

Where: W1 represents the weight of the original specimen in grams, and W2 represents the weight of the dry material acquired after measurement.

Biochemical oxygen demand (BOD)

The experiment was conducted using seawater, which was placed in glass bottles and kept at room temperature. Every bottle was tightly sealed using an oxygen-measuring device called OxiTop. Additionally, a carbon dioxide scavenger was used to capture any carbon dioxide produced during the biodegradation process. The measurement of oxygen consumption involved observing the decrease in pressure resulting from the process. To account for any potential background oxygen consumption, we used reference samples of seawater that were free from any material. The findings were standardized based on the mass of the sample. The results were presented as the amount of oxygen consumed per 100mg of the sample, which offers valuable information about the material's biodegradability.

SEM

A scanning electron microscope (JEOL, JSM-6490LA) was employed in high vacuum mode, utilizing a tungsten thermionic electron source, to capture images of the microstructure of various materials. To improve the conductivity and imaging quality of the samples, a 10 nm thin layer of gold was applied using the JEOL auto fine coater model JFC-1600. Subsequently, the samples were examined under the scanning electron microscope (SEM) with an accelerating voltage of 5 kV.

Density

The symbol ρ is utilized to denote the absolute density, a term that refers to the mass per unit volume. In preparation for the test, the films were initially segmented into small circular sections measuring approximately 22 mm in diameter using scissors. Subsequently, the segmented film pieces were weighed. Subsequently, the volume was determined by employing a calliper. The experiment was repeated twice, with a minimum of five measurements recorded for each sample. The collected data was then averaged to calculate the mean value. The density of each individual piece is determined by utilizing the following formula.

$$\rho = m/v$$

Where: m is the weight of the original specimen in grams, and V is the volume.

Thermal conductivity

The thermal conductivity of thermostats and Styrofoam was assessed using the reclaimed transient plane source method. This method was implemented using the TCI Thermal Conductivity Analyzer, a tool that enables accurate measurement of thermal properties. The measuring instrument consists of a sensor, control electronics, and computer software. The MTPS sensor comprises a spiral-shaped heater/sensor element that is encased by a protector ring. The protector ring serves to enhance the heat transfer to the spiral-shaped structure, enabling a unidirectional flow of heat from the sensor to the material under examination. This effectively eliminates any thermal boundary effects. The study utilizes the MTPS method, which leverages advanced material and electronic technologies to achieve a precision level exceeding 5%. The MTPS measurements were performed under controlled temperature conditions.

Compression testing

To investigate the foam properties of thermosets through mechanical compression testing, Samples with a standardized size of 8mm were directly cut from cured materials. The compression tests were carried out at room temperature using an Instron 3366 testing machine equipped with a 10 N cell load, following the guidelines outlined in ASTM D3410. The compression rate was set to 1mm/min. This testing procedure was repeated 3 times, and each sample underwent a minimum of five measurements. The obtained results were averaged to obtain a representative value.

Chapter 3: Biobased and biodegradable imine vitrimers from epoxidized soybean oil as packaging

Abstract

A vitrimer with flexible and stretchable properties was successfully synthesized, using solely biobased building blocks and adhering to the principles of green chemistry. A composite material was developed utilizing epoxidized soybean oil (ESO), vanillin, the biobased diamine, Priamine[®], and oleic acid with the aim of providing an alternative to non-biodegradable packaging derived from fossil sources. The crosslinker was developed using Vanillin and Priamine[®] to effectively react with the epoxide groups of ESO. This synthesis method eliminates the requirement for solvents and does not produce any waste or by-products, making it a catalyst-free and environmentally friendly process. The inclusion of oleic acid was implemented in order to adjust the characteristics of the resulting material. This is due to the ability of oleic acid to react with ESO and regulate the crosslink density. The vitrimers synthesized in this study exhibited exceptional reprocessability and recyclability. They have the capacity to be shaped and exhibit strong adhesion to various surfaces. Furthermore, the materials demonstrated oxygen and water vapor barrier properties that are comparable to those of low-density polyethylene. Additionally, they exhibited minimal migration into food simulants, making them highly suitable for use in the flexible food and general packaging market. The vitrimers also demonstrated the ability to undergo biodegradation in seawater, offering a secure means of disposal in the event of improper handling.

3.1 OVERVIEW

The global production of plastics exceeds 450 million tonnes annually [208], with a significant portion used for packaging, contributing to over 140 million tonnes of plastic waste generated each year. The mismanagement of packaging waste, which makes up nearly 40% of municipal solid waste, has resulted in environmental pollution [209]. There is an increasing interest in using biobased, recyclable, and compostable materials for packaging purposes. The production capacity of biodegradable plastics made from renewable biomass sources is expected to double by 2027, indicating a growing interest in their development [349]. There is ongoing exploration of

commercially available compostable plastics like PBAT, PLA, and PBS, along with other biodegradable polymers [229]. However, the conditions necessary for composting these biodegradable plastics are frequently not present in the environment. As a result, pollution occurs, particularly in marine ecosystems. The utilization of vegetable oils as a renewable source for creating new materials shows great potential. However, the challenge lies in the formation of thermosets instead of thermoplastics. It's crucial to understand that merely considering the renewability and recyclability of the feedstock isn't enough to assert that your materials are a sustainable solution. Instead, it's important to also take into account the environmental impact of the precursor syntheses. While natural building blocks like diacids or polyols offer promise, some biobased synthons are still obtained through intricate syntheses that involve harmful or fossil-based reagents, leading to a considerable amount of waste being produced [271, 350]. While conducting an LCA analysis is crucial, it was not within the scope of this thesis. The focus of this thesis was on the synthesis of materials in emerging fields like vitrimers. In these fields, the emphasis is often on innovation, functionality, and creating new materials, sometimes without giving enough thought to their environmental impact. In the future, it would be beneficial to conduct a life cycle assessment (LCA) on these materials. This assessment would provide valuable insights into their environmental performance and help identify areas for improvement to enhance their sustainability even more.

Vitrimers are a specific type of polymeric material that possess properties that fall between those of thermoplastics and thermosets [192]. These materials are known for their exceptional thermal stability, mechanical strength, and chemical resistance [261]. Vitrimers, unlike traditional thermoset materials, have the unique ability to undergo exchange reactions. This means that they can flow and be reprocessed without changing the number of chemical bonds and cross-links they have [192, 261]. Although vitrimers have been studied for various applications, such as recyclable fiber-reinforced and functional composites [351, 352], removable adhesives [353], coatings [354], and electronics [355], there is currently no available information on their direct utilization in food packaging. This can be attributed to factors such as their high cost, limited research, and strict safety and regulatory standards [356]. The synthesis of sustainable epoxy vitrimers from epoxidized soybean oil (ESO) and vanillin has gained significant attention in recent years. Researchers have focused on simplifying the fabrication procedures of biobased epoxy vitrimers by curing

commercially available biobased epoxy resins, such as epoxidized soybean oils, with dynamic covalent bond-containing hardeners. For instance, According to a study by Geng et al. (2018) introduces the integration of dynamic imine covalent bonds into vanillin-based vitrimers networks, endowing thermosets with the hot-reprocessing ability and chemical recyclability under acid hydrolysis. Their crosslinker was prepared using vanillin, anhydrous K_2CO_3 , and CH_3CN , with 1,4-dibromo butane as a catalyst. Following overnight vacuum-drying in an oven, a white powder of DAV was obtained with an 86% yield. To prepare the vitrimer, the cross-linked films were prepared by dissolving DAV in an appropriate amount of CH_2Cl_2 solvent; then, a precise amount of diethylenetriamine and tris (2-aminoethyl)amine were added into the solution [357]. Liu et al. (2022) pioneered catalyst-free room-temperature-curable vanillin-based vitrimers. This vitrimer has exceptional properties: Due to Schiff base network and enamine–ylen click reactions, vitrimers can be recycled successfully. They fully degrade in mild organic acid, organic base, and amine solutions. Glass transition temperature is $55^\circ C$ to $62^\circ C$, tensile strength is 13–15 MPa, and elongation at break is 77–98% in vitrimer networks. However, vanillin was dissolved in DMSO, followed by the addition of dicyclohexyl carbodiimide, 4-dimethylaminopyridine, p-toluenesulfonic acid monohydrate, and propiolic acid into the vanillin solvent. Following the filtration process, a yellow solid 4-formyl-2-methoxy phenylpropionate (VNL-P) was obtained with a yield of 64%. Next, to create the vitrimer, Tris (2-aminoethyl) amine and Priamine 1074 or Priamine 1071 were combined with a mixture of VNL-P. Finally, the value for VNL-1071 is 51 kJ/mol and for VNL-1074 is 47 kJ/mol [358]. The article by Li (2023) discusses the development of bio-based thermosetting polyimine vitrimers with exceptional adhesion, rapid self-healing, multi-recyclability, and antibacterial properties. The vitrimers are constructed using renewable feedstocks, including castor oil, cysteamine, and vanillin, through imination between cysteamine functionalized castor oil and divanillin to form covalent adaptive networks (CANs). The resulting polyimine vitrimers exhibit a unique structure comprising flexible chains, aromatic hydrocarbons, and imine bonds, which contribute to their multifunctional properties. However, for the preparation of the vitrimers, 2,2-dimethoxy-2-phenylacetophenone (DMPA) was used. Also, they utilized chloroform solvent and DMF solvent for the material mixture [359]. According to a study carried out by (Zhang et al., 2023). researchers prepared bio-based vitrimers derived from divanillic acid (DVA) and epoxidized soybean oil (ESO)

formed via dynamic covalent bonds. Two series, OHESO-x and BuESO-x, were cured with varying COOH/epoxy ratios. The research investigated dynamic transesterification, reprocessability, and self-healing properties of these bio-based vitrimers. Nevertheless, The crosslinker was created by mixing divanillic acid and KOH in a THF solvent and BuDVA and KOH in a methanol solvent. Additionally, a catalyst must be present in order to combine the crosslinker and ESO to create the vitrimer. Additionally, activation energy (E_a) values were provided for OHESO-1.0, and BuESO-1.0 had 111.8 ± 18.7 and 118.6 ± 22.7 kJ mol^{-1} , respectively [360]. According to The paper presented by (Zhao et al., 2020) details the synthesis of sustainable epoxy vitrimers through the curing of epoxidized soybean oil (ESO) with a vanillin-derived Schiff base (VSB) dynamic hardener. The dynamic Schiff base bonds provided excellent reprocessability, weldability, reconfigurability, and programmability to the epoxy vitrimers, facilitating recycling and processing of cured epoxy materials. The vitrimer prepared in the literature has good mechanical properties. The main reason would be they utilized 4,4-diaminodiphenyl methane (DAM) which has 2 phenyl groups inside the structure, making that vitrimer strong. The vitrimer prepared in the literature has good mechanical properties. The main reason would be they utilized 4,4-diaminodiphenyl methane (DAM) which has 2 phenyl groups inside the structure, making that vitrimer stronger than of our vitrimers. It's worth mentioning that they utilized 4,4-diaminodiphenyl methane (DAM) as the crosslinker, a potential occupational carcinogen. For the crosslinker produce needs to be heated between 65° and 70° , raising concerns about energy consumption. Also, because the crosslinker is solid, it must be melted before combining with Soybean Oil. Additionally, vitrimer was formed using 1,2-dimethylimidazole as a catalyst during the mixing process with ESO. Furthermore, due to the utilization of hard VSB, the activation energy (E_a) for the reaction is approximately $108.9 \text{ kJ}\cdot\text{mol}^{-1}$ [361]. The studies reviewed demonstrate the diverse approaches to creating bio-based vitrimers with unique properties and applications. While some studies utilized toxic solvents and chemicals in the synthesis process, in this chapter, we report fully bio-based vitrimers were synthesized using epoxidized soybean oil (ESO) and a bio-based imine crosslinker derived from vanillin and Priamine™ 1071 (VPI) without requiring a solvent or a catalyst. Additionally, oleic acid was incorporated to regulate the crosslink density. The material that was produced showed a level of oxygen and water vapor resistance similar to polyethylene. It also demonstrated promising thermal and

mechanical properties, as well as low migration in food simulants. These characteristics make it a potential option for sustainable packaging material. Furthermore, the vitrimers have shown the capability to undergo biodegradation in seawater, indicating their potential to decrease their accumulation in marine ecosystems in case of accidental release into the environment.

3.2 RESULTS AND DISCUSSION

3.2.1 Synthesis of vitrimer

The initial stage in acquiring the vitrimer involved synthesizing a bio-based crosslinker for epoxy soybean oil (ESO). The VPI crosslinker was synthesized through the reaction between the aldehyde group of vanillin and the amino group of Priamine[®] 1071. This reaction resulted in the formation of dynamic imine bonds, as depicted in **(Figure 33a)**. The synthesis was performed in ethanol, an economic and green solvent, and the mixture was stirred at room temperature for one day in nitrogen atmosphere. The product was obtained as a viscous orange liquid in a quantitative yield without a need for further purification. Its structure was confirmed by ¹H and ¹³C NMR **(Figure 33b)** and **(Figure 33c)**. In the ¹H NMR spectrum of VPI the disappearance of the vanillin's aldehyde proton (-C(=O)H, 9.79 ppm) and the Priamine's methylene group next to the amine (-CH₂-NH₂, 2.67 ppm) can be observed. Instead, a new signal at 8.13 ppm appears that can be ascribed to the proton of the newly formed imine (-CH=N-) as well as a new signal at 3.57 ppm attributed to the methylene group next to the imine bond (-CH₂-N=CH-). Similarly, in the ¹³C NMR spectrum of VPI the carbons of the vanillin's aldehyde group (-C(=O)H, 191.14 ppm) and Priamine's methylene group next to the amine (-CH₂-NH₂, 42.22 ppm) disappear and new signals corresponding to the carbon of the imine bond (-CH=N-, 161.01 ppm) and the methylene group next to the imine bond (-CH₂-N=CH-, 61.39 ppm) are visible.

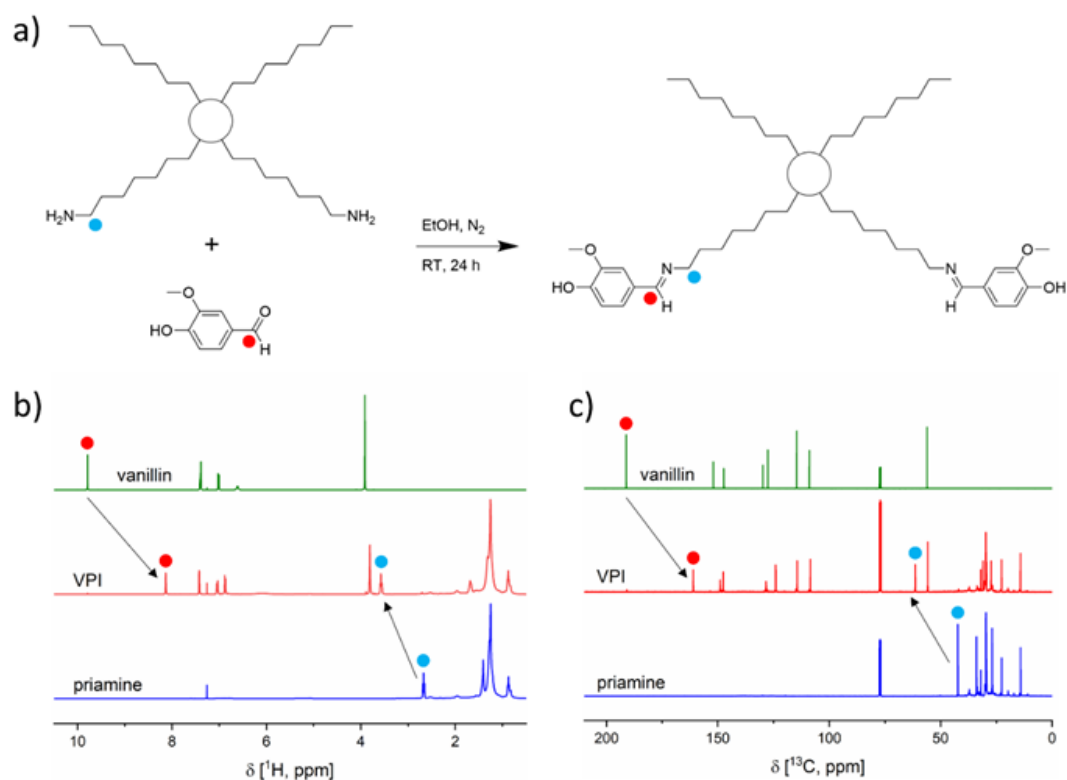


Figure 33. a) Schematic of synthesis of VPI crosslinker. b) ^1H NMR (RT, 400 MHz) and c) ^{13}C (RT, 100 MHz) NMR spectra of VPI and the two reagents Priamine 1071 and Vanillin.

The vitrimer was formed by crosslinking ESO and VPI through a coupling reaction between the epoxide group of ESO and the hydroxyl group of VPI, as illustrated in (Figure 41). The experiment was conducted in a vacuum oven at a temperature of 180 °C, utilizing a ratio of 4 parts ESO (epoxy group) to 2.2 parts VPI (hydroxyl groups), as documented in (Table 2). In a subsequent set of samples, oleic acid (OA) was introduced to both oils in order to adjust the level of crosslinking. The carboxyl group of OA has the ability to undergo a reaction with the epoxy groups, leading to the displacement of the bond with VPI. As a consequence, this reaction yields a material with reduced cross-linking. It is important to note that the combined amount ratio of hydroxyl and carboxylic acid groups should always be equal to the number of epoxy groups (4 epoxy groups of ESO) in order to react with all the available epoxy groups. So it is important to note that if one does not use OA to increase the softness and flexibility of the sample, and instead adds a lower amount of VPI crosslinker (such as 3VPI, 2.5VPI, or 2.1VPI) without incorporating any OA or functional groups (such as carboxylic acid or aromatic -OH) to block the remaining epoxy groups, there will be some unreacted epoxy groups from ESO. Consequently, when an epoxy is opened with the VPI, an OH group is formed. This hydroxyl group has the capability of reacting

with another unopened epoxide in the event that there is insufficient VPI. This reaction will result in the creation of a static bond, which is a non-dynamic bond analogous to that of typical thermoset materials, rather than a dynamic bond like vitrimer. Because of this, the major purpose of the OA is to prevent the epoxy groups from functioning. The crosslink density and, thus, the final macroscopic properties of the material were subjected to testing in order to determine the effectiveness of this technique. Additionally, the substitution of OA for a portion of the VPI guarantees that all of the epoxy groups will react and that there will be no side reactions that will result in static crosslinking. For example, an OH group that is created by opening an epoxy can react with an epoxy that is closed. (**Table 2**) presents the various ratios of ESO to VPI to OA that have been calculated.

Table 2. Composition and Properties of ESO–VPI, OA Vitrimers and ESO–VPI Vitrimer

| Sample Code | ESO [g] | Vanillin-Priamine [g] | Oleic acid [g] | Gel fraction [%] | Tg (DMTA) [°C] | Tg (DSC) [°C] | MFI | Youngs modulus [MPa] | Stress at break [MPa] | Elongation at break [%] |
|-------------------|---------|-----------------------|----------------|------------------|----------------|---------------|-----|----------------------|-----------------------|-------------------------|
| <i>Vitrimer 1</i> | 3.63 | 6.37 | 0 | 93.8 | 12.44 | 0 | - | 2.41±0.2 | 1.74±0.16 | 91±11 |
| <i>Vitrimer 2</i> | 3.83 | 5.03 | 1.14 | 89.5 | -5.85 | -15 | - | 1.49±0.15 | 0.88±0.08 | 68±8 |
| <i>Vitrimer 3</i> | 3.93 | 4.31 | 1.76 | 83.5 | -14.72 | -25 | - | 0.78±0.09 | 0.40±0.12 | 60±5 |
| <i>Vitrimer 4</i> | 4.02 | 3.70 | 2.28 | 80.2 | -19.83 | -30 | 0.7 | 0.66±0.15 | 0.29±0.06 | 59±12 |

3.2.1.1 Gel fraction:

In order to ascertain the most effective duration for achieving optimal crosslinking, the samples underwent curing for a range of 1 to 8 days at a temperature of 180 °C within the vacuum oven (refer to **Figure 34a**). To assess the extent of crosslinking, the gel fraction was measured at each curing interval. Based on the findings presented in (**Figure 34b**), it was determined that the optimal duration for curing the material and achieving a significant level of crosslinking was observed to be 4 days at a temperature of 180 °C. During this period, all samples exhibited a gel fraction exceeding 80%. The results indicate that the gel fraction of the samples decreased when they were modified with OA. The reason for this phenomenon is that OA effectively decreases the level of crosslinking within the material. The subsequent results presented pertain to samples that were cured for a duration of 4 days at a temperature of 180 °C under vacuum conditions.

Considering the sensitivity of the imine bond to water, an experiment was conducted to assess the water stability of the vitrimer. The gel fraction before and after immersing it in water for 24 hours was compared. The results can be found in **Table 3**. The gel

fraction of the materials exhibited minimal changes: The material with the highest crosslinking density, Vitrimer 1, did not exhibit a statistically significant difference in gel fraction. Prior to immersion in water, the gel fraction was 93.5%, which decreased slightly to 92.3% after immersion. On the other hand, Vitrimer 4, the material with the lowest crosslinking density, experienced a slight decrease in gel fraction from 80.2% to 74.5%.

Table 3. Gel fraction of the vitrimers before and after being placed in water.

| | Gel fraction of the vitrimers cured at 180 °C after 4 days | after being placed 24h at RT in water |
|-------------------|---|--|
| Vitrimer 1 | 93.50% ± 1.5% | 92.30% ± 1.2% |
| Vitrimer 2 | 89.50% ± 1.0% | 86.65% ± 1.1% |
| Vitrimer 3 | 83.50% ± 0.7% | 77.12% ± 0.8% |
| Vitrimer 4 | 80.20% ± 0.5% | 74.50% ± 0.4% |

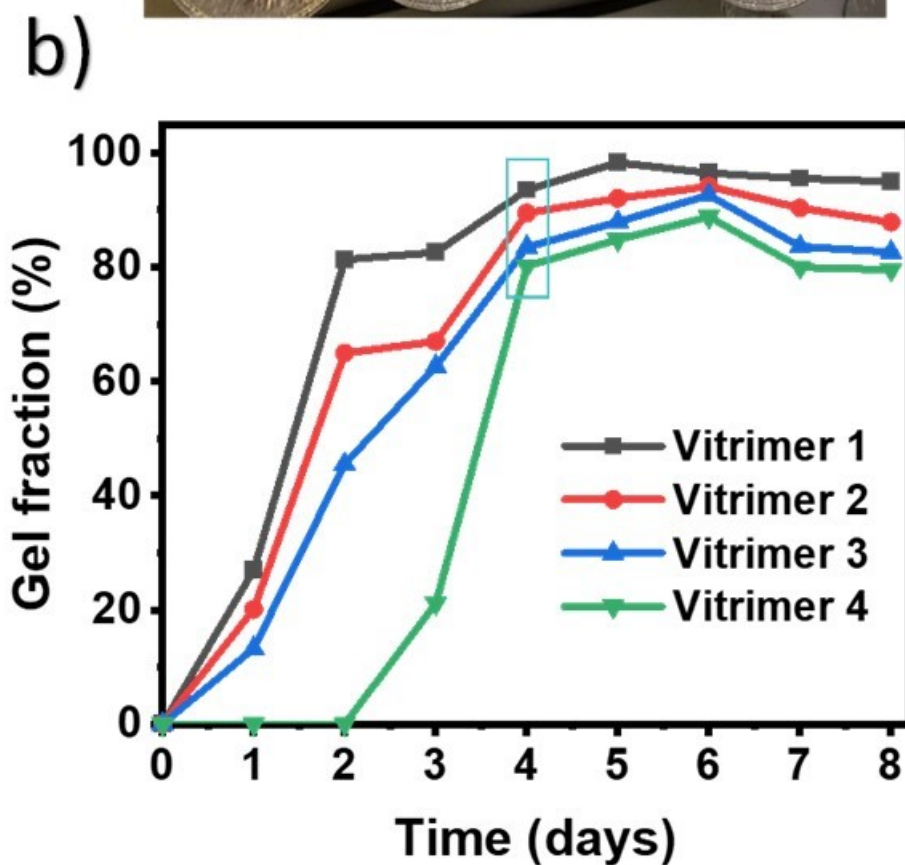
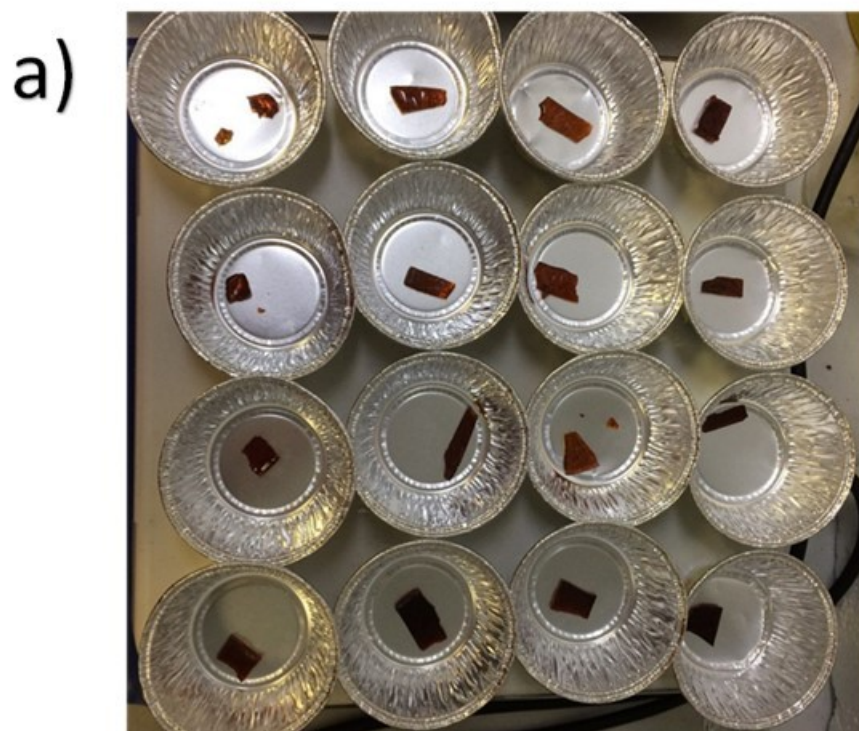


Figure 34. Gel fraction of the vitrimers cured at 180 °C for different days after the ethyl acetate was removed, a) drying under hood at 100°C, b) Representative gel fraction curves of composite with ESO, VPI, and OA.

3.2.2 Thermomechanical properties and adhesion tests

3.2.2.1 Thermogravimetric analysis (TGA) and differential scanning calorimete (DSC)

According to the TGA analysis, it has been confirmed that the ESO-VPI vitrimers, both with and without oleic acid, exhibited no weight loss when subjected to temperatures of approximately 300 °C (**Figure 35**). The DSC analysis indicated the existence of a glass transition temperature near 0°C. With the inclusion of OA, the Tg experienced a significant decrease, going from 0°C to -30 °C, as illustrated in (**Figure 36a**). This finding supports our idea that oleic acid functions as an internal plasticizer, creating additional space between chains and lowering the energy needed to exchange imine bonds. The DSC curve of polyethylene (PE) was also obtained for comparison reasons and showed a relatively low melting temperature of approximately 105–115 °C, as reported in (**Figure 36b**).

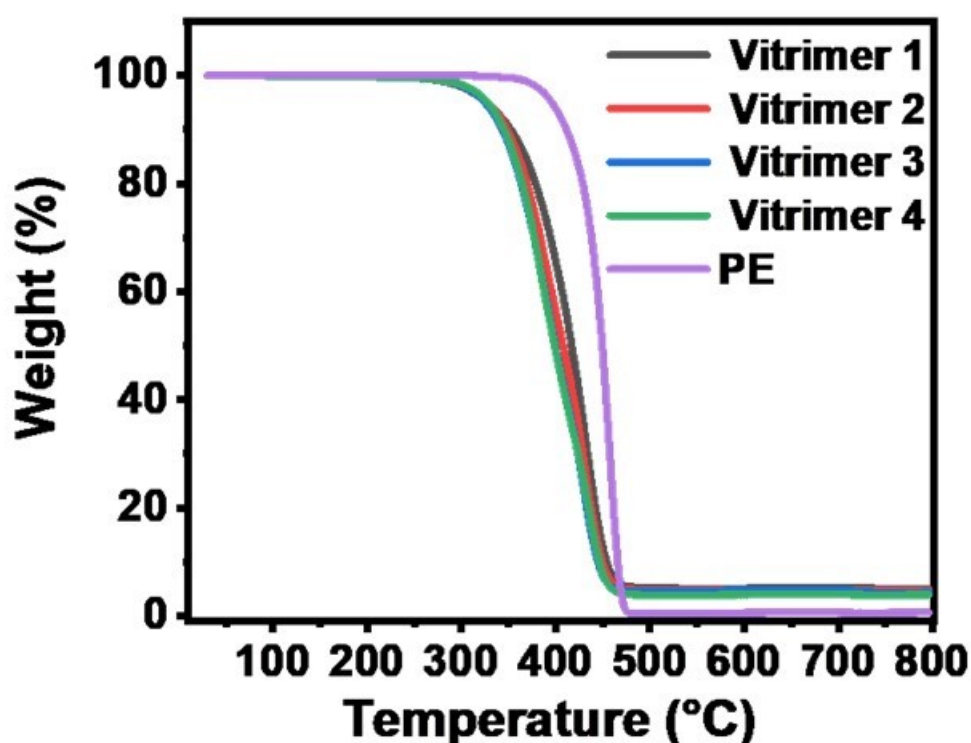


Figure 35. TGA of vitrimers with ESO and VPI and different amount of OA. The TGA of LLDPE is also shown for comparison reasons.

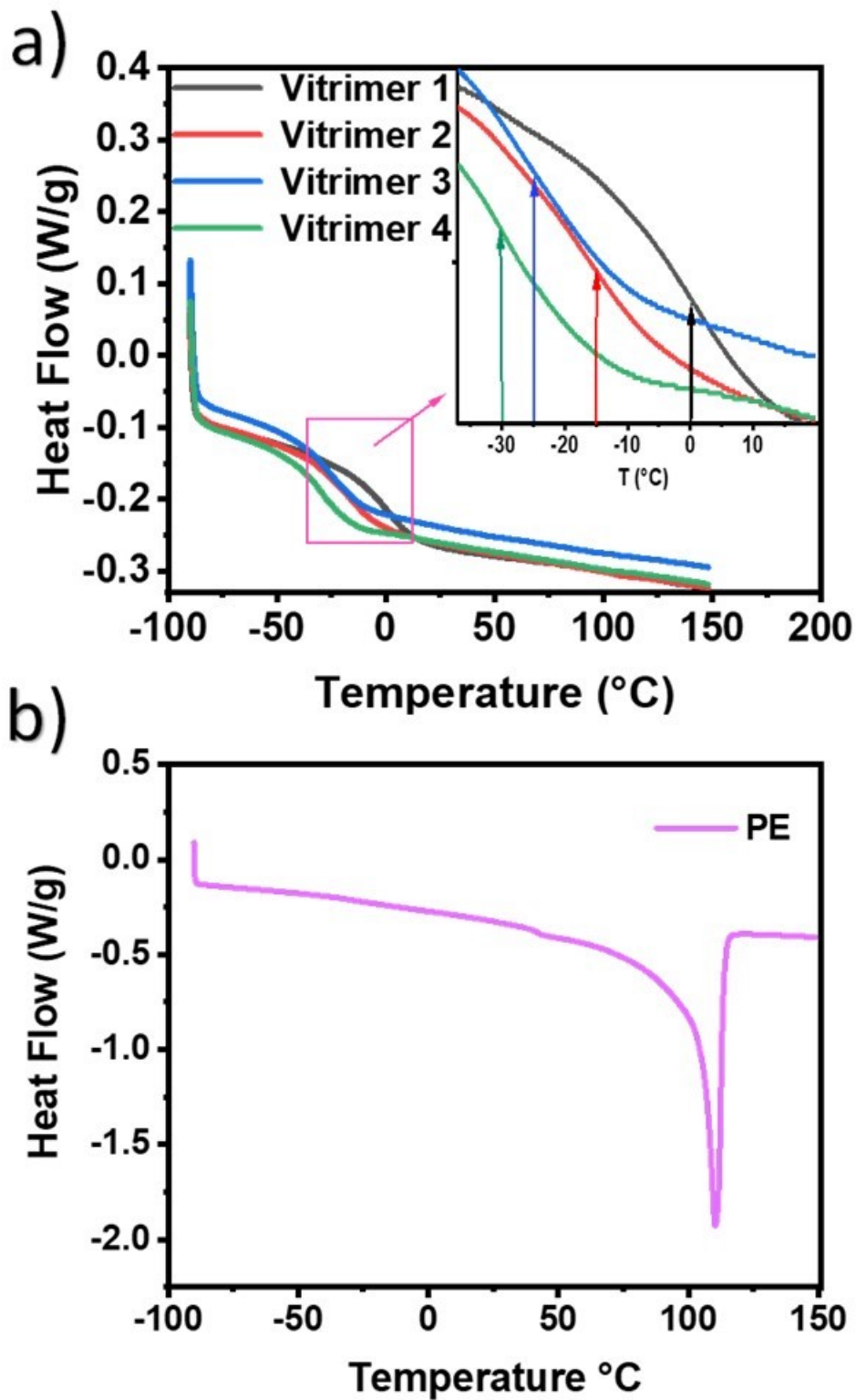


Figure 36. a) DSC of vitrimers with ESO and VPI and different amount of OA, b) DSC second heating curve of PE.

3.2.2.2 Dynamic mechanical analysis (DMA):

A DMA analysis was conducted on ESO-VPI vitrimers, both with and without the presence of OA. The experimental results depicted in (**Figure 37**), indicate that the α -relaxation (T_α) temperature of ESO-VPI follow a similar decrease, when OA is added, for instance in the absence of oleic acid is approximately 30°C higher than that of the vitrimer with the highest amount of oleic acid. These results are in agreement with the DSC results shown before. The small discrepancy between T_g and T_α is due to the fact that glass transition is a non-equilibrium state and the transition temperature depends on experimental conditions, so small differences are known to occur [362].

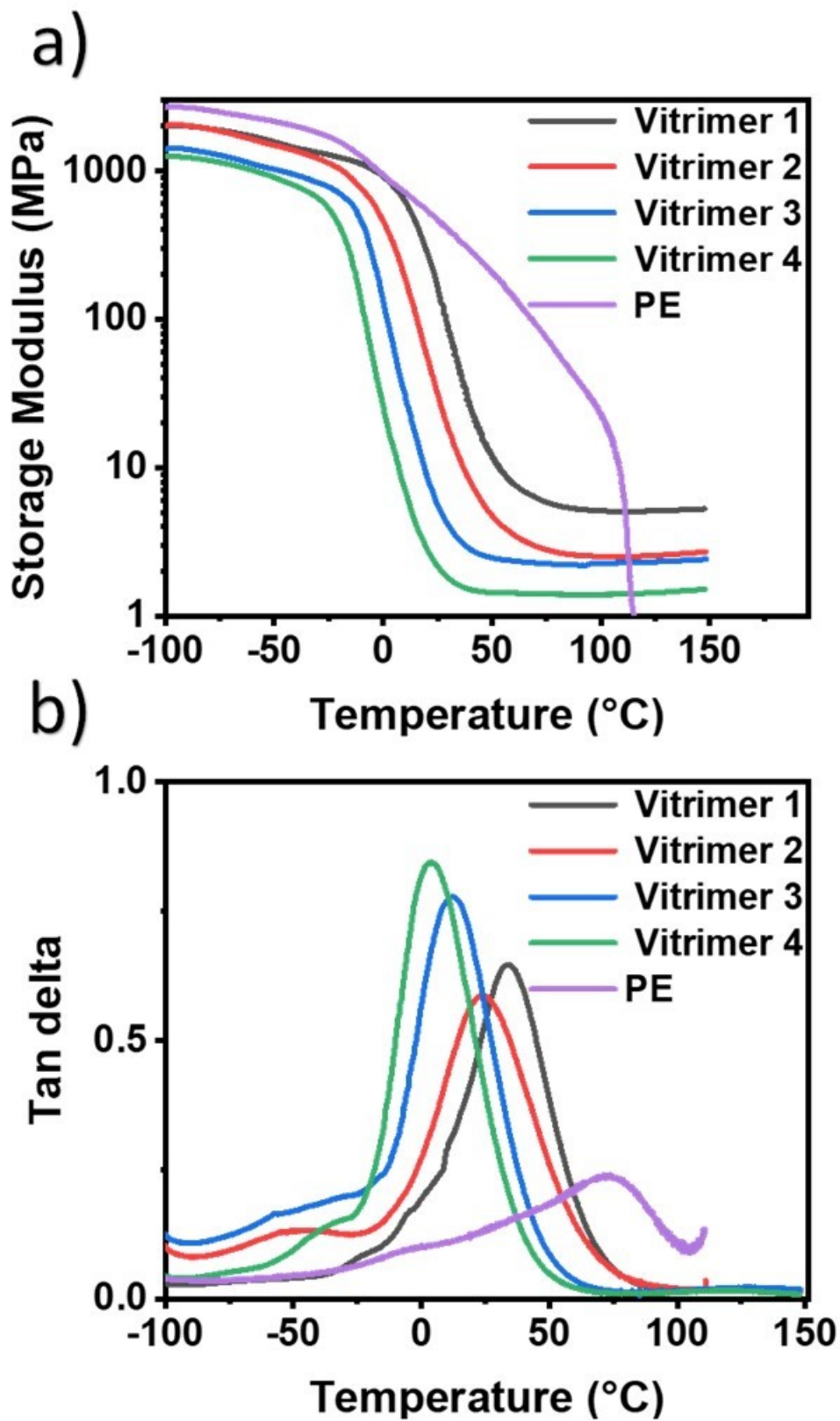
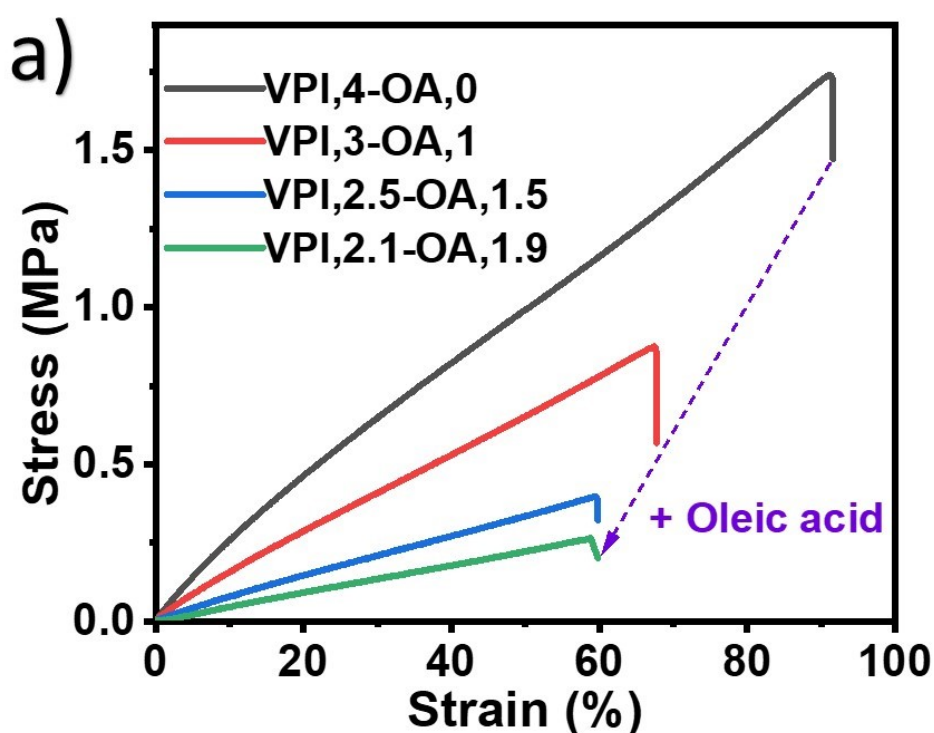


Figure 37. DMA test curves of the vitrimers and LLDPE for comparison reasons.

3.2.2.3 Mechanical test:

The mechanical tests conducted on the vitrimers provide insights into the correlation between their macroscopic properties and the degree of cross-linking, which is influenced by the quantity of OA present in the oil thermoset. The stress-strain graphs for the vitrimers are presented in **Figure 38a**. The corresponding values of Young's modulus, maximum stress, and elongation at break are provided in **Table 2**. The gradual decrease in tensile strength, from 1.74 MPa to 0.26 MPa, was observed as the amount of oleic acid in the samples increased. This decrease was accompanied by a reduction in the elongation at break, from 91% to 59%. The incorporation of extended chains of organic acids (OA) in the materials results in a softer texture and facilitates the mobility of these chains. The mechanical analysis for polyethylene (PE) is presented in (**Figure 38b**) for the purpose of comparison.

Moreover, since the imine bond is known to be sensitive to water, the water stability of the vitrimer was evaluated by comparing the mechanical properties of the vitrimer before and after it was immersed in water for a period of 24 hours. **Figure 38c** presents the findings that were carried out. After being submerged in water for 24 hours, the mechanical properties of all four vitrimers exhibit only slight variations from one another. This confirms how the aliphatic nature of the material helps to protect the sensitive imine bond from the influence of water.



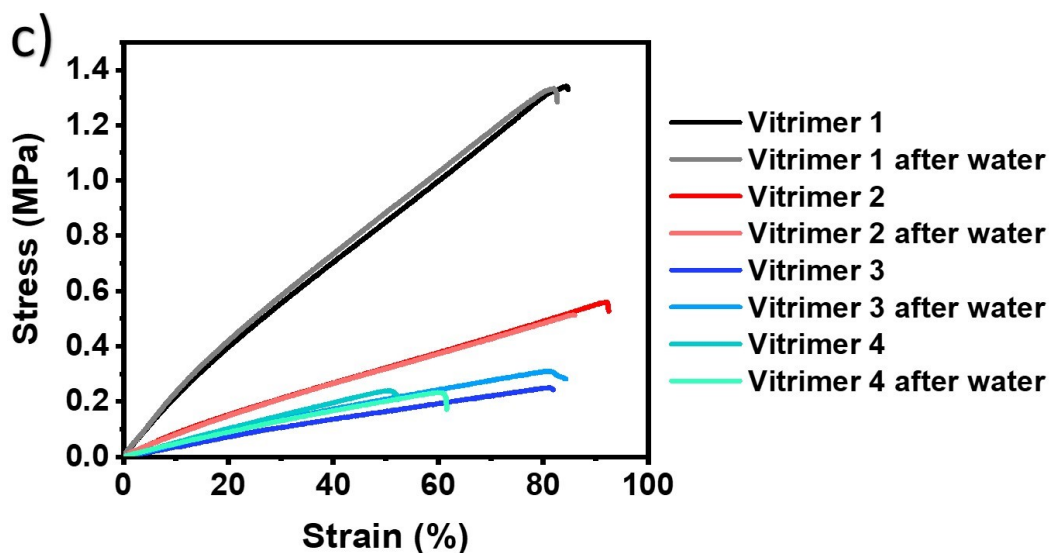
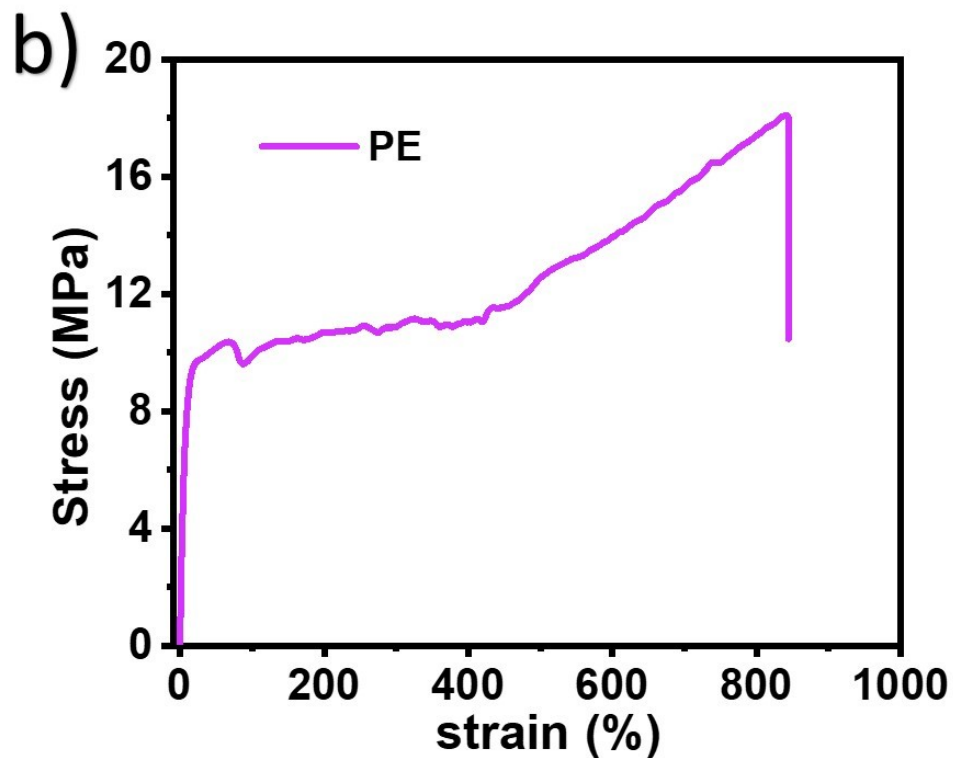


Figure 38. a) Representative tensile test curves of the vitrimers, b) Representative tensile test curves of PE. c) Representative tensile test curves of vitrimers before and after being placed in water.

3.2.2.4 Creep-recovery

The dimensional stability of the vitrimer samples was assessed using a creep test conducted at a temperature of 30 °C, under a constant load of 0.05 MPa. The results, depicted in **Figure 39**, demonstrate the different dimensional stability of the four synthesized materials. Vitrimer 1 exhibited a mere 2.2% creep, whereas the softer and more plasticized Vitrimer 4 demonstrated a more consistent 10.6% creep. The results indicate that the crosslink density of the various synthesized materials aligns with their characteristics. Specifically, the increased presence of oleic acid in Vitrimer 4 contributed to the enhanced flexibility of the material.

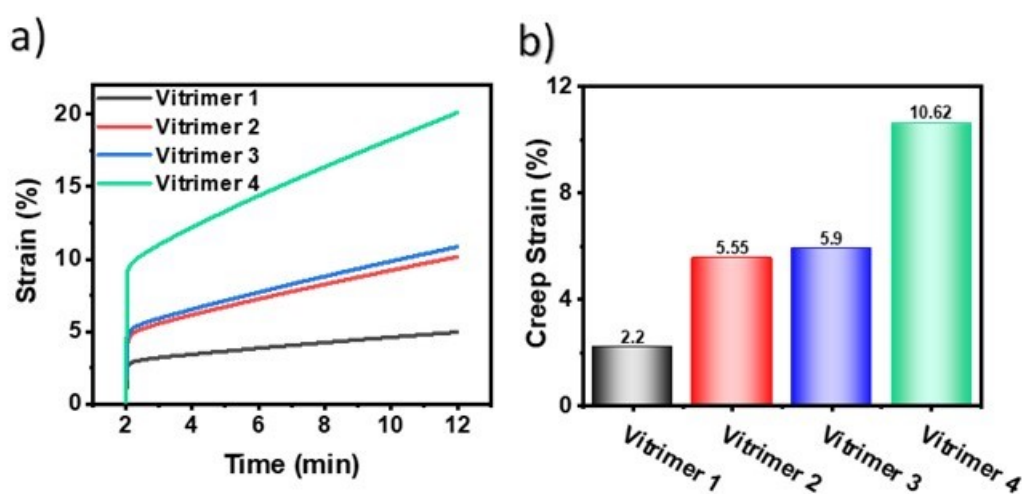


Figure 39. Creep test curves of vitrimers.

3.2.2.5 Adhesion strength:

The potential of utilizing cross-linked vitrimers as adhesives was examined through the execution of adhesion strength tests. T-peel tests were conducted to measure the adhesive strength between the samples and pieces of paper. Prior to the tests, the samples were subjected to hot pressing at a pressure of 1.5 tons for a duration of 20 minutes at a temperature of 140°C. According to the findings presented in **Figure 40**, Vitrimer 1 exhibited a notably higher adhesion value of 377 N m⁻¹ compared to PE embossed on paper under identical conditions, which yielded an adhesion value of 131 N m⁻¹. The reported values for the Velcro loop/hook adhesive tape are more than double in comparison [363].

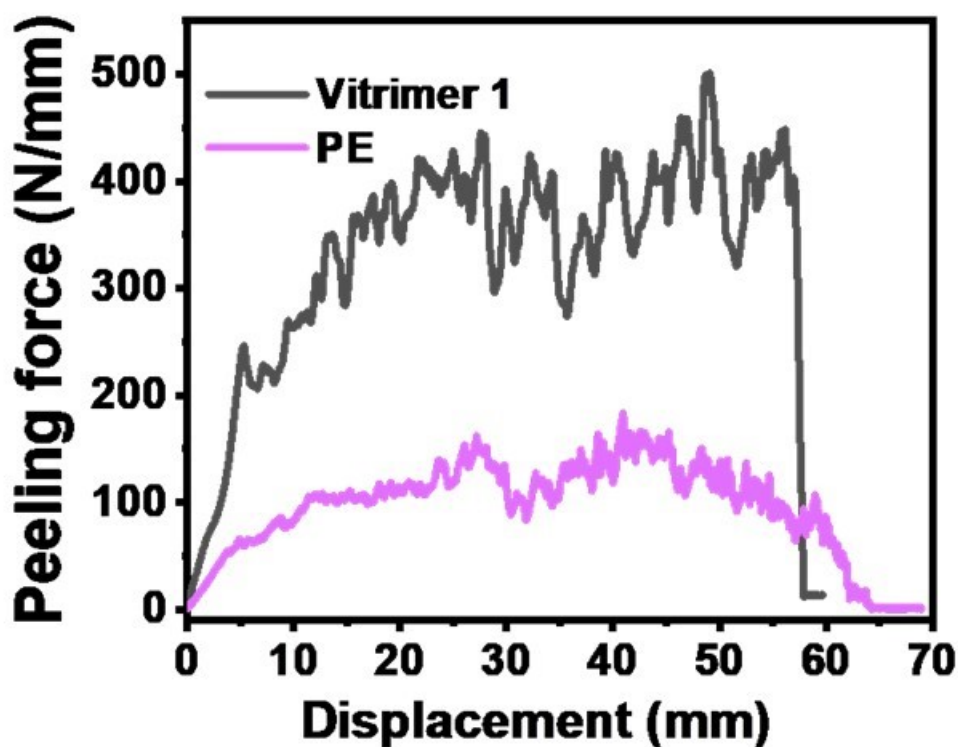


Figure 40. Representative T peel tests curves of the vitrimer1 and LLDPE for comparison.

3.2.3 Reprocessing of vitrimers

One notable attribute of vitrimers is their capacity to undergo bond exchange in the presence of adequate thermal energy. The rearrangement of bonds is illustrated in (Figure 41), in the present study, the vitrimers under investigation demonstrate the ability of two imine bonds to undergo exchange, facilitating chain rearrangement. This phenomenon enables stress relaxation and material flow, thereby enabling reprocessing when the heat provided is above a certain activation energy.

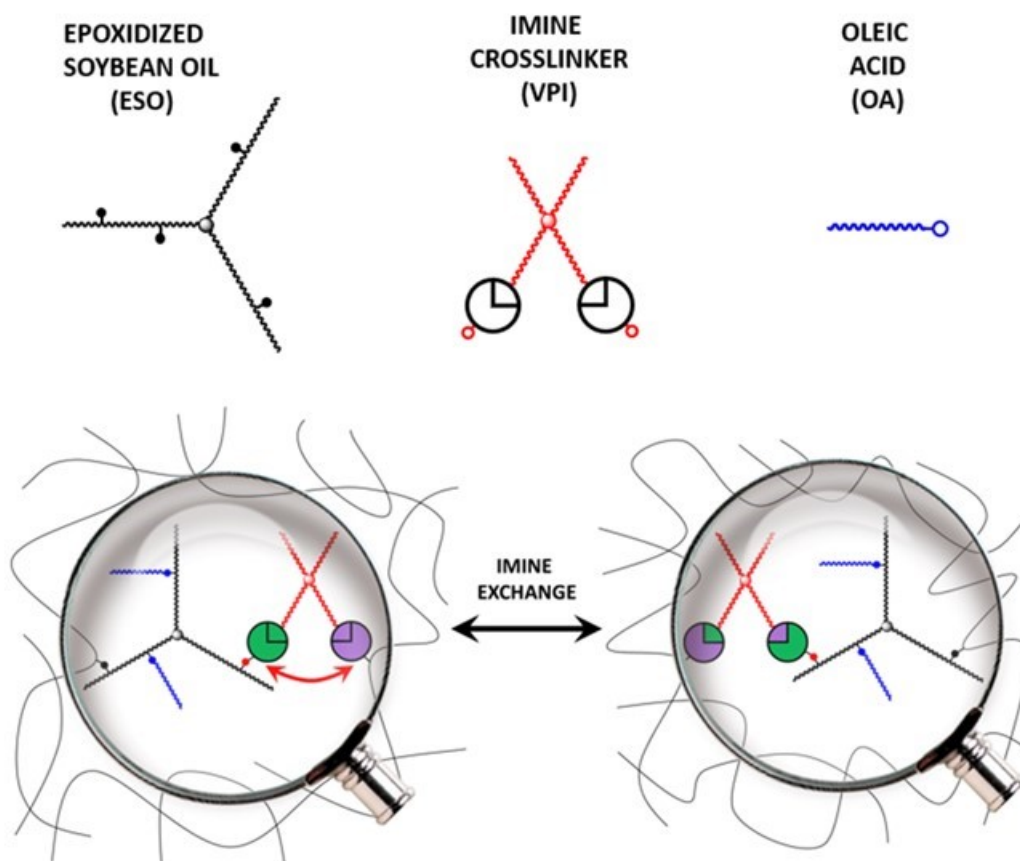


Figure 41. Illustration that shows the three components of the vitrimer: ESO–VPI, OA and the exchange of imine that allows the vitrimer to rearrange its structure.

3.2.3.1 Stress relaxation:

The stress relaxation behaviours of ESO-VPI vitrimers with and without oleic acid (OA) at a temperature of 100 °C are depicted in **Figure 42**. All of the samples have demonstrated the ability to alleviate applied stress at high temperatures. This suggests that they possess the capability to reconfigure their network structure and relieve the imposed stress by means of the exchange reaction involving the imine bonds facilitated by the VPI crosslinker. Nevertheless, as the concentration of oleic acid (OA) within the sample increases, the stress relaxation time of the vitrimer requires less energy, this is due to the fact that OA reduces the number of crosslinks and acts as a plasticizer, resulting in increased free volume within the material. In order to validate this, the activation energy (E_a) associated with the topological rearrangement and the temperature (T_v) at which the topology-freezing transition occurs were determined. This was accomplished by measuring the relaxation times and plotting them on an

Arrhenius plot, as shown in [192]. The activation energy (E_a) and glass transition temperature (T_v) for vitrimer 1 were determined to be 33.6 kJ/mol and -152.64 °C, respectively. When the concentration of organic additives (OA) was increased within the vitrimers, both the activation energy (E_a) and the temperature at which vitrification occurs (T_v) exhibited a decrease. The activation energy (E_a) and glass transition temperature (T_v) values for vitrimer 2 were determined to be 29.15 kJ/mol and -166.96 °C, for vitrimer 3, the E_a and T_v values were found to be 28.82 kJ/mol and -171.02 °C. Lastly, vitrimer 4 exhibited E_a and T_v values of 27.89 kJ/mol and -175.5 °C.

Analysis of activation energy (E_a) of vitrimers

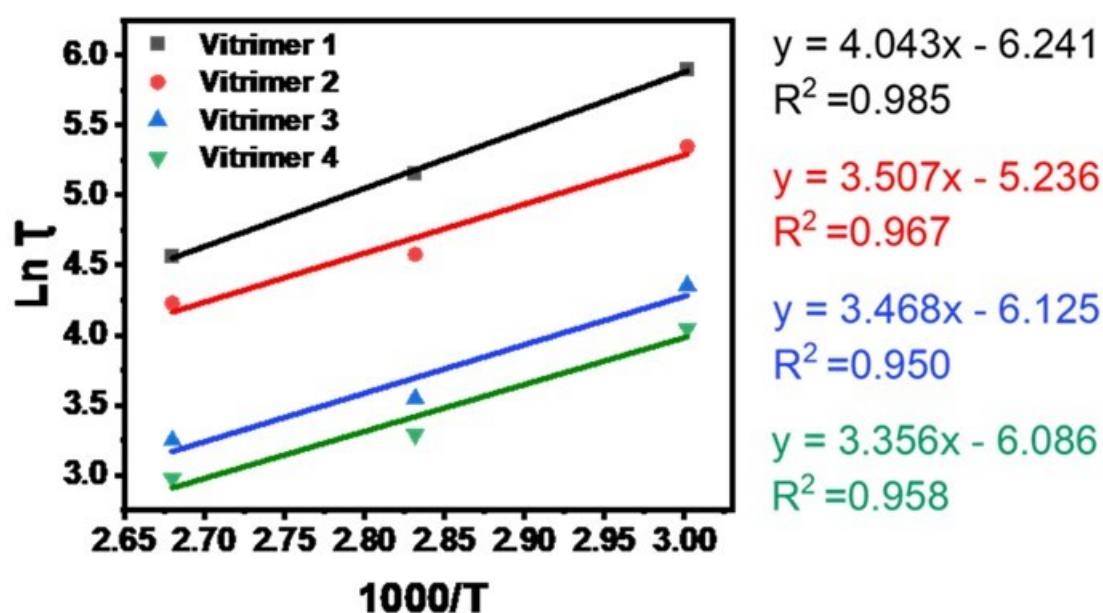


Figure 42. Arrhenius plot of relaxation times of vitrimers.

To calculate the topology-freezing transition temperature (T_v) of vitrimers, Arrhenius equation was used, which relates the rate constant (τ) of a reaction to its activation energy (E_a), temperature (T), and a constant (τ_0):

$$\text{(Equation 1)} \quad \tau = \tau_0 e^{\frac{E_a}{RT}}$$

Where R is the universal gas constant (8.31 J/(K·mol)).

Taking the natural logarithm of both sides of Equation 1 gives:

$$\text{(Equation 2)} \quad \ln \tau = \frac{E_a}{RT} + \ln \tau_0$$

Equation 2 has the form of a linear equation, $y = ax + b$, where $y = \ln \tau$, $x = 1/T$, $a = Ea/R$, and $b = \ln \tau_0$.

To determine Ea , we need to plot $\ln \tau$ versus $1/T$ and find the slope of the line. We can then use the value of the slope to calculate Ea using the equation:

$$\text{(Equation 3)} \quad Ea = a \cdot R$$

Where a is the slope of the $\ln \tau$ versus $1/T$ plot, and R is the gas constant.

Once we have determined Ea , we can use Equation 1 to calculate the topology-freezing transition temperature (T_v) of vitrimers. We can rearrange Equation 1 to solve for T :

$$\text{(Equation 4)} \quad T = \frac{Ea}{R \cdot \ln(\tau/\tau_0)}$$

Where τ is the relaxation time at a given temperature, and τ_0 is the relaxation time at a reference temperature.

To summarize, the steps to calculate the topology-freezing transition temperature (T_v) of vitrimers are:

Measure the relaxation time (τ) of vitrimers at different temperatures.

Calculate $\ln \tau$ and $1/T$ for each temperature.

Plot $\ln \tau$ versus $1/T$ and find the slope of the line.

Use the slope to calculate Ea using Equation 3.

Choose a reference temperature and calculate τ_0 using Equation 1.

Use Equation 4 to calculate T_v for a given τ .

Analysis of topology-freezing transition temperature (T_v) of vitrimers.

T_v represents the temperature at which a material reaches a viscosity of 10^{12} Pa. The relationship between a substance's viscosity (η) and its characteristic relaxation time (τ^*) can be determined using the Maxwell equation.

$$\text{(Equation 5)} \quad \eta = G\tau = \frac{E'\tau}{2(1+\nu)}$$

G -shear modulus, E' – plateau modulus just after the glass transition (MPa), ν - Poisson's ratio (for ESO based epoxy $\nu = 0.34$)

T_v can be determined by using eq (2), eq (5), and Figure 42 from the equation (6).

$$\text{(Equation 6)} \quad T_v = \frac{1000a}{\ln \frac{2\eta(1+\nu)}{E'} - b}$$

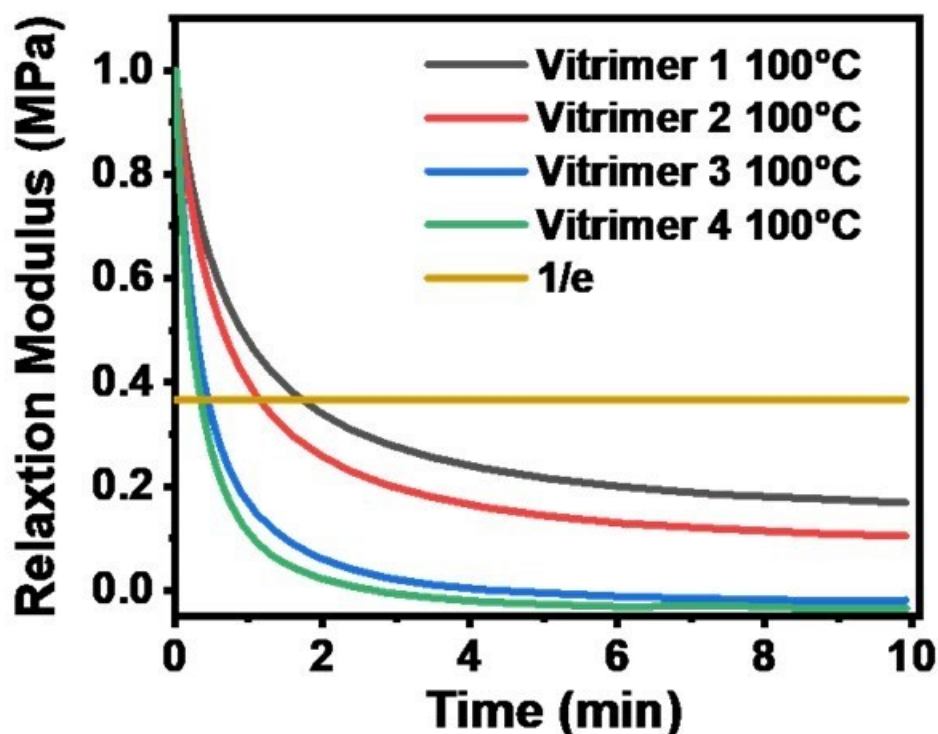


Figure 43. Comparison stress relaxation between vitrimers and PE at 100 °C.

3.2.3.2 Melt Flow Index (MFI):

The utilization of tuning and facilitating the reprocessing of materials with organic acid (OA) enables the potential to achieve a flow of the cross-linked vitrimer that is comparable to that of a thermoplastic. The flow was characterized through the measurement of the melt flow index (MFI). Among the tested vitrimers, Vitrimer 4 exhibited the highest flow rate, as evidenced by the Melt Flow Index (MFI) data presented in (Figure 44a). The remaining vitrimers (1, 2, or 3) exhibited significant resistance to flow, leading to their confinement within the device in a compressed state, thereby rendering the measurement of MFI unfeasible. The melt flow index (MFI) of vitrimer 4 was determined to be $0.698 + 0.045$ g/10 min at 190°C/10 kg. Although this value is relatively low, it is sufficient for enabling the processing of the material through melt extrusion and even injection molding techniques (Figure 44b) [248].

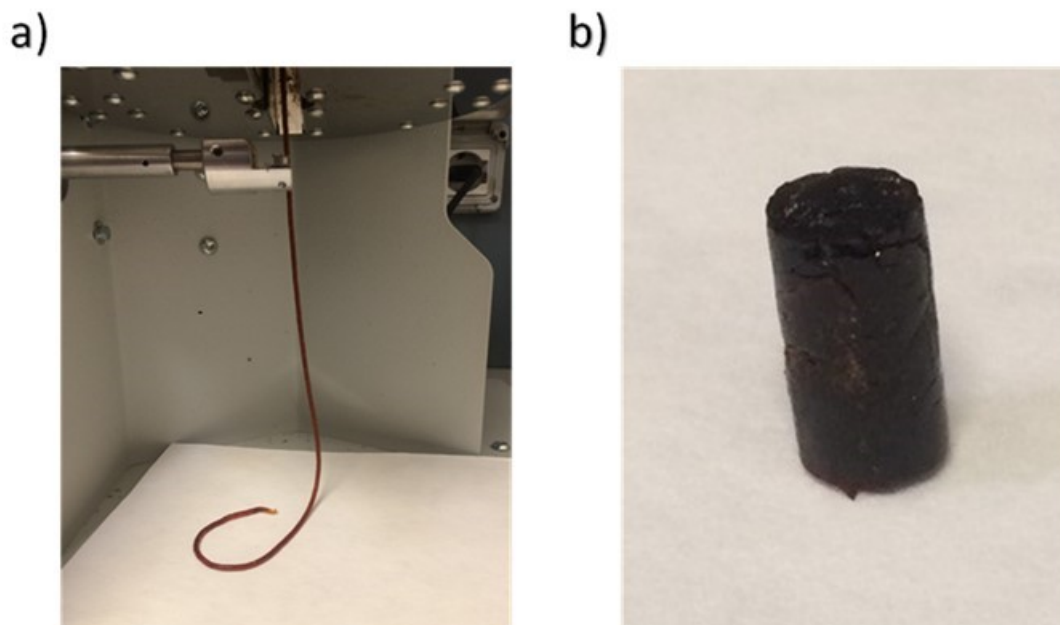


Figure 44. a) ESO-VPI, 2.1 OA, 1.9 during the MFI measurement (190 °C/10 kg). b) Other vitrimers (1, 2, or 3).

3.2.3.3 Reprocessability:

Vitrimer 1 was utilized to assess the reprocessing capability via compression molding, as depicted in (Figure 45a), this approach leverages the exchange reaction of imine bonds in the ESO-VPI. In order to showcase the reprocessability of the vitrimer, the material was divided into smaller sections and subsequently subjected to compression molding. This process was carried out at a temperature of 140 °C, applying a pressure of 5 tons for a duration of 20 minutes. Following these procedures, a cohesive and uniform material was successfully obtained. The mechanical properties of the recycled vitrimer were subsequently evaluated and found to exhibit no significant deviations compared to the original sample prior to undergoing compression molding during reprocessing. This observation remained consistent even after undergoing four cycles of reprocessing, suggesting that the vitrimers possess the ability to undergo multiple mechanical recycling processes without experiencing any detrimental effects on their mechanical properties. The cross-link density and chemical structure exhibited minimal changes following the reprocessing, as depicted in (Figure 45b).

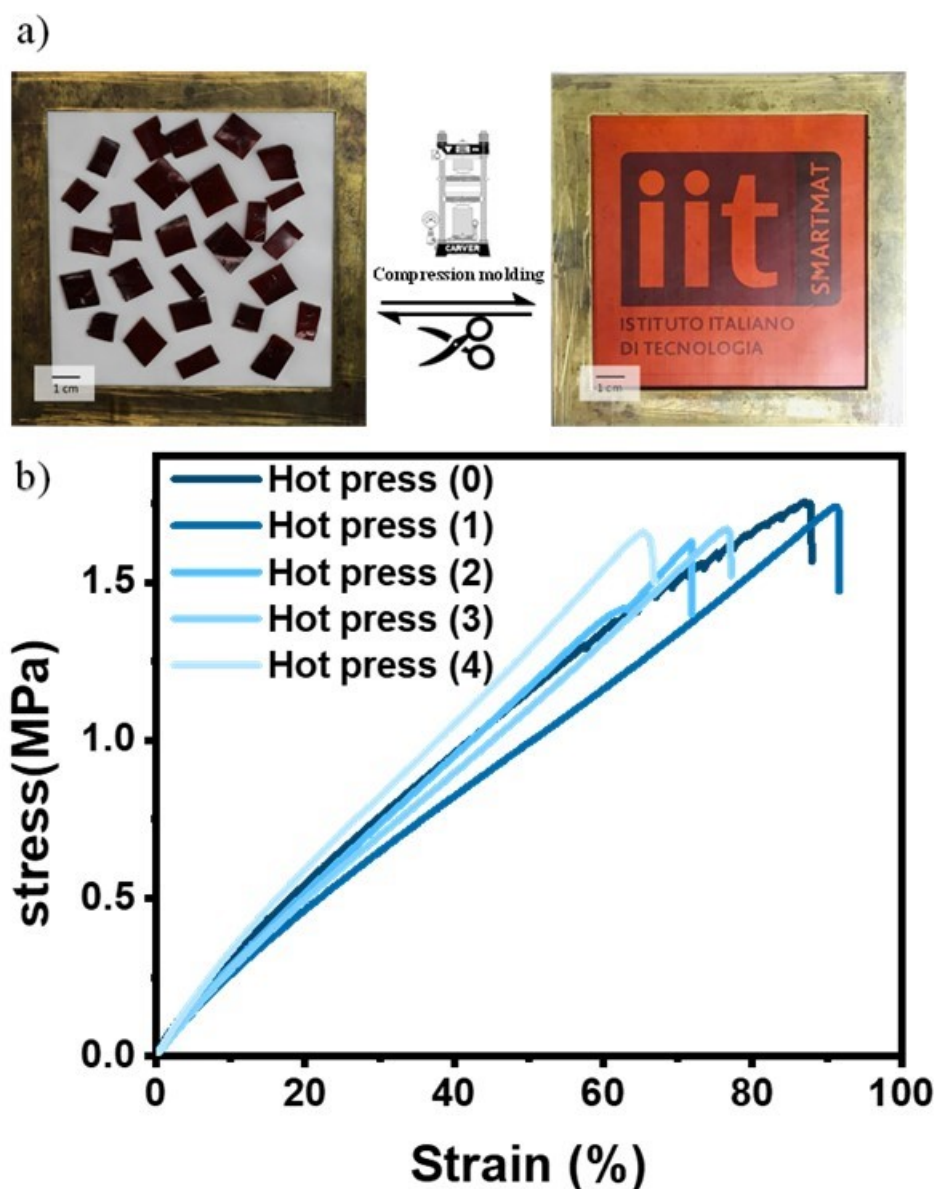


Figure 45. a) Recycling of vitrimer 1 by steps of fragmentation and melt compression molding. b) Representative reprocessability test curves of Vitrimer 1.

3.2.3.4 Biochemical oxygen demand (BOD):

One of the primary drawbacks associated with highly cross-linked thermosets pertains to their end-of-life implications. In the absence of viable reprocessing, recycling, or biodegradation/composting methods, the only available means of disposing these items are through landfilling, incineration, and pyrolysis. Following the demonstration of the ability of vitrimers to undergo multiple reprocessing cycles through imine bond exchange, an investigation was conducted to assess the biodegradation of the material. According to the data presented in (Figure 46), it can be observed that the biochemical

oxygen demand (BOD) in the marine environment exhibits a progressive increase over time. This finding provides evidence to support the assertion that vitrimers possess biodegradable properties. The results of the test indicate that ESO begins to biodegrade within a relatively short period of 3-4 days when exposed to seawater. Similarly, ESO-VPI vitrimer exhibited signs of biodegradation after a duration of 15 days. The observed delay in the biodegradation of ESO-VPI vitrimer, in comparison to ESO, can be attributed to the cross-linked structure of the vitrimer. Additionally, the biodegradation kinetics of ESO-VPI vitrimer are slower.

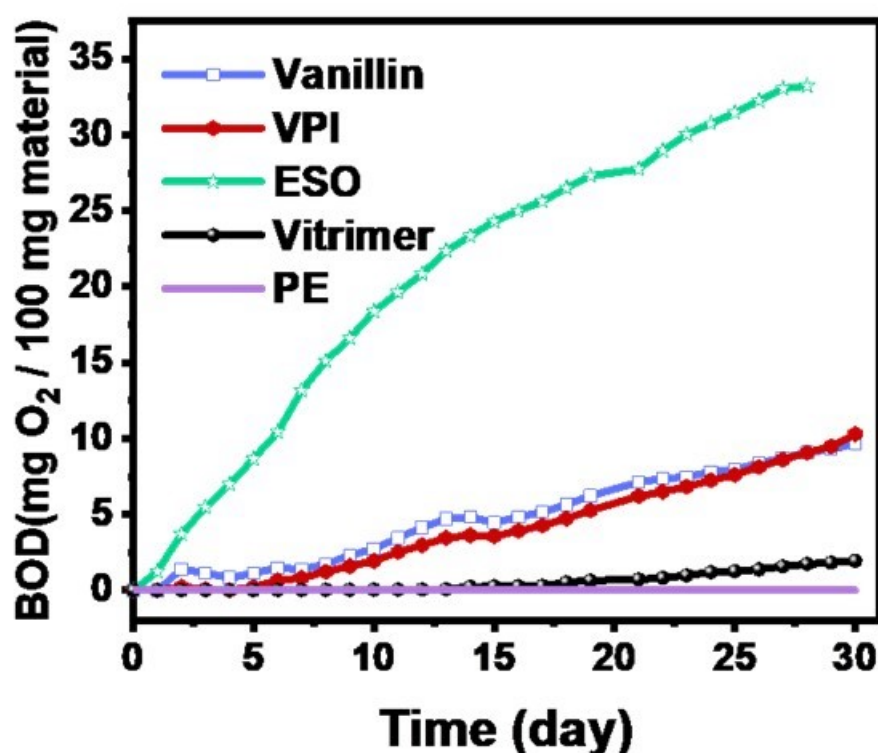


Figure 46. Biodegradation of the vitrimer1 and its components in seawater.

3.2.3.5 Scanning electron microscopy (SEM):

The process of biodegradation in aquatic environments holds great importance, as a considerable amount of plastics ultimately become marine litter as a result of inadequate management practices during their end-of-life stage. Aquatic ecosystems present significant challenges for biodegradation processes, primarily attributed to factors such as low temperature and a relatively smaller microbial population. Scanning electron microscopy (SEM) images of the vitrimers were captured both

before and after the BOD test, as depicted in (Figure 47). The analysis demonstrates that the vitrimer experienced substantial biodegradation following a 30-day exposure to seawater. Upon examination, it was observed that the pristine samples exhibited a smooth and dense composition. However, after a period of 30 days immersed in seawater, these samples displayed a porous structure, indicating the significant progression of the biodegradation process.

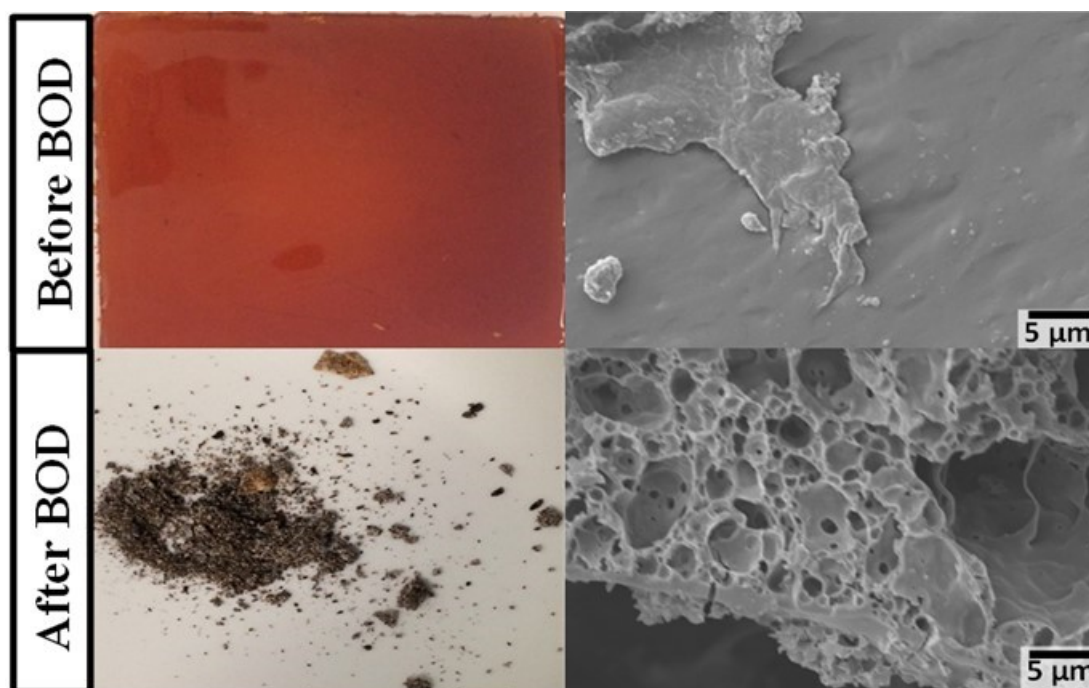


Figure 47. SEM images of the vitrimers 1 before and after BOD.

3.2.4 Vitrimers for packaging

The various processing options, the biobased composition of building blocks, and the environmentally friendly end-of-life characteristics collectively position the vitrimer proposed in this study as a compelling and sustainable alternative to traditional plastics. Additionally, was investigated its potential as a material for packaging by utilizing its good adhesion to paper. This allowed to us explore its application as a freestanding film and as a coating for paper. Due to this, a thorough investigation into the barrier properties, specifically towards oxygen and water vapor, and the migration into food simulatant was evaluated.

3.2.4.1 Water vapor permeability (WVP):

The water vapor permeability (WVP) tests, as depicted in (Figure 48), demonstrate that the WVP of all vitrimers is comparable to that of polyethylene (PE). As an

illustration, Vitrimer 1 exhibited a water vapor permeability (WVP) value of 105.732 ± 1.03 , whereas its permeation efficiency (PE) was measured at 89.17 ± 2.33 . Furthermore, the data demonstrates that the inclusion of oleic acid results in a notable enhancement of water vapor permeability values. The varying quantities of oleic acid present resulted in a notable enhancement of chain mobility in the vitrimers. This, in turn, expanded the potential for water molecule diffusion, ultimately leading to an increase in water vapor permeability (WVP).

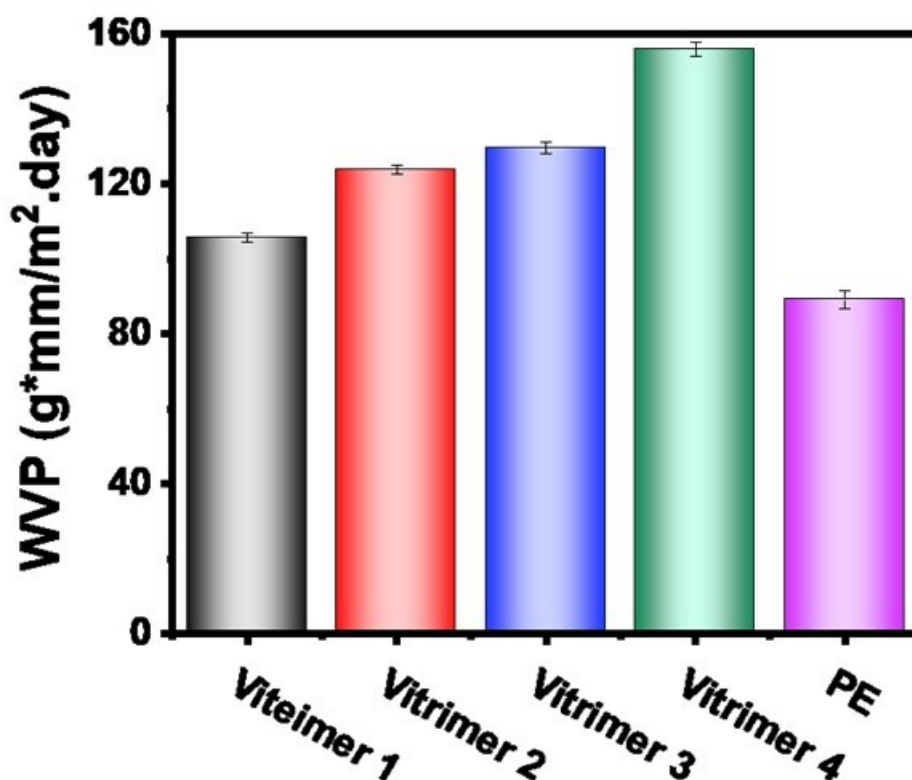


Figure 48. Water vapor permeability of vitrimers and PE.

3.2.4.2 Oxygen permeability (OP):

The measurement of oxygen permeability (OP) is a vital characteristic to consider when evaluating materials intended for packaging applications. According to the data presented in (Figure 49), the OP value for the ESO-VPI vitrimer is $138.16 \text{ (cm}^3\text{.mm/m}^2\text{.24 h)}$, which is significantly lower than that of PE at $866.6 \text{ (cm}^3\text{.mm/m}^2\text{.24 h)}$. However, it is comparable to other packaging materials such as polypropylene (PP) films, which have an OP range of 50 to 100 $\text{(cm}^3\text{.mm/m}^2\text{.24 h)}$ [364], and polystyrene (PS) films with an OP range of 100 to 150 $\text{(cm}^3\text{.mm/m}^2\text{.24 h)}$ [364].

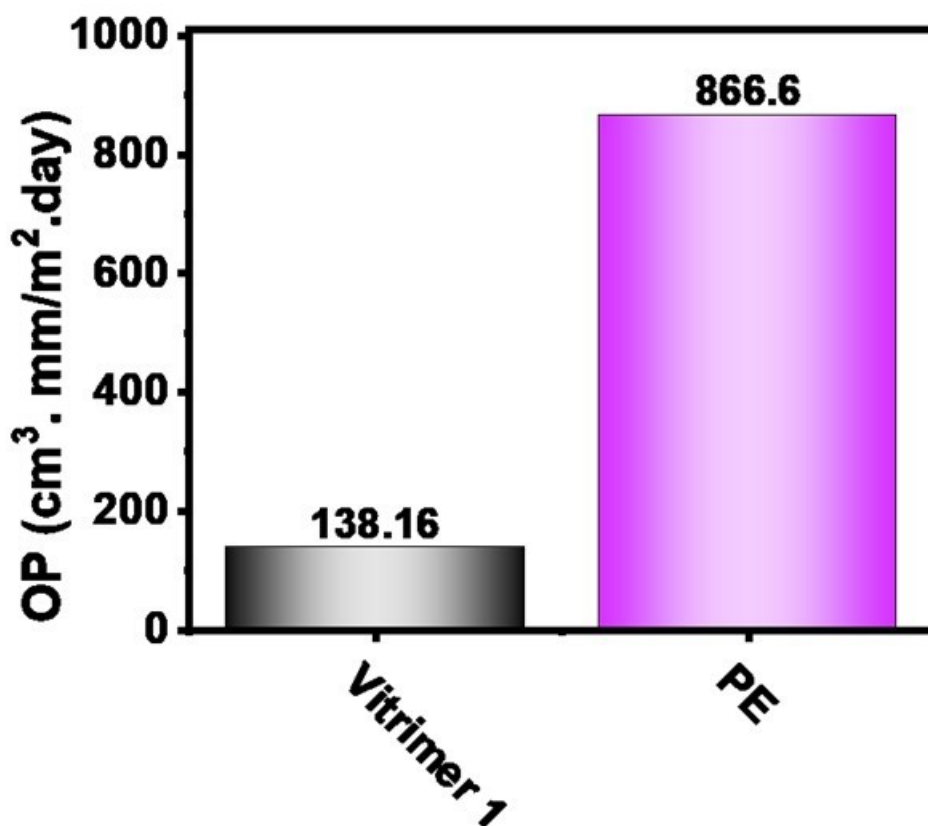


Figure 49. Oxygen permeability of vitrimer1 and PE.

3.2.4.3 Food Contact Migration:

Tests were conducted to assess the migration of compounds into food using a solid food simulant known as Tenax[®]. The results of the comprehensive migration tests indicate that all vitrimers exhibited migration levels significantly below the European Union's limit of 10 mg/dm², as specified in Regulation No 10/2011. This is demonstrated in the data provided (**Figure 50**).

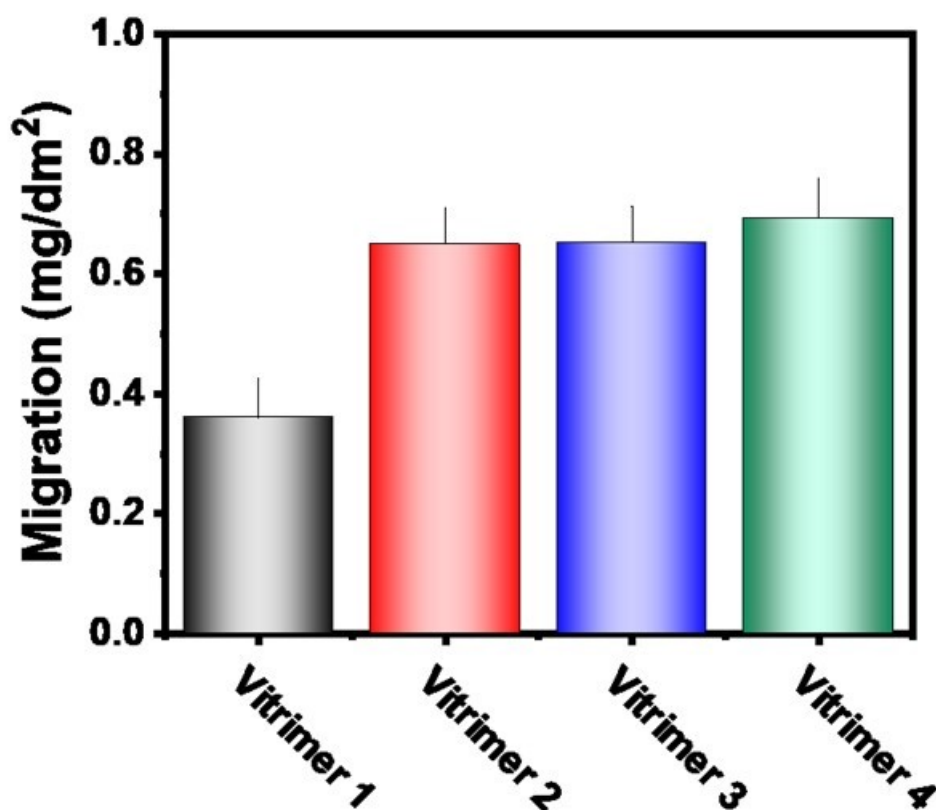


Figure 50. Migration levels of vitrimers samples using Tenax® as food simulants

3.2.4.4 Water contact angle (WCA):

The hydrophobicity of the vitrimers' surface was assessed by conducting a static water contact angle (WCA) measurement. The data are presented, and the WCA (water contact angle) of PE (polyethylene) is illustrated in (Figure 51). All materials were determined to exhibit hydrophobic properties, as evidenced by their water contact angles (WCA) ranging from 115 °C to 110 °C. An observed trend indicated a modest reduction in the water contact angle (WCA) as the OA content increased. Additionally, it was observed that all vitrimers exhibited higher hydrophobicity in comparison to conventional packaging plastic, polyethylene (PE). The discovery indicates that ESO-VPI vitrimer has the potential to serve as a viable substitute for traditional plastics, such as PE, in the realm of flexible food packaging. This innovation could play a significant role in advancing the creation of environmentally sustainable packaging options.

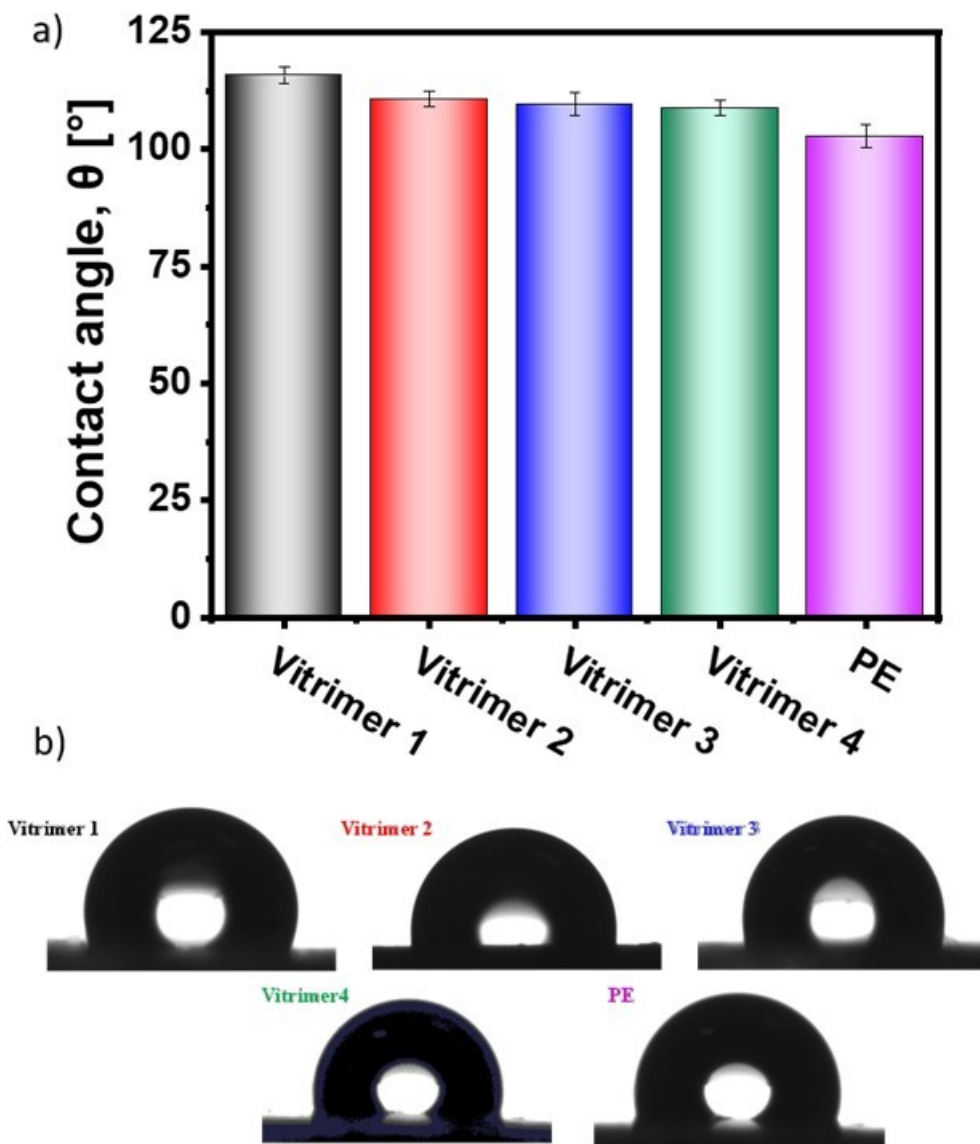


Figure 51. Water Contact Angle of vitrimers and PE.

3.2.4.5 Packaging applications:

Two demonstrators, which utilize the various advantageous properties of vitrimers for packaging applications, include a vitrimer sealed bag and a paper box with a vitrimer coating. These demonstrators, constructed using vitrimer 3, are depicted in (Figure 52a, b). The utilization of the sealed bag capitalizes on the flexibility facilitated by OA and the potential for thermal reprocessing, which is enabled by the exchange of imine bonds, in order to effectively seal the edges. The construction of the box capitalizes on the exceptional adhesive properties between paper and vitrimer. After subjecting the vitrimer to hot pressing on paper, a strong adhesion was successfully obtained, as evidenced by the scanning electron microscopy (SEM) image in (Figure 52c),

Furthermore, the paper coated with the vitrimer exhibited the ability to be folded into a box. The application of a vitrimer coating can enhance the water resistance and oxygen barrier properties of paper, while maintaining the biodegradability of the composite material.

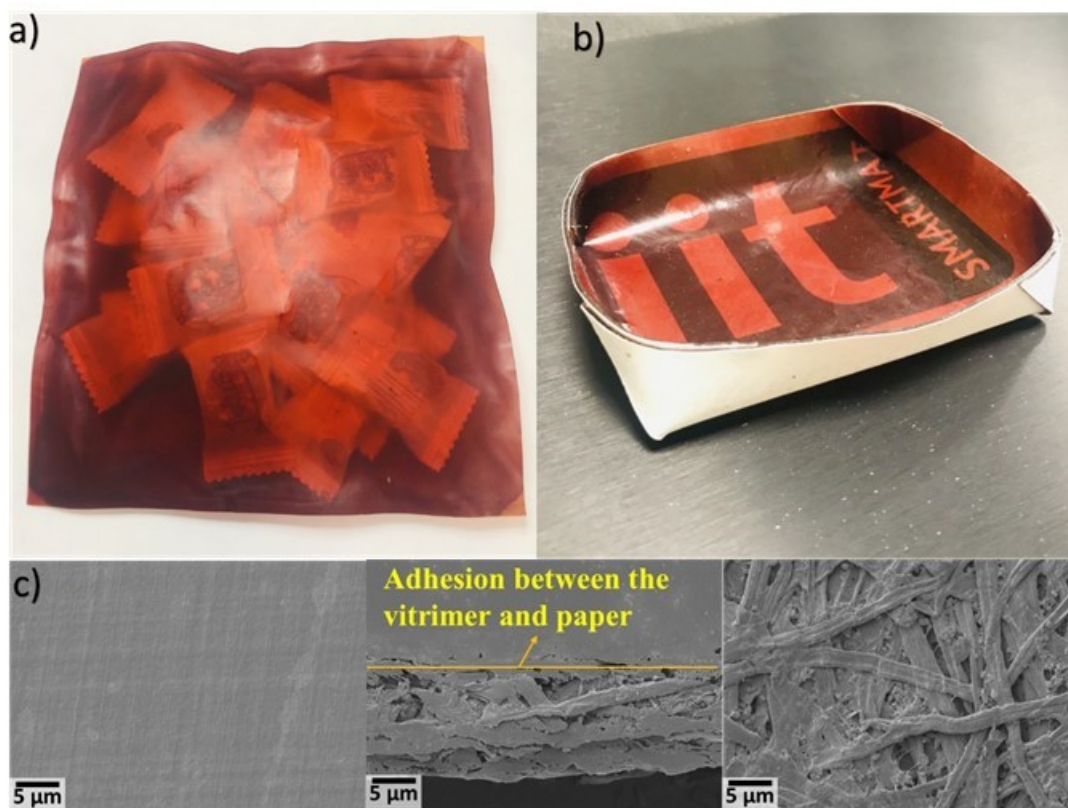


Figure 52. Rectangular container (Pouch) made of vitrimer sealed at the edges. b) Paper box coated with vitrimer, and c) SEM images of the adhesion between the vitrimer and paper.

3.3 CONCLUSIONS

Compared to the previous literature reported the crosslinker was synthesized generally with a lower yield, compared to ours. The process, in these examples, required solvents such as CH_2Cl_2 (in ACS Sustainable Chem. Eng. 2018)[357], or DMSO (in Polymer Testing, 2022)[358], or DMF (in Industrial Crops and Products, 2023) [359] or THF (in RSC Sustain., 2023) [360]. In other papers (e.g., ACS Sustainable Chem. Eng. 2020, 8, 15020–15029)[361], 4,4-diamino diphenyl methane is used as a building block to create the crosslinker, a chemical that has safety concerns and has been included in the Substance of very high concern from the European Chemical Agency. The synthesis between DAM and vanillin takes place at 70°C. The DAM-Vanillin

crosslinker is solid and needs to be melted or dissolved to react. The activation energy (E_a) for the exchange reaction is approximately $108.9 \text{ kJ}\cdot\text{mol}^{-1}$ for the material reported in the paper referenced. The present investigation involved the production of a novel vitrimer by employing only components derived from bio-based sources. In order to accomplish this, epoxidized soybean oil (ESO) was cross-linked with a crosslinker (VPI) that was produced by the coupling of Priamine 1071 with vanillin. All steps were executed in accordance with the principles of green chemistry. In order to produce the vitrimer, a reaction was carried out between the epoxy groups of ESO and the hydroxyl group of VPI, without the requirement of a solvent or catalyst. This process is considered environmentally friendly since it does not generate waste or by-products. Oleic acid (OA) was utilized in addition to the VPI crosslinker in order to react with some of the epoxides that were present in the ESO rather than the VPI. This allowed for the regulation of the crosslink density, which in turn allowed for the fine-tuning of the performance and processing of the vitrimers. It was demonstrated in the thermo-mechanical properties that the presence of OA lowered the glass transition temperature, functioning as an internal plasticizer in the material, increasing the free volume between molecules and decreasing the rigidity of the material. Vitrimers created by ESO-VPI exhibit reversible cross-linking bonds. Two imine bonds can exchange between them when sufficient temperature is provided, enabling the material to be reprocessed and reshaped multiple times without compromising its mechanical properties. In addition, the vitrimers that have been developed offer a barrier against oxygen and water vapor that is comparable to that of polyethylene, and they are able to fulfil the requirements that have been established by the European Commission in relation to the limitations of food migration, which positions them as a potential material for the market of flexible food packaging. The ability to reprocess, recycle, and biodegrade in seawater makes the materials presented here particularly interesting due to their distinctive blend of good mechanical properties and barrier performance characteristic of highly cross-linked thermosets, along with the recyclability of

thermoplastics and environmentally friendly disposal of biopolymers. With the reprocessing of thermoplastics and the benign end-of-life of biopolymers.

3.4 EXPERIMENTAL SECTION

3.4.1 Materials

The Epoxidized Soybean Oil (ESO) was generously supplied by ATP R&D SRL (Italy) and possesses an average molecular weight of 950 g/mol, along with four epoxide groups per molecule. Priamine®1071 is a dimer diamine functional building block, with an average molecular weight of 620 g/mol and 2.2 amino groups per molecule. This compound was generously supplied by Cargill (United Kingdom). Vanillin, ethanol (with a concentration of 96%), oleic acid, and ethyl acetate (also known as EtOAc) were acquired from Merck.

3.4.2 Preparation of VPI cross-linker (Vanillin- Priamine®)

A solution of vanillin (54.5g, 0.358 mol) was prepared by dissolving it in 250 mL of ethanol. Subsequently, Priamine® (100.7 g, 0.1624 mol) was diluted with 50 mL of ethanol (EtOH) and added dropwise to the vanillin solution. The solution was agitated at ambient temperature for a duration of 24 hours in the presence of a nitrogen atmosphere. The chemical reaction took place between the amino group of Priamine® and the aldehyde group of vanillin, resulting in the formation of an orange liquid product. Afterwards, the solvent was eliminated using a rotary evaporator, and the resulting product was dried under vacuum to yield the final product as a dark red liquid with a high viscosity (120 g, 83.2% yield).

3.4.3 Typical Procedure for ESO cross-linking

A predetermined quantity of ESO (epoxidized soybean oil) and VPI (Vanillin-Priamine®) as a cross-linker was introduced into a glass vial and thoroughly blended. Given that both ESO and VPI exhibit liquid properties at room temperature (RT), they can be conveniently combined to yield a uniform reaction mixture, obviating the necessity for solvents. The mixture was introduced into a Teflon mold, and the film was produced through the process of crosslinking ESO and VPI in a vacuum oven, maintained at a temperature of 180 °C for a duration of four days.

3.4.4 Measurements

¹H NMR

The ¹H NMR analysis was conducted at room temperature using 5 mm diameter tubes on a Bruker Avance III 400 MHz spectrometer equipped with a broadband inverse probe. The chemical shifts were expressed in parts per million (ppm) and were calculated relative to tetramethylsilane (TMS).

DSC

The thermal properties of vitrimers were analyzed using a differential scanning calorimeter (DSC) model Discovery DSC 250 TA. The temperature range for the experiment was from -90 degrees Celsius to 150 degrees Celsius at a rate of 10 degrees Celsius per minute. All temperature controls stated above were conducted by using nitrogen as a cell purge gas, with a flow rate of fifty milliliters per minute. The glass transition temperatures were determined based on the results obtained during the second heating process.

TGA

Thermogravimetric analysis (TGA) was employed to assess the thermal stability of the vitrimers. TGA was conducted using a TGA Q 500 analyzer manufactured by TA Instruments. The analysis was performed under a nitrogen atmosphere (flux: 50 mL/min) with the heating rate employed was 10 °C/minute, and the temperature range investigated spanned from 30 to 800 °C.

Mechanical properties

The mechanical characteristics of the cross-linked films of the vitrimers were assessed using a dual-column Instron 3365 universal testing machine equipped with a 10 N load cell and pneumatic clamps. The tests were conducted at room temperature, employing a tensile rate of 10 mm/min. The mechanical test samples were obtained by directly cutting cured materials into dumbbell shapes, adhering to the specifications outlined in ISO 527-2 type 5A (length x breadth x thickness: 2.5 mm³). A minimum of three measurements were undertaken for each sample, and the collected data were subsequently averaged to determine the mean value.

Reprocessability

For conducting reprocessability tests of vitrimers, the compression molding technique was utilized. In order to conduct this test, the films were cut into small pieces with scissors and then were placed inside a square metal mold with a diameter of 10 cm and

a thickness of 1.5 mm. The vitrimer pieces were gradually subjected to compression molding, applying 5 tons of pressure for 20 min at 140°C using a Carver 3853 CE press. After being cooled to room temperature, the obtained films were cut into dog bones and subjected to tensile test. At least five measurements were conducted for each sample. The process described above was subsequently repeated 4 times.

Adhesion strength

The adhesion strength between the samples, namely vitrimers, and a piece of paper, as well as polyethylene and a piece of paper, was assessed through T-peel tests conducted on a dual-column Instron 3365 universal testing equipment. During the adhesion step, the samples (either vitrimer or polyethylene) were carefully pressed onto pieces of paper under the pressure of 1.5 tons for 20 minutes at a temperature of 140°C using a Carver 3853 CE press into the form of rectangle with dimensions of 40 mm by 10 mm by 2.5 mm. During the test, the samples were pulled at a rate of 10 mm/minute, and the force needed to peel the samples from the paper was measured and then divided by the width of the sample to determine the peeling strength, which was expressed in $\text{N}\cdot\text{m}^{-1}$.

DMA

To conduct dynamic mechanical analysis (DMA) on vitrimers, the samples were initially shaped into rectangles measuring 20 mm × 4 mm × 2 mm. Subsequently, the measurements were performed using a Mettler Toledo DMA-1 instrument in the tension mode. During this experiment, the samples underwent temperature variations spanning from -100 to 150°C with a heating rate employed was 3°C/min and a maximum strain amplitude of 0.1% at a single frequency oscillation mode with a frequency of 1 Hz.

Stress relaxation

Stress relaxation tests were conducted on the TA Instruments DMA Q800 using the tensile mode, with a temperature range of 40°C to 160°C. The rectangular specimens, measuring 20 mm × 4 mm × 2 mm, were first preloading with a force of 0.001 N. They were then allowed to reach thermal equilibrium at each test temperature for a duration of 4 minutes. Following that, the specimens underwent an isothermal process lasting 5 minutes. During this time, the specimens were stretched by 1%. After the stretching, the specimens were allowed to recover for 10 minutes to enable the material to relax back to its original state. After that, the temperature was raised by 20 °C, and the

previous steps were repeated until the temperature reached 165°C. The alteration of the relaxation modulus (MPa) versus time was recorded.

Gel fraction

In order to achieve successful crosslinking, the samples underwent a curing process at 180°C within a vacuum oven for a duration of 1 to 8 days. A small piece of the resulting materials, with an approximate mass of 200 mg, was then placed in a vial, followed by the addition of approximately 20 ml of ethyl acetate to the sample. After waiting for 24 hours, the ethyl acetate was discarded, and anything of the material that had not dissolved was washed with ethyl acetate, dried in a fume hood at a temperature of 100 °C for 3 days, and then weighed once more. The gel fraction, which indicates the degree of crosslinking, was determined by comparing the mass of the vitrimer before and after it was exposed to ethyl acetate.

Biochemical oxygen demand (BOD)

The purpose of the experiment was to determine whether or not vitrimers are capable of biodegrading in seawater by measuring the amount of oxygen that was consumed by the microorganisms that were present in the seawater. The seawater was utilized as collected and it contains nutrients as well as microorganisms that are normally found in their natural environments. The experiment was conducted using glass bottles at room temperature, which were sealed with an oxygen-measuring device (OxiTop), additionally, a carbon dioxide scavenger was employed to capture any carbon dioxide generated during the process of biodegradation. The decrease in pressure due to the consumption of oxygen was used to measure the oxygen consumption. To account for any background oxygen consumption, blank samples (seawater without any sample) were utilized, and the results were normalized based on the mass of the sample. Finally, the results were reported as the quantity of oxygen consumed per 100mg of the sample, which provides an indication of the material's biodegradability.

SEM

The morphology of vitrimers was observed using a scanning electron microscope (SEM) model JEOL JSM-6490LA, which was operated in high vacuum mode and utilized a tungsten thermionic electron source. In this experiment, the samples were coated with a 10 nm layer of gold using an auto fine coater (JEOL, JFC-1600). The coated samples were then observed under a scanning electron microscope (SEM) with an accelerating voltage of 5 kV.

Oxygen Permeability

The oxygen permeation properties of ESO-VPI vitrimers and PE film were assessed using an Oxysense 525oi device (Oxysense, USA) that was equipped with a film permeation chamber and OxyDot fluorescence sensor. The system was configured in accordance with the American Society for Testing and Materials (ASTM) Method F3136-15. The tests were carried out under standard laboratory conditions, namely 21 ± 2 °C and 40 ± 10 % relative humidity. In a nutshell, the permeation chamber is a cylinder with two sections (sensing well and driving well). The films were cut into rectangular pieces measuring 6 cm × 6 cm. These pieces were then placed between two wells in the testing module. The sensing well is equipped with a fluorescence sensor called oxydot, which directly measures the concentration of oxygen. This section (sensing well) was purged with nitrogen, while the other one (driving well) was kept open to ambient air. The amount of oxygen that reached the sensing well was measured over time until a constant value was found. This quantity is expressed in cubic centimeters of oxygen that permeated a film measuring 1 millimeter in thickness over an area of 1 square meter within a 24-hour timeframe. It is represented by the formula $OP ((\text{cm}^3 \text{ mm})/(\text{m}^2 \text{ 24 h}))$.

Food Contact Migration

The migration of vitrimers films into food was measured using Tenax[®] as a solid food simulant, following the procedure described in previous studies. Briefly, a circular piece of material measuring approximately 22 mm in diameter was cut and carefully placed inside a clean glass vial. Around 160 mg of Tenax[®] (solid food simulant) were then added to the vial. The vial, with its contents, was subsequently placed in an oven set at a temperature of 70 °C and left undisturbed for a duration of 2 hours. The overall migration was determined through the analysis of the sample's mass differential prior to and after the treatment.

MFI

The melt flow index (MFI) test is conducted by quantifying the mass of the sample that passes through a standardized orifice under consistent temperature and pressure conditions over a predetermined duration. The experimental procedure involved utilizing an Instron CEAST MF20 instrument, following the ISO 1133 standard, at a temperature of 190 °C and applying a load of 10 kg. The MFI value is determined by calculating the average of 10 measurements.

Creep-recovery

The creep behavior was evaluated using DMA (TA-Q800). The dimensions of the sample were 13 mm × 4 mm × 1.3 mm. At first, the sample was heated to 30°C and left to equilibrate for 2 minutes. Following that, a consistent force was applied to stretch the material, with the stress maintained at 0.05 MPa, and after 10 minutes, the force was removed, and the material was recovered.

Chapter 4: Conclusions

In conclusion, the global reliance on petroleum-based materials, particularly in the production of plastics and packaging, has led to severe environmental consequences, including pollution of oceans and marine ecosystems. The persistence of non-biodegradable materials, such as polyethylene and styrofoam, poses significant threats to the environment, marine life, and human health. The escalating production of plastics and the projected increase in plastic waste emphasize the urgent need for sustainable alternatives. The emergence of bioplastics, derived from renewable resources like plant-based materials, presents a promising avenue for reducing the environmental impact of packaging materials. Biodegradable plastics, such as PLA, PHA, and PBS, offer the potential to mitigate the long-lasting effects of traditional plastics, although their optimal degradation depends on specific environmental conditions. Moreover, the development of vitrimers, especially those derived from bio-based sources like epoxidized soybean oil, represents a noteworthy advancement in the quest for eco-friendly packaging materials. The incorporation of epoxidized soybean oil (ESO) in the synthesis of eco-friendly epoxy resins showcases a potential shift towards sustainable industrial operations. The utilization of ESO, a bio-based substance, offers advantages such as high reactivity, cost-effectiveness, and non-toxicity. The resulting composites, engineered for low-temperature curing and enhanced mechanical properties, represent a step forward in developing environmentally friendly alternatives. Vitrimers exhibit characteristics of both thermoplastics and thermosets, allowing for recycling, reprocessing, and remolding without compromising their chemical makeup. Our study introduces an entirely bio-based vitrimer synthesized from epoxidized soybean oil and a bio-based imine crosslinker, offering oxygen and water vapor barrier properties comparable to polyethylene. Importantly, these vitrimers demonstrated the potential for biodegradation in seawater, addressing concerns about their environmental impact.

In conclusion, this thesis highlights the successful synthesis of two distinct bio-based materials with promising applications in sustainable packaging. The first material, a thermoset composite, was produced by cross-linking soybean oil (ESO) with pripol and incorporating carrot waste. This environmentally friendly approach, aligned with

green chemistry principles, resulted in a film-forming process without the generation of waste or byproducts. The incorporation of carrot waste not only enhanced the mechanical properties of the composite but also introduced a naturally occurring foam, showcasing the versatility and potential of utilizing vegetable waste in thermoset materials. Moreover, the composites exhibited superior foaming capabilities after a humidity treatment, demonstrating a novel method to further improve their inherent qualities. In future research and development on soybean oil-based composites with agri-waste for foamed materials, exploring various agricultural by-products beyond carrot powder could shed light on how different agri-waste types impact composite properties. Variations in moisture content, fiber composition, and structural characteristics of different agri-waste materials may influence foaming, mechanical attributes, and thermal insulation properties. Additionally, refining the foaming process by utilizing moisture as the foaming agent could be a focal point. Enhancing foaming techniques may enhance foam uniformity, density, and thermal insulation properties through the manipulation of bubble size, distribution, and foaming conditions such as temperature, pressure, and curing time. Long-term durability assessments under diverse environmental conditions, including sunlight exposure, moisture, and temperature fluctuations, could offer insights into the stability and degradation kinetics of the biobased foam material over time. Furthermore, investigating the commercial feasibility and scalability of manufacturing these biobased foams for applications in construction, insulation, packaging, and other industries is crucial. This evaluation would involve analyzing the economic viability of large-scale production, ensuring consistent quality control, and optimizing manufacturing processes. Delving into the biodegradation behavior of these materials is essential, understanding degradation pathways, rates, and the influence of environmental factors like temperature, pH, and microbial activity. Conducting a life cycle assessment to compare the environmental impact and sustainability benefits of biobased foams with traditional fossil-based materials would provide a comprehensive understanding of their ecological footprint and advantages. The second material, a bio-based vitrimer synthesized from ESO and a crosslinker (VPI), showcased a unique combination of desirable properties. The green chemistry principles were strictly adhered to throughout the synthesis, emphasizing the environmentally friendly nature of the process. The inclusion of oleic acid alongside the crosslinker allowed for the fine-tuning of the vitrimers' performance and processing, resulting in improved

thermal-mechanical properties. The vitrimers exhibited reversible cross-linking bonds, enabling multiple cycles of reprocessing and reshaping without sacrificing mechanical integrity. Additionally, these vitrimers demonstrated oxygen and water vapor barrier properties comparable to polyethylene, meeting European Commission migration limit requirements. This positions them as highly promising materials for the flexible food packaging market. The future plans of this scientific project involve developing prototypes with high shape memory properties that can replace frozen food packaging. In addition, the vitrimer material has the potential to be used in various industries, including robotics, water treatment, automotive, construction, and electronics. Another suggestion is to conduct an LCA (Life Cycle Assessment) analysis, as no existing articles have addressed this topic, and there is a lack of research on this subject. Conducting such an analysis is crucial for the development of sustainable materials in the future. Moreover, while the material has shown promise in biodegradability in seawater, further research could delve deeper into understanding the degradation mechanisms, which often involve a consortium of living microorganisms, and also assess its environmental impact in various disposal scenarios. Transitioning from laboratory-scale to commercial-scale production can be quite challenging. Research efforts should prioritize addressing scalability issues, optimizing cost-effectiveness, and ensuring consistent quality control to facilitate the commercialization of the like this vitrimer material.

Both materials discussed in this thesis offer unique advantages, including recycling potential, and biodegradability in marine environments. The utilization of vegetable waste not only contributes positively to the environment but also enhances the foaming qualities and malleability of thermoset composites. The vitrimers, on the other hand, provide an innovative solution for sustainable and flexible food packaging with a combination of desirable mechanical properties and environmental compatibility. In essence, these bio-based materials represent a significant step towards developing sustainable alternatives to conventional packaging materials, addressing environmental concerns associated with plastic waste. Their diverse properties and eco-friendly synthesis methods make them promising candidates for a greener and more sustainable future in the field of packaging materials.

Bibliography

1. Alamri, M., et al., *Food packaging's materials: A food safety perspective*. 2021. **28**(8): p. 4490-4499.
2. Morris, B.A., *The science and technology of flexible packaging: multilayer films from resin and process to end use*. 2022: William Andrew.
3. Cutter, C.N.J.C.r.i.f.s. and nutrition, *Microbial control by packaging: a review*. 2002. **42**(2): p. 151-161.
4. Saha, N., et al., *Flexible Packaging Material—Manufacturing Processes and Its Application*, in *Food Packaging: Materials, Techniques and Environmental Issues*. 2022, Springer. p. 47-87.
5. Roy, S., et al., *Curcumin and its uses in active and smart food packaging applications-a comprehensive review*. 2022. **375**: p. 131885.
6. Tiwari, M., et al., *Smart Packaging Technology in Food Processing*. p. 202.
7. Rejeesh, C. and T.J.M.T.P. Anto, *Packaging of milk and dairy products: Approaches to sustainable packaging*. 2023. **72**: p. 2946-2951.
8. Dobrucka, R., R.J.J.o.F.P. Przekop, and Preservation, *New perspectives in active and intelligent food packaging*. 2019. **43**(11): p. e14194.
9. Adeyemi, J.O. and O.A.J.B. Fawole, *Metal-Based Nanoparticles in Food Packaging and Coating Technologies: A Review*. 2023. **13**(7): p. 1092.
10. Hamouda, A.F. and S.J.M. Felemban, *A Bio-Indicator Pilot Study Screening Selected Heavy Metals in Female Hair, Nails, and Serum from Lifestyle Cosmetic, Canned Food, and Manufactured Drink Choices*. 2023. **28**(14): p. 5582.
11. Mohamad Haron, D.E., et al., *PFAS, bisphenol, and paraben in Malaysian food and estimated dietary intake*. 2023. **16**(2): p. 161-175.
12. Kokoszka, P. and A.J.M. Milenin, *The Impact of Temperature Conditions on the Manufacturing Process and Mechanical Behavior of Beverage Can Ends during Operation*. 2023. **16**(18): p. 6137.
13. Deshwal, G.K., et al., *An overview of paper and paper based food packaging materials: health safety and environmental concerns*. 2019. **56**: p. 4391-4403.
14. Bauer, A.-S., et al., *Cereal and Confectionary Packaging: Background, Application and Shelf-Life Extension*. 2022. **11**(5): p. 697.
15. Oloyede, O.O. and S.J.F. Lignou, *Sustainable paper-based packaging: A consumer's perspective*. 2021. **10**(5): p. 1035.
16. Ferrara, C. and G.J.J.o.C.P. De Feo, *Comparative life cycle assessment of alternative systems for wine packaging in Italy*. 2020. **259**: p. 120888.
17. Tumuluru, J.S.J.F.P. and P.T.-R. Advances, *Introductory Chapter: Food Processing, Preservation, and Packaging—A Brief Overview*. 2023.
18. Nwosu, J.C. and G.C. Ebuor, *Food packaging materials: Health and environment*.
19. Zhao, X., et al., *Sustainable bioplastics derived from renewable natural resources for food packaging*. 2023. **6**(1): p. 97-127.
20. Ribeiro, L.S., et al., *Use of Post-Consumer Plastics in the Production of Wood-Plastic Composites for Building Components: A Systematic Review*. 2023. **16**(18): p. 6549.
21. Hemavathi, A. and H.J.E.o.p.a.C.P.B.R. Siddaramaiah, *Food packaging: polimers as packaging materials in food supply chains*. 2018: p. 1374-1397.
22. Khanam, P.N., M.A.A.J.A.M.P. AlMaadeed, and C. Science, *Processing and characterization of polyethylene-based composites*. 2015. **1**(2): p. 63-79.

23. Nakamura, A., et al., *Ortho-phosphinobenzenesulfonate: A superb ligand for palladium-catalyzed coordination–insertion copolymerization of polar vinyl monomers*. 2013. **46**(7): p. 1438-1449.
24. Kaminsky, W., *Polyolefins: 50 Years After Ziegler and Natta. II*. Vol. 258. 2013: Springer.
25. Ronca, S., *Polyethylene*, in *Brydson's plastics materials*. 2017, Elsevier. p. 247-278.
26. Gerassimidou, S., et al., *Unpacking the complexity of the polyethylene food contact articles value chain: A chemicals perspective*. 2023. **454**: p. 131422.
27. Geyer, R., J.R. Jambeck, and K.L.J.S.a. Law, *Production, use, and fate of all plastics ever made*. 2017. **3**(7): p. e1700782.
28. Litauski, K., et al., *Environmentally friendly packaging foams: Investigation of the compostability of poly (lactic acid)-based syntactic foams*. 2023. **35**: p. e00527.
29. Kim, Y.T., B. Min, and K.W. Kim, *General characteristics of packaging materials for food system*, in *Innovations in food packaging*. 2014, Elsevier. p. 13-35.
30. Camann, A., et al., *Properties, recycling and alternatives to PE bags*. 2010.
31. Barlow, A.J.I.E.I.M., *The chemistry of polyethylene insulation*. 1991. **7**(1): p. 8-19.
32. Manoli, E. and D.J.H.C.A.w.P.i.t.M.E. Voutsas, *Food containers and packaging materials as possible source of hazardous chemicals to food*. 2019: p. 19-50.
33. Chairat, S. and S.H.J.E.R. Gheewala, *Life cycle assessment and circularity of polyethylene terephthalate bottles via closed and open loop recycling*. 2023. **236**: p. 116788.
34. Siracusa, V. and I.J.P. Blanco, *Bio-polyethylene (Bio-PE), Bio-polypropylene (Bio-PP) and Bio-poly (ethylene terephthalate)(Bio-PET): Recent developments in bio-based polymers analogous to petroleum-derived ones for packaging and engineering applications*. 2020. **12**(8): p. 1641.
35. Song, Y.K., et al., *Combined effects of UV exposure duration and mechanical abrasion on microplastic fragmentation by polymer type*. 2017. **51**(8): p. 4368-4376.
36. Maleki, F., et al., *Synthesis and characterization of waste Styrofoam hypercrosslinked polymer as an adsorbent for CO2 capture*. 2023. **42**(1): p. e13954.
37. Ahmad, A., et al., *Nano packaging–Progress and future perspectives for food safety, and sustainability*. 2023. **35**: p. 100997.
38. Oduneye, T.V., *Migration of Styrene from Polystyrene Food Containers into Food Simulants: A Meta-Analysis*. 2020.
39. Ugoeze, K., et al., *Environmental and public health impacts of plastic wastes due to healthcare and food products packages: A Review*. 2021. **5**(1): p. 1-31.
40. Ngugi, H.N., et al., *Use of expanded polystyrene technology and materials recycling for building construction in Kenya*. 2017. **2**(5): p. 64-71.
41. Arfin, T., et al., *Applications of polystyrene and its role as a base in industrial chemistry*. 2015: p. 269-280.
42. Chandra, M., et al., *Real cost of styrofoam*. 2016.
43. Williams, A.T. and N.J.M.P.B. Rangel-Buitrago, *The past, present, and future of plastic pollution*. 2022. **176**: p. 113429.
44. Farrelly, T.A. and I.C.J.H.h.w.m. Shaw, *Polystyrene as hazardous household waste*. 2017. **45**.
45. An, R., et al., *Recent advances in degradation of polymer plastics by insects inhabiting microorganisms*. 2023. **15**(5): p. 1307.
46. Neal, A., M. Johnson, and M. Havrda, *Multi-level climate action through circular supply chain management of ocean plastic*, in *Handbook of Multi-Level Climate Actions*. 2023, Edward Elgar Publishing. p. 215-241.
47. Guo, C., L.-Q. Zhang, and W.J.C. Jiang, *Biodegrading plastics with a synthetic non-biodegradable enzyme*. 2023. **9**(2): p. 363-376.

48. Bennett, N.J., et al., *Environmental (in) justice in the Anthropocene ocean*. 2023. **147**: p. 105383.
49. MacArthur, E.J.S., *Beyond plastic waste*. 2017, American Association for the Advancement of Science. p. 843-843.
50. Banton, M., et al., *Evaluation of potential health effects associated with occupational and environmental exposure to styrene—an update*. 2019. **22**(1-4): p. 1-130.
51. Sathish, H.J.P.i.f.p., *PLASTICS BASED PACKAGE FORMS & SPECIALITY PACKAGING FOR FOOD PRODUCTS*.
52. Deng, J., et al., *Microplastics released from food containers can suppress lysosomal activity in mouse macrophages*. 2022. **435**: p. 128980.
53. Peñate, C.O., *Microplastics in drinking water, food, and everyday products*. 2021.
54. Becerril-Arreola, R. and R.E.J.S.r. Bucklin, *Beverage bottle capacity, packaging efficiency, and the potential for plastic waste reduction*. 2021. **11**(1): p. 3542.
55. Erceg, T., et al., *Preparation and characterization of biodegradable cellulose acetate-based films with novel plasticizer obtained by polyethylene terephthalate glycolysis intended for active packaging*. 2023: p. 1-20.
56. Su, Z., et al., *Designed biomass materials for “green” electronics: A review of materials, fabrications, devices, and perspectives*. 2022. **125**: p. 100917.
57. Nisticò, R.J.P.T., *Polyethylene terephthalate (PET) in the packaging industry*. 2020. **90**: p. 106707.
58. Ghosh, T., et al., *Comparing Parallel Plastic-to-X Pathways and Their Role in a Circular Economy for PET Bottles*. 2023: p. 2300068.
59. Ncube, L.K., et al., *Environmental impact of food packaging materials: A review of contemporary development from conventional plastics to polylactic acid based materials*. 2020. **13**(21): p. 4994.
60. Yan, Y., et al., *Dibutyl phthalate release from polyvinyl chloride microplastics: Influence of plastic properties and environmental factors*. 2021. **204**: p. 117597.
61. Srivastav, P.J.I.J.o.N.R. and Development, *USE OF PLASTIC BOTTLE AS LOW COST BUILDING MATERIAL: A SUSTAINBLE MATERIAL*. 2023. **8**(3): p. 462-469.
62. Jiménez, L., et al., *Polylactic acid (PLA) as a bioplastic and its possible applications in the food industry*. 2019. **5**(2): p. 2-6.
63. Morales, G.E.M. and S.M.A. Calle, *Best uses of PLA plastic type and agricultural environmental alternatives*. 2020, EasyChair.
64. Kumari, S.V.G., K. Pakshirajan, and G.J.I.J.o.B.M. Pugazhenthii, *Recent advances and future prospects of cellulose, starch, chitosan, polylactic acid and polyhydroxyalkanoates for sustainable food packaging applications*. 2022.
65. Shogren, R., et al., *Plant-based materials and transitioning to a circular economy*. 2019. **19**: p. 194-215.
66. Ada, E., et al., *Identifying the Drivers of Circular Food Packaging: A Comprehensive Review for the Current State of the Food Supply Chain to Be Sustainable and Circular*. 2023. **15**(15): p. 11703.
67. Six, W., et al., *Prediction of interphase strength in 2K injectionmolding of thermoset rubbers and thermoplastics*. 2020.
68. Khan, M.I., et al., *Investigation of impact properties of para-aramid composites made with a thermoplastic-thermoset blend*. 2023. **36**(2): p. 866-866.
69. Velpuri, V.R., S. Kumari, and K.J.J.o.C.S. Muralidharan, *Rapid capture of flow carbon dioxide by hard Epoxy thermosets with the high glass transition temperature*. 2023. **135**(2): p. 24.
70. Zhang, F., et al., *A review on the self-healing ability of epoxy polymers*. 2021. **138**(16): p. 50260.

71. KILINÇ, K.B. and S.A. SELÇUK. *Re-Formation of Waste Plastics through Digital Manufacturing: An architectural point of view*. in *IDU SPAD'20 International Spatial Planning and Design Symposium*.
72. Bhagat, G.V. and P.P.J.J.o.B.E. Savoikar, *Durability related properties of cement composites containing thermoplastic aggregates—A review*. 2022. **53**: p. 104565.
73. Alsaadi, M., et al., *Liquid-based 4D printing of shape memory nanocomposites: a review*. 2023. **7**(1): p. 35.
74. Beach, M., et al., *Self-healing organic coatings—Fundamental chemistry to commercial application*. 2023. **183**: p. 107759.
75. Shree, V., et al., *Use of a combination of phosphorous-containing epoxy resin and silica fillers for development of flame retardant thermoset polymer composites*. 2023. **29**(1): p. 130-143.
76. Cao, Z., et al., *A robust fully bio-based aromatic–aliphatic ketone epoxide monomer for high-performance epoxy resin containing an imine structural moiety*. 2023. **14**(34): p. 3978-3988.
77. Zainuddin, N.A.M.N., et al., *Surface profile analysis of laminated transfemoral prosthetic socket fabricated with different ratios of epoxy resin and acrylic resin*. 2023. **13**(1): p. 2664.
78. Pappa, C.P., S. Torofias, and K.S.J.C. Triantafyllidis, *Sub-Micro Organosolv Lignin as Bio-Based Epoxy Polymer Component: A Sustainable Curing Agent and Additive*. 2023: p. e202300076.
79. Zhao, Y., et al., *Uncovering the mechanism of size effect on the thermomechanical properties of highly cross-linked epoxy resins*. 2022. **126**(13): p. 2593-2607.
80. Poynton, G., *Multi-component epoxy resin formulation for high temperature applications*. 2014: The University of Manchester (United Kingdom).
81. Fpanse, S., et al., *Impact of polymer crosslinking on release mechanisms from long-acting levonorgestrel intrauterine systems*. 2022. **612**: p. 121383.
82. Xie, H., et al., *A critical review on performance and phase separation of thermosetting epoxy asphalt binders and bond coats*. 2022. **326**: p. 126792.
83. Tomić, N.Z. and M.N. Saleh, *Bio-Derived Self-healing Epoxy Resins, in Multifunctional Epoxy Resins: Self-Healing, Thermally and Electrically Conductive Resins*. 2023, Springer. p. 175-208.
84. Lasenko, I., et al., *The Mechanical Properties of Nanocomposites Reinforced with PA6 Electrospun Nanofibers*. 2023. **15**(3): p. 673.
85. Liu, Y., et al., *Closed-Loop Recycling of Carbon Fiber-Reinforced Composites Enabled by a Dual-Dynamic Cross-linked Epoxy Network*. 2023.
86. Zhao, L., et al., *Accelerated-curing epoxy structural film adhesive for bonding lightweight honeycomb sandwich structures*. 2023. **140**(6): p. e53458.
87. Issa, C.A., *Introduction to Multifunctional Epoxy Composites, in Multifunctional Epoxy Resins: Self-Healing, Thermally and Electrically Conductive Resins*. 2023, Springer. p. 1-13.
88. Pulikkalparambil, H., et al., *Corrosion protective self-healing epoxy resin coatings based on inhibitor and polymeric healing agents encapsulated in organic and inorganic micro and nanocontainers*. 2018. **16**: p. 381-395.
89. Ding, X.-M., et al., *Biomass-derived dynamic covalent epoxy thermoset with robust mechanical properties and facile malleability*. 2022. **33**(6): p. 3245-3248.
90. Urbiña-Alvarez, J., et al., *Ammonia surrogates in the synthesis of primary amines*. 2023.
91. Cao, Q., et al., *Achieving higher performances without an external curing agent in natural magnolol-based epoxy resin*. 2022. **33**(4): p. 2195-2199.
92. Yang, Q., et al., *A phosphorus-containing aliphatic amine curing agent towards intrinsic flame-retardant and smoke-suppressive epoxy resins*. 2023. **30**(2): p. 51.

93. Orduna, L., et al., *Are ionic liquids effective curing agents for preparing epoxy adhesives?* 2023. **125**: p. 103438.
94. Farooq, U., J. Teuwen, and C.J.P. Dransfeld, *Toughening of epoxy systems with interpenetrating polymer network (IPN): A review.* 2020. **12**(9): p. 1908.
95. Wang, H., et al., *Study of the epoxy/amine equivalent ratio on thermal properties, cryogenic mechanical properties, and liquid oxygen compatibility of the bisphenol A epoxy resin containing phosphorus.* 2020. **32**(4): p. 429-443.
96. Yung, T.-Y., et al., *Reinforcement of epoxy resin by additives of amine-functionalized graphene nanosheets.* 2020. **11**(1): p. 35.
97. Naeemikhah, E. and H.J.P.S. Behniafar, *Series B, Silica Loaded Binary Epoxy Resins Cured by an Imide–Amine Hardener Suitable for Preparing Transparent and Flexible Coatings.* 2023: p. 1-9.
98. Aziz, T., et al., *Correction: The epoxy resin system: function and role of curing agents.* Carbon Letters, 2023.
99. Gomez-Lopez, A., et al., *Poly (hydroxyurethane) adhesives and coatings: State-of-the-art and future directions.* 2021. **9**(29): p. 9541-9562.
100. Wang, C., et al., *AP/Si-containing polyethylenimine curing agent towards transparent, durable fire-safe, mechanically-robust and tough epoxy resins.* 2023. **451**: p. 138768.
101. Wang, Z., et al., *Curing behavior and thermomechanical performance of bioepoxy resin synthesized from vanillyl alcohol: Effects of the curing agent.* 2021. **13**(17): p. 2891.
102. Wan, J., et al., *Preparation, curing kinetics, and properties of a novel low-volatile starlike aliphatic-polyamine curing agent for epoxy resins.* 2011. **171**(1): p. 357-367.
103. Gobiraman, A., S. Nagaraja, and V. Sathiyamoorthi, *Epoxy Resin as Matrix for Polymer Composites: Factors Influencing the Properties of Polymers and Their Composites*, in *Epoxy-Based Biocomposites*. 2023, CRC Press. p. 1-19.
104. Coenraads, P.A. and L.J.M.A.o.C.A. Marie, *Allergic contact dermatitis in two employees of an ethylene amine-producing factory.* 2019. **76**: p. 181.
105. Gou, H., et al., *Development of molding compounds based on epoxy resin/aromatic amine/benzoxazine for high-temperature electronic packaging applications.* 2022. **307**(12): p. 2200351.
106. Ding, C., et al. *Research and application of fast-curing anticorrosion inner coatings for vessels in an acid environment.* in *Journal of Physics: Conference Series*. 2023. IOP Publishing.
107. Silau, H., et al., *Bio-based amine curing agents prepared from lignin by ring-opening functionalization with cyclic aza-silanes and their curing kinetics investigated for aliphatic and aromatic epoxy species.* 2023. **184**: p. 107822.
108. Xiong, D., et al., *Selective separation of aliphatic and aromatic amines with CO₂ switchable ionic liquids aqueous two-phase systems.* 2013. **15**(7): p. 1941-1948.
109. Chugunova, E., et al., *On the Nucleophilic Reactivity of 4, 6-Dichloro-5-nitrobenzofuroxan with Some Aliphatic and Aromatic Amines: Selective Nucleophilic Substitution.* 2020. **85**(21): p. 13472-13480.
110. Datar, P.M. and E.N.G.J.A.C. Marsh, *Decarboxylation of Aromatic Carboxylic Acids by the Prenylated-FMN-dependent Enzyme Phenazine-1-carboxylic Acid Decarboxylase.* 2021. **11**(18): p. 11723-11732.
111. Zhang, Y., et al., *Bismaleimide resin modified by a propargyl substituted aromatic amine with ultrahigh glass transition temperature, thermomechanical stability and intrinsic flame retardancy.* 2023: p. 105740.
112. Shao, Z.-B., et al., *Phosphorus/sulfur-containing aliphatic polyamide curing agent endowing epoxy resin with well-balanced flame safety, transparency and refractive index.* 2020. **187**: p. 108417.

113. Helal, M.A., et al., *In-vitro comparative evaluation for the surface properties and impact strength of CAD/CAM milled, 3D printed, and polyamide denture base resins*. 2022. **12**(1): p. 126.
114. Baig, Z., et al., *Influence of amine-terminated additives on thermal and mechanical properties of diglycidyl ether of bisphenol A (DGEBA) cured epoxy*. 2020. **137**(8): p. 48404.
115. Fu, K., et al., *Molecular dynamics simulation and experimental studies on the thermomechanical properties of epoxy resin with different anhydride curing agents*. 2019. **11**(6): p. 975.
116. Wang, H., et al., *Synthesis of rosin-based flexible anhydride-type curing agents and properties of the cured epoxy*. 2009. **58**(12): p. 1435-1441.
117. Yoon, M. and C.-S.J.J.o.P.R. Lim, *Comparative experiments on amine vs. acid anhydride curing agents for epoxy resin required for automotive parts*. 2023. **30**(1): p. 9.
118. Saeedi, I.A., T. Andritsch, and A.S.J.P. Vaughan, *On the dielectric behavior of amine and anhydride cured epoxy resins modified using multi-terminal epoxy functional network modifier*. 2019. **11**(8): p. 1271.
119. Li, J., H.H. Aung, and B.J.M. Du, *Curing regime-modulating insulation performance of anhydride-cured epoxy resin: A review*. 2023. **28**(2): p. 547.
120. Sprenger, S.J.J.o.m.s., *Fiber-reinforced composites based on epoxy resins modified with elastomers and surface-modified silica nanoparticles*. 2014. **49**(6): p. 2391-2402.
121. Hamerton, I. and J. Kratz, *The use of thermosets in modern aerospace applications*, in *Thermosets*. 2018, Elsevier. p. 303-340.
122. Russell, B.K., et al., *Examining the influence of carboxylic anhydride structures on the reaction kinetics and processing characteristics of an epoxy resin for wind turbine applications*. 2019. **144**: p. 104353.
123. Rhodes, P.S.J.A.M.A.P., *Advances in anhydride epoxy systems*. 1991. **23**: p. 442-455.
124. Cavezza, F., et al., *A review on adhesively bonded aluminium joints in the automotive industry*. 2020. **10**(6): p. 730.
125. Marotta, A., et al., *Curing behavior and properties of sustainable furan-based epoxy/anhydride resins*. 2019. **20**(10): p. 3831-3841.
126. Suliga, A., I. Hamerton, and A.J.C.P.B.E. Viquerat, *Cycloaliphatic epoxy-based hybrid nanocomposites reinforced with POSS or nanosilica for improved environmental stability in low Earth orbit*. 2018. **138**: p. 66-76.
127. Jia, X.-W., et al., *Flame-Retardant Cycloaliphatic Epoxy Systems with High Dielectric Performance for Electronic Packaging Materials*. 2023. **24**(3): p. 2301.
128. Vidil, T., et al., *Control of reactions and network structures of epoxy thermosets*. 2016. **62**: p. 126-179.
129. Zielinski, D., et al., *Mono N-Alkylated DABCO-Based Ionic Liquids and Their Application as Latent Curing Agents for Epoxy Resins*. 2021. **3**(11): p. 5481-5493.
130. Lee, J.H.J.P., *Using Dihydrazides as Thermal Latent Curing Agents in Epoxy-Based Sealing Materials for Liquid Crystal Displays*. 2020. **13**(1): p. 109.
131. Bantchev, G.B., et al., *Heat-and light-induced thiol-ene oligomerization of soybean oil-based polymercaptopan*. 2018. **135**(17): p. 46150.
132. Sitthiracha, M., *Organic-inorganic hybrid polymer composites*. 2014, ResearchSpace@ Auckland.
133. Owuor, P.S., et al., *Interface chemistry of atomic-scale structures for building bioinspired 3D light-weight and porous architectures*. 2021: p. 115-141.
134. Pradhan, S., et al., *Insight on the chemistry of epoxy and its curing for coating applications: a detailed investigation and future perspectives*. 2016. **55**(8): p. 862-877.

135. Yang, S., et al., *Direct and Catalyst-Free Ester Metathesis Reaction for Covalent Adaptable Networks*. 2023.
136. Chen, J., W. Li, and X. Nie, *Applications of Electrically Conductive Epoxy Adhesives*, in *Multifunctional Epoxy Resins: Self-Healing, Thermally and Electrically Conductive Resins*. 2023, Springer. p. 415-434.
137. Dhanasekar, S., et al., *Study of polymer matrix composites for electronics applications*. 2022. **2022**.
138. Zhao, Y., et al., *Preparation of polyaniline/cellulose nanofiber composites with enhanced anticorrosion performance for waterborne epoxy resin coatings*. 2023.
139. Kim, H.J., et al., *Synthesis of acid anhydride-modified flexible epoxy resins and enhancement of impact resistance in the epoxy composites*. 2023. **140**(1): p. e53249.
140. Taurino, R., F. Bondioli, and M.J.M.T.S. Messori, *Use of different kinds of waste in the construction of new polymer composites*. 2023. **21**: p. 100298.
141. Mishra, K., et al., *Ionic Liquid-Based Polymer Nanocomposites for Sensors, Energy, Biomedicine, and Environmental Applications: Roadmap to the Future*. 2022. **9**(26): p. 2202187.
142. Kazemi, F., *DÉVELOPPEMENT DE NOUVEAUX PRODUITS ÉPOXY BIOSOURCÉS À BASE DE DIOXYDE DE LIMONÈNE*.
143. Zheng, N., et al., *Dynamic covalent polymer networks: a molecular platform for designing functions beyond chemical recycling and self-healing*. 2021. **121**(3): p. 1716-1745.
144. Borrero-López, A.M., et al., *A Review of Rigid Polymeric Cellular Foams and Their Greener Tannin-Based Alternatives*. 2022. **14**(19): p. 3974.
145. Mougel, C., et al., *Phenolic foams: A review of mechanical properties, fire resistance and new trends in phenol substitution*. 2019. **164**: p. 86-117.
146. Tessianan, W., P. Phinyocheep, and T.J.P. Amornsakchai, *Development of Biodegradable Thermosetting Plastic Using Dialdehyde Pineapple Stem Starch*. 2023. **15**(18): p. 3832.
147. Hejna, A., et al., *Waste tire rubber as low-cost and environmentally-friendly modifier in thermoset polymers—A review*. 2020. **108**: p. 106-118.
148. Li, X., et al., *Bismaleimide/phenolic/epoxy ternary resin system for molding compounds in high-temperature electronic packaging applications*. 2022. **61**(12): p. 4191-4201.
149. Yang, W., et al., *Formaldehyde-free self-polymerization of lignin-derived monomers for synthesis of renewable phenolic resin*. 2021. **166**: p. 1312-1319.
150. Thébault, M., et al., *Properties data of phenolic resins synthesized for the impregnation of saturating Kraft paper*. 2018. **20**: p. 345-352.
151. Vaithilingam, S., R. ThangavelRavivarman, and A.J.P.C. Muthukaruppan, *Development of cashew nut shell carbon reinforced thiourea based biophenolic benzoxazine-epoxy composites: High performance biobased coating materials*. 2020. **41**(5): p. 1950-1961.
152. Lerma-Canto, A., et al., *Epoxidized and Maleinized Hemp Oil to Develop Fully Bio-Based Epoxy Resin Based on Anhydride Hardeners*. 2023. **15**(6): p. 1404.
153. Petkov, V.I., et al., *The Influence of Ethynyl In-Chain Crosslinkers on the Properties of 6FDA-Based Polyimides*. 2022. **16**(1): p. 169.
154. Lee, B.M., et al., *Effect of bulky and hydroxyl groups on gas separation performance of polyimide membranes*. 2015. **15**(3): p. 2351-2355.
155. Zhou, Z.-X., et al., *High-performance cyanate ester resins with interpenetration networks for 3D printing*. 2020. **12**(34): p. 38682-38689.

156. Xu, M., et al., *Thermal stability of allyl-functional phthalonitriles-containing benzoxazine/bismaleimide copolymers and their improved mechanical properties*. 2018. **10**(6): p. 596.
157. Wang, B., et al., *A review on prediction and control of curing process-induced deformation of continuous fiber-reinforced thermosetting composite structures*. 2022: p. 107321.
158. PEREIRA, L.d.F.C., *Multiphysics simulation and optimization of the curing process of thick thermosetting epoxy samples: multi-objective genetic algorithm and a conversion rate driven approach*. 2022, Universidade Federal de Pernambuco.
159. Hameed, N., et al., *Rapid cross-linking of epoxy thermosets induced by solvate ionic liquids*. 2020. **2**(7): p. 2651-2657.
160. Unno, N. and T.J.N. Mäkelä, *Thermal Nanoimprint Lithography—A Review of the Process, Mold Fabrication, and Material*. 2023. **13**(14): p. 2031.
161. Mathew, C., S. Naina Mohamed, and L.S.J.P.C. Devanathan, *A comprehensive review of current research on various materials used for developing composite bipolar plates in polymer electrolyte membrane fuel cells*. 2022. **43**(7): p. 4100-4114.
162. Brounstein, Z., et al., *Long-term thermal aging of modified sylgard 184 formulations*. 2021. **13**(18): p. 3125.
163. Auvergne, R., et al., *Biobased thermosetting epoxy: present and future*. 2014. **114**(2): p. 1082-1115.
164. Pham, H.Q. and M.J.J.U.s.E.o.I.C. Marks, *Epoxy resins*. 2000.
165. Williams, J.G. *Composite material offshore corrosion solutions*. in *International workshop on corrosion control of marine structures and pipelines*. Galveston, Texas. 1999.
166. Li, X., et al., *Preparation of low- κ polyimide resin with outstanding stability of dielectric properties versus temperature by adding a reactive Cardo-containing diluent*. 2019. **177**: p. 107401.
167. Laurenzi, S., M.J.C. Marchetti, and t. properties, *Advanced composite materials by resin transfer molding for aerospace applications*. 2012: p. 197-226.
168. Norkhairunnisa, M., et al., *Evolution of aerospace composite materials*, in *Advanced Composites in Aerospace Engineering Applications*. 2022, Springer. p. 367-385.
169. Sayam, A., et al., *A review on carbon fiber-reinforced hierarchical composites: Mechanical performance, manufacturing process, structural applications and allied challenges*. 2022. **32**(5): p. 1173-1205.
170. Zhang, J., et al., *Past, present and future prospective of global carbon fibre composite developments and applications*. 2022: p. 110463.
171. Mohanty, A.K., et al., *Sustainable polymers*. 2022. **2**(1): p. 46.
172. Liu, G., et al., *Additive manufacturing of structural materials*. 2021. **145**: p. 100596.
173. Daehn, K., et al., *Innovations to decarbonize materials industries*. 2022. **7**(4): p. 275-294.
174. Shehab, E., et al., *Cost modelling for recycling fiber-reinforced composites: State-of-the-art and future research*. 2022. **15**(1): p. 150.
175. Wu, M., et al., *A novel life cycle assessment and life cycle costing framework for carbon fibre-reinforced composite materials in the aviation industry*. 2023. **28**(5): p. 566-589.
176. Dunky, M.J.B.A.S., *Characteristics and Applications, Applications and Industrial Implementations of Naturally-Based Adhesives*. 2023: p. 659-704.
177. Anni, I.A., et al. *Repair of Damaged Fiber Reinforced Polymer Composites with Cold Spray*. in *ITSC 2023*. 2023. ASM International.
178. Kandelbauer, A., et al., *Unsaturated polyesters and vinyl esters*, in *Handbook of thermoset plastics*. 2022, Elsevier. p. 97-158.

179. Post, W., et al., *A review on the potential and limitations of recyclable thermosets for structural applications*. 2020. **60**(2): p. 359-388.
180. Yan, B., et al., *Research and Application Progress of Resin-Based Composite Materials in the Electrical Insulation Field*. 2023. **16**(19): p. 6394.
181. Bangash, M.K., *Polymer Recycling Techniques*, in *Advanced Functional Polymers: Synthesis to Applications*. 2023, Springer. p. 199-216.
182. Morici, E. and N.T.J.P. Dintcheva, *Recycling of thermoset materials and thermoset-based composites: challenge and opportunity*. 2022. **14**(19): p. 4153.
183. Okajima, I., et al., *Chemical recycling of carbon fiber reinforced plastic using supercritical methanol*. 2014. **91**: p. 68-76.
184. Al Rashid, A. and M.J.M.T.S. Koç, *Additive Manufacturing for Sustainability and Circular Economy: Needs, Challenges, and Opportunities for 3D Printing of Recycled Polymeric Waste*. 2023: p. 100529.
185. Agbo, P., et al., *Bio-Oil-Based Epoxy Resins from Thermochemical Processing of Sustainable Resources: A Short Review*. 2023. **7**(9): p. 374.
186. Eze, W.U., et al., *Plastics waste management: A review of pyrolysis technology*. 2021. **1**(1): p. 50-69.
187. Chen, Y., et al., *Flame-Retardant and Recyclable Soybean Oil-Based Thermosets Enabled by the Dynamic Phosphate Ester and Tannic Acid*. 2023. **15**(4): p. 5963-5973.
188. Xue, X., et al., *A technology review of recycling methods for fiber-reinforced thermosets*. 2022. **41**(11-12): p. 459-480.
189. de Luzuriaga, A.R., et al., *Epoxy resin with exchangeable disulfide crosslinks to obtain reprocessable, repairable and recyclable fiber-reinforced thermoset composites*. 2016. **3**(3): p. 241-247.
190. Cárdenas-Alcaide, M.F., et al., *Environmental impact and mitigation of micro (nano) plastics pollution using green catalytic tools and green analytical methods*. 2022. **3**: p. 100031.
191. Chen, X., et al., *Degradable and recyclable bio-based thermoset epoxy resins*. 2020. **22**(13): p. 4187-4198.
192. Zych, A., et al., *Biobased, biodegradable, self-healing boronic ester vitrimers from epoxidized soybean oil acrylate*. 2020. **3**(2): p. 1135-1144.
193. Patil, N.V. and A.N.J.J.o.A.P.S. Netravali, *Microfibrillated cellulose-reinforced nonedible starch-based thermoset biocomposites*. 2016. **133**(45).
194. Wang, C., S.S. Kelley, and R.A.J.C. Venditti, *Lignin-based thermoplastic materials*. 2016. **9**(8): p. 770-783.
195. Walker, W., *Photopolymer Networks with Tunable Command Destruct Properties*. 2021.
196. Wang, B., et al., *Facile synthesis of "digestible", rigid-and-flexible, bio-based building block for high-performance degradable thermosetting plastics*. 2020. **22**(4): p. 1275-1290.
197. Chia, W.Y., et al., *Nature's fight against plastic pollution: Algae for plastic biodegradation and bioplastics production*. 2020. **4**: p. 100065.
198. Asyraf, M., et al., *Thermal properties of oil palm lignocellulosic fibre reinforced polymer composites: a comprehensive review on thermogravimetry analysis*. 2023. **30**(5): p. 2753-2790.
199. Yu, S., et al., *Topological network design toward high-performance vegetable oil-based elastomers*. 2023.
200. Sobhan, A., et al., *Derivation and characterization of epoxidized soybean oil and epoxy resin film produced using a three step-washing neutralization process*. 2023. **198**: p. 116675.

201. Qian, Z., et al., *Versatile Epoxidized Soybean Oil-Based Resin with Excellent Adhesion and Film-Forming Property*. 2023.
202. Kumar, V., A. Khan, and M.J.P.i.O.C. Rabnawaz, *A plant oil-based eco-friendly approach for paper coatings and their packaging applications*. 2023. **176**: p. 107386.
203. Nepomuceno, N., et al., *Bio-Based Epoxy Resins of Epoxidized Soybean oil Cured with Salicylic acid Loaded with Chitosan: Evaluation of Physical–Chemical Properties*. 2023. **31**(6): p. 2566-2575.
204. Sobhan, A., et al. *Green synthesis of epoxidized soybean oil for bio-resin in sustainable packaging application*. in *2023 ASABE Annual International Meeting*. 2023. American Society of Agricultural and Biological Engineers.
205. Fadda, M., et al., *Hydrophobic and water resistant fish leather: a fully sustainable combination of discarded biomass and by-products of the food industry*. 2024. **26**(1): p. 542-555.
206. Zeng, R.-T., et al., *Curing behavior of epoxidized soybean oil with biobased dicarboxylic acids*. 2017. **57**: p. 281-287.
207. Ma, S. and D.C.J.M. Webster, *Naturally occurring acids as cross-linkers to yield VOC-free, high-performance, fully bio-based, degradable thermosets*. 2015. **48**(19): p. 7127-7137.
208. Zúñiga, M., F.L. Aranda, and B.L.J.J.o.t.C.C.S. Rivas, *POLYMERS RECYCLING: UPCYCLING TECHNIQUES. AN OVERVIEW*. 2023. **68**(2): p. 5876-5886.
209. SK, M.M., *SPATIAL ANALYSIS OF SOLID WASTE GENERATION PATTERNS IN A FAST-GROWING INDUSTRIAL CITY-DURGAPUR, INDIA*. 2023.
210. Alali, S.A., M.K. Aldaihani, and K.M.J.A.S. Alanezi, *Plant Design for the Conversion of Plastic Waste into Valuable Chemicals (Alkyl Aromatics)*. 2023. **13**(16): p. 9221.
211. Sari, D., et al. *Reduce marine debris policy in Indonesia*. in *IOP Conference Series: Earth and Environmental Science*. 2021. IOP Publishing.
212. MacArthur, E., *Beyond plastic waste*. *Science*, 2017. **358**(6365): p. 843.
213. Veettil, B.K., et al., *Coastal and marine plastic litter monitoring using remote sensing: A review*. 2022: p. 108160.
214. Gallo, F., et al., *Marine Litter Plastics and Microplastics and Their Toxic Chemicals Components*. 2020. **159**.
215. Kruse, K., et al., *Plastic Debris and Its Impacts on Marine Mammals*, in *Marine Mammals: A Deep Dive into the World of Science*. 2023, Springer International Publishing Cham. p. 49-62.
216. Singh, N., et al., *Recycling of plastic solid waste: A state of art review and future applications*. 2017. **115**: p. 409-422.
217. Wróblewska-Krepsztul, J., et al., *Recent progress in biodegradable polymers and nanocomposite-based packaging materials for sustainable environment*. 2018. **23**(4): p. 383-395.
218. Emadian, S.M., T.T. Onay, and B.J.W.m. Demirel, *Biodegradation of bioplastics in natural environments*. 2017. **59**: p. 526-536.
219. Zimmermann, L., et al., *Are bioplastics and plant-based materials safer than conventional plastics? In vitro toxicity and chemical composition*. 2020. **145**: p. 106066.
220. Abdur Rahman, M., et al., *A review of environmental friendly green composites: production methods, current progresses, and challenges*. 2023: p. 1-25.
221. Ortiz, S.P.J.P.b., *Are bioplastics the solution to the plastic pollution problem?* 2023. **21**(3).
222. Rashdan, W. and A. Ashour. *MYCELIUM-BASED MATERIALS: AN ALTERNATIVE FOR SUSTAINABLE INTERIOR DESIGN*. in *Ideas*.

223. Rathinamoorthy, R., et al., *Mycelium as sustainable textile material—review on recent research and future prospective*. 2023.
224. Kim, M.S., et al., *A Review of Biodegradable Plastics: Chemistry, Applications, Properties, and Future Research Needs*. 2023. **123**(16): p. 9915-9939.
225. Mazumder, M.A.R., M.F. Jubayer, and T.V.J.B.f.Z.W.E.W.M.T. Ranganathan, *Biodegradation of plastics by microorganisms*. 2022: p. 123-141.
226. Moshood, T.D., et al., *Biodegradable plastic applications towards sustainability: A recent innovations in the green product*. 2022. **6**: p. 100404.
227. Idris, S.N., et al., *The degradation of single-use plastics and commercially viable bioplastics in the environment: A review*. 2023. **231**: p. 115988.
228. <https://www.european-bioplastics.org/>. *Bioplastics market development update 2023*. 2023; Available from: manuscript.
229. Haider, T.P., et al., *Plastics of the future? The impact of biodegradable polymers on the environment and on society*. 2019. **58**(1): p. 50-62.
230. Simó-Cabrera, L., et al., *Haloarchaea as cell factories to produce bioplastics*. 2021. **19**(3): p. 159.
231. Rosenboom, J.-G., R. Langer, and G.J.N.R.M. Traverso, *Bioplastics for a circular economy*. 2022. **7**(2): p. 117-137.
232. Alshehrei, F.J.J.o.A. and E. Microbiology, *Biodegradation of synthetic and natural plastic by microorganisms*. 2017. **5**(1): p. 8-19.
233. Akshaykranth, A., T.V. Rao, and R.R.J.M.L. Kumar, *Growth of ZnO nanorods on biodegradable poly (lactic acid)(PLA) substrates by low temperature solution method*. 2020. **259**: p. 126807.
234. Strangis, G., et al., *Seawater Biodegradable Poly (butylene succinate-co-adipate)—Wheat Bran Biocomposites*. 2023. **16**(7): p. 2593.
235. Meereboer, K.W., M. Misra, and A.K.J.G.C. Mohanty, *Review of recent advances in the biodegradability of polyhydroxyalkanoate (PHA) bioplastics and their composites*. 2020. **22**(17): p. 5519-5558.
236. Mealing, V.S., A.E.J.C.T. Landis, and E. Policy, *A life cycle assessment of guar agriculture*. 2023: p. 1-8.
237. Li, Y., et al., *Effects of soybean varieties on life-cycle greenhouse gas emissions of biodiesel and renewable diesel*. 2023. **17**(3): p. 449-462.
238. Romeiko, X.X., et al., *Spatially and temporally explicit life cycle environmental impacts of soybean production in the US Midwest*. 2020. **54**(8): p. 4758-4768.
239. Riaz, B., et al., *Life cycle environmental and cost implications of isostearic acid production for pharmaceutical and personal care products*. 2019. **7**(18): p. 15247-15258.
240. Huang, X., et al., *Upcycling of plastic wastes and biomass to mechanically robust yet recyclable energy-harvesting materials*. 2023. **116**: p. 108843.
241. Arias, A., et al., *Cradle-to-gate Life Cycle Assessment of bio-adhesives for the wood panel industry. A comparison with petrochemical alternatives*. 2020. **738**: p. 140357.
242. Ghasemi, S., et al., *A preliminary environmental assessment of epoxidized sucrose soyate (ESS)-based biocomposite*. 2020. **25**(12): p. 2797.
243. Liu, Y., et al., *Versatile levulinic acid-derived dynamic covalent thermosets enabled by in situ generated imine and multiple hydrogen bonds*. 2023. **451**: p. 139053.
244. Jeon, D., et al., *Fully Recyclable Covalent Adaptable Network Composite with Segregated Hexagonal Boron Nitride Structure for Efficient Heat Dissipation*. 2023.
245. Montarnal, D., et al., *Silica-like malleable materials from permanent organic networks*. 2011. **334**(6058): p. 965-968.
246. He, C., et al., *Poly (oxime–ester) vitrimers with catalyst-free bond exchange*. 2019. **141**(35): p. 13753-13757.

247. Denissen, W., J.M. Winne, and F.E.J.C.s. Du Prez, *Vitrimers: permanent organic networks with glass-like fluidity*. 2016. **7**(1): p. 30-38.
248. Röttger, M., et al., *High-performance vitrimers from commodity thermoplastics through dioxaborolane metathesis*. 2017. **356**(6333): p. 62-65.
249. Li, W., et al., *Readily recyclable, high-performance catalyst-free tung oil-derived vitrimer and carbon fiber reinforced composites*. 2023.
250. Dahlke, J., et al., *How to design a self-healing polymer: general concepts of dynamic covalent bonds and their application for intrinsic healable materials*. 2018. **5**(17): p. 1800051.
251. Obadia, M.M., et al., *Reprocessing and recycling of highly cross-linked ion-conducting networks through transalkylation exchanges of C–N bonds*. 2015. **137**(18): p. 6078-6083.
252. Hendriks, B., et al., *Poly (thioether) vitrimers via transalkylation of trialkylsulfonium salts*. 2017. **6**(9): p. 930-934.
253. Jin, Y., et al., *Malleable and recyclable thermosets: the next generation of plastics*. 2019. **1**(6): p. 1456-1493.
254. Peng, J., et al., *High-performance epoxy vitrimer with superior self-healing, shape-memory, flame retardancy, and antibacterial properties based on multifunctional curing agent*. 2022. **242**: p. 110109.
255. Capelot, M., et al., *Metal-catalyzed transesterification for healing and assembling of thermosets*. 2012. **134**(18): p. 7664-7667.
256. Zhang, H., et al., *Recycling strategies for vitrimers*. 2022. **13**(3): p. 367-390.
257. Liu, Y.-Y., et al., *Biobased high-performance epoxy vitrimer with UV shielding for recyclable carbon fiber reinforced composites*. 2021. **9**(12): p. 4638-4647.
258. Chen, Y., et al., *Mechanically robust, self-healable, and reprocessable elastomers enabled by dynamic dual cross-links*. 2019. **52**(10): p. 3805-3812.
259. Zheng, J., et al., *Vitrimers: Current research trends and their emerging applications*. 2021. **51**: p. 586-625.
260. Wang, S., et al., *Fully recyclable and reprocessable polystyrene-based vitrimers with improved thermal stability and mechanical properties through nitrogen-coordinating cyclic boronic ester bonds*. 2021. **570**: p. 151157.
261. Van Zee, N.J. and R.J.P.i.P.S. Nicolaÿ, *Vitrimers: Permanently crosslinked polymers with dynamic network topology*. 2020. **104**: p. 101233.
262. Legrand, A.I. and C.J.M. Soulié-Ziakovic, *Silica–epoxy vitrimer nanocomposites*. 2016. **49**(16): p. 5893-5902.
263. Zhou, Z., et al., *Synthesis of vanillin-based polyimine vitrimers with excellent reprocessability, fast chemical degradability, and adhesion*. 2020. **2**(12): p. 5716-5725.
264. Subramaniyan, S., et al., *Vanillin-Derived Thermally Reprocessable and Chemically Recyclable Schiff-Base Epoxy Thermosets*. 2023. **7**(4): p. 2200234.
265. Chen, M., et al., *Rapid stress relaxation and moderate temperature of malleability enabled by the synergy of disulfide metathesis and carboxylate transesterification in epoxy vitrimers*. 2019. **8**(3): p. 255-260.
266. Chen, H., et al., *Spiroborate-Linked Ionic Covalent Adaptable Networks with Rapid Reprocessability and Closed-Loop Recyclability*. 2023. **145**(16): p. 9112-9117.
267. De, S., et al., *Biomass-derived composites for various applications*, in *Advances in Bioenergy*. 2023, Elsevier. p. 145-196.
268. Haida, P., et al., *Starch-Reinforced Vinylogous Urethane Vitrimer Composites: An Approach to Biobased, Reprocessable, and Biodegradable Materials*. 2023.
269. Li, J., S. Zhang, and B.J.J.o.A.P.S. Ju, *Soft, fully bio-based poly-hydroxyl thermosets based on catalyst-free transesterification with decent re-processability*. 2022. **139**(30): p. e52676.

270. Zhao, W., et al., *Vitrimer-cellulose paper composites: a new class of strong, smart, green, and sustainable materials*. 2019. **11**(39): p. 36090-36099.
271. Lucherelli, M.A., A. Duval, and L.J.P.i.P.S. Avérous, *Biobased vitrimers: Towards sustainable and adaptable performing polymer materials*. 2022. **127**: p. 101515.
272. Wang, S., et al., *Robust, fire-safe, monomer-recovery, highly malleable thermosets from renewable bioresources*. 2018. **51**(20): p. 8001-8012.
273. Paipa-Álvarez, H., W.P. Alvarado, and B.M. Delgado. *Biodegradable thermosets polymers as an alternative solution to pollution generated by plastics*. in *Journal of Physics: Conference Series*. 2020. IOP Publishing.
274. Chen, Z., et al., *Tough epoxy vitrimer with hybrid networks and its applications in reprocessable composites*. 2023.
275. Yang, S., et al., *Enhanced Shape Memory Metal-Coordinated Poly (aryl ether ketone) s with Tunable Gradient-Deformation Behaviors as well as Self-Healing and Reprocessing Abilities*. 2022. **14**(17): p. 20032-20041.
276. Okubo, H., S.J.J.o.M.C. Yao, and W. Management, *Restoring mechanism of mechanical properties of recycled polyethylene pellet moldings by a repelletizing treatment using a twin-screw extruder*. 2021. **23**: p. 1152-1176.
277. Zhong, L., et al., *Closed-loop recyclable fully bio-based epoxy vitrimers from ferulic acid-derived hyperbranched epoxy resin*. 2022. **55**(2): p. 595-607.
278. Hubbard, A.M., et al., *Recyclability of Vitrimer Materials: Impact of Catalyst and Processing Conditions*. 2022. **7**(33): p. 29125-29134.
279. Kim, S., et al., *Closed-loop additive manufacturing of upcycled commodity plastic through dynamic cross-linking*. 2022. **8**(22): p. eabn6006.
280. Sun, X., et al., *Biobased plastic: A plausible solution toward carbon neutrality in plastic industry?* 2022. **435**: p. 129037.
281. Kwesiga, D.J.R.J.o.E., Science, Technology and Environment, *Strategies for managing plastic waste from construction and manufacturing projects*. 2018. **1**(1).
282. Barbault, L., V.J.I.j.o.e.s. Revest, and n. resources, *Bio-based Plastics: a 'Sustainable' Alternative for the Plastic Industry?* 2023. **31**(5).
283. Zhang, J., et al., *Malleable and recyclable conductive mwcnt-vitrimer composite for flexible electronics*. 2020. **3**(5): p. 4845-4850.
284. Zhao, Y., et al., *Mechanically Robust, Heat-Resistant, and Reprocessable Polyethylene Vitrimers Cross-Linked by β -Hydroxy Ester Bonds via Reactive Processing*. 2022. **61**(35): p. 13126-13135.
285. Gao, H., et al., *White Light Emissive Vitrimers for Phosphor-free Light Emitting Diode Encapsulations*. 2022.
286. Ahn, B.K., et al., *Thermally stable, transparent, pressure-sensitive adhesives from epoxidized and dihydroxyl soybean oil*. 2011. **12**(5): p. 1839-1843.
287. Francioso, L., et al., *PDMS/Kapton interface plasma treatment effects on the polymeric package for a wearable thermoelectric generator*. 2013. **5**(14): p. 6586-6590.
288. Cho, S., et al., *Recent progress in self-healing polymers and hydrogels based on reversible dynamic B–O bonds: boronic/boronate esters, borax, and benzoxaborole*. 2021. **9**(26): p. 14630-14655.
289. Kim, N.K., et al., *3D hierarchical scaffolds enabled by a post-patternable, reconfigurable, and biocompatible 2D vitrimer film for tissue engineering applications*. 2019. **7**(21): p. 3341-3345.
290. Kim, W., et al., *Manufacture of antibacterial carbon fiber-reinforced plastics (CFRP) using imine-based epoxy vitrimer for medical application*. *Heliyon*, 2023. **9**(6): p. e16945.

291. Niu, W., et al., *Photonic vitrimer elastomer with self-healing, high toughness, mechanochromism, and excellent durability based on dynamic covalent bond*. 2021. **31**(13): p. 2009017.
292. Prathumrat, P., et al., *Shape memory elastomers: A review of synthesis, design, advanced manufacturing, and emerging applications*. 2022. **33**(6): p. 1782-1808.
293. Kausar, A.J.e.-P., *Shape memory polymer/graphene nanocomposites: State-of-the-art*. 2022. **22**(1): p. 165-181.
294. Joe, J., et al., *A 4D Printable Shape Memory Vitrimer with Repairability and Recyclability through Network Architecture Tailoring from Commercial Poly(ϵ -caprolactone)*. *Adv Sci (Weinh)*, 2021. **8**(24): p. e2103682.
295. Yang, Z., et al., *Dual-triggered and thermally reconfigurable shape memory graphene-vitrimer composites*. 2016. **8**(33): p. 21691-21699.
296. Yue, L., et al., *One-pot Synthesis of Depolymerizable δ -lactone Based Vitrimers*. 2023: p. 2300954.
297. Bui, K., et al., *Tailoring electromechanical properties of natural rubber vitrimers by cross-linkers*. 2022. **61**(25): p. 8871-8880.
298. Choi, S., et al., *Weldable and Reprocessable Shape Memory Epoxy Vitrimer Enabled by Controlled Formulation for Extrusion-Based 4D Printing Applications*. 2022. **24**(4): p. 2101497.
299. Schenk, V., et al., *Vitrimer composites: Current state and future challenges*. 2022.
300. Wang, S., et al., *Facile preparation of polyimine vitrimers with enhanced creep resistance and thermal and mechanical properties via metal coordination*. 2020. **53**(8): p. 2919-2931.
301. Cuminet, F., et al., *Neighboring Group Participation and Internal Catalysis Effects on Exchangeable Covalent Bonds: Application to the Thriving Field of Vitrimer Chemistry*. 2021. **54**(9): p. 3927-3961.
302. Liu, T., et al., *Glycerol induced catalyst-free curing of epoxy and vitrimer preparation*. 2019. **40**(7): p. 1800889.
303. Ruiz de Luzuriaga, A., et al., *Aero Grade Epoxy Vitrimer towards Commercialization*. 2022. **14**(15): p. 3180.
304. Ike, E.J.G.J.o.P. and A. Sciences, *The study of viscosity-temperature dependence and activation energy for palm oil and soybean oil*. 2019. **25**(2): p. 209-217.
305. Biswal, A.K., et al., *Ultrasonic welding of fiber reinforced vitrimer composites*. 2023. **242**: p. 110202.
306. Zhang, Y.-h., et al., *Sustainable castor oil-based vitrimers: Towards new materials with reprocessability, self-healing, degradable and UV-blocking characteristics*. 2023. **193**: p. 116210.
307. Li, J., et al., *Hydroxyl-Terminated Polybutadiene-Based Polyurethane with Self-Healing and Reprocessing Capabilities*. *ACS Omega*, 2022. **7**(12): p. 10156-10166.
308. Berne, D., et al., *Catalyst-Free Epoxy Vitrimers Based on Transesterification Internally Activated by an α -CF₃ Group*. 2022. **55**(5): p. 1669-1679.
309. Singh, G., *Computational Studies of Vitrimers, Semicrystalline Polymers and Metals: Deformation, Actuation and Fabrication*. 2023.
310. Zhou, Z., et al., *Unraveling a path for multi-cycle recycling of tailored fiber-reinforced vitrimer composites*. 2022. **3**(9).
311. Kim, G., C. Caglayan, and G.J.J.A.o. Yun, *Epoxy-Based Catalyst-Free Self-Healing Elastomers at Room Temperature Employing Aromatic Disulfide and Hydrogen Bonds*. 2022. **7**(49): p. 44750-44761.
312. Rinehart, J.M., J.R. Reynolds, and S.K.J.A.A.P.M. Yee, *Limitations of Diels–Alder Dynamic Covalent Networks as Thermal Conductivity Switches*. 2022. **4**(2): p. 1218-1224.

313. Liu, F., et al., *Diels–Alder Reactivities of Strained and Unstrained Cycloalkenes with Normal and Inverse-Electron-Demand Dienes: Activation Barriers and Distortion/Interaction Analysis*. *Journal of the American Chemical Society*, 2013. **135**(41): p. 15642-15649.
314. Carneiro de Oliveira, J., M.-P. Laborie, and V.J.M. Roucoules, *Thermodynamic and Kinetic Study of Diels–Alder Reaction between Furfuryl Alcohol and N-Hydroxymaleimides—An Assessment for Materials Application*. 2020. **25**(2): p. 243.
315. van den Tempel, P., F. Picchioni, and R.K.J.M.R.C. Bose, *Designing End-of-Life Recyclable Polymers via Diels–Alder Chemistry: A Review on the Kinetics of Reversible Reactions*. 2022. **43**(13): p. 2200023.
316. Chakma, P. and D.J.A.C.I.E. Konkolewicz, *Dynamic covalent bonds in polymeric materials*. 2019. **58**(29): p. 9682-9695.
317. Jiang, Z.C., et al., “Self-Lockable” *Liquid Crystalline Diels–Alder Dynamic Network Actuators with Room Temperature Programmability and Solution Reprocessability*. 2020. **132**(12): p. 4955-4961.
318. Mukherjee, S., et al., *Oximes as reversible links in polymer chemistry: dynamic macromolecular stars*. 2014. **5**(24): p. 6923-6931.
319. Li, F., et al., *Photopolymerizable Ionogel with Healable Properties Based on Dioxaborolane Vitriimer Chemistry*. 2022. **8**(6): p. 381.
320. Liu, W.-X., et al., *Oxime-based and catalyst-free dynamic covalent polyurethanes*. 2017. **139**(25): p. 8678-8684.
321. Yan, L., et al., *A Robust Strategy for Photoinitiated Macromolecular Thiol-Ene Radical Coupling Reaction with High-Efficiency Based on a RAFT-Generated Thiol-Terminated PDPA Reactant*. 2023. **224**(2): p. 2200321.
322. Findik, V., et al., *Insight into the Thiol-yne Kinetics via a Computational Approach*. 2021. **125**(17): p. 3556-3568.
323. Lyon, G.B., et al., *Remoldable thiol–ene vitrimers for photopatterning and nanoimprint lithography*. 2016. **49**(23): p. 8905-8913.
324. Breuillac, A., A. Kassalias, and R.J.M. Nicolaÿ, *Polybutadiene vitrimers based on dioxaborolane chemistry and dual networks with static and dynamic cross-links*. 2019. **52**(18): p. 7102-7113.
325. Chen, X., et al., *Causality analysis of the impacts of petroleum use, economic growth, and technological innovation on carbon emissions in Bangladesh*. 2023. **267**: p. 126565.
326. Fadda, M., et al., *Hydrophobic and water resistant fish leather: a fully sustainable combination of discarded biomass and by-products of the food industry*. 2023.
327. Negrell, C., et al., *New bio-based epoxy materials and foams from microalgal oil*. 2017. **119**(4): p. 1600214.
328. Altuna, F.I., et al., *Biobased thermosetting epoxy foams: mechanical and thermal characterization*. 2015. **3**(7): p. 1406-1411.
329. Pradeep, S.A., et al., *Effect of silane-treated pine wood fiber (PWF) on thermal and mechanical properties of partially biobased composite foams*. 2022. **8**: p. 100278.
330. Bonnaillie, L.M. and R.P.J.J.o.a.p.s. Wool, *Thermosetting foam with a high bio-based content from acrylated epoxidized soybean oil and carbon dioxide*. 2007. **105**(3): p. 1042-1052.
331. Mazzon, E., A. Habas-Ulloa, and J.-P.J.E.P.J. Habas, *Lightweight rigid foams from highly reactive epoxy resins derived from vegetable oil for automotive applications*. 2015. **68**: p. 546-557.
332. Khundamri, N., et al., *Bio-based flexible epoxy foam synthesized from epoxidized soybean oil and epoxidized mangosteen tannin*. 2019. **128**: p. 556-565.
333. Huang, X., et al., *Bio-based thermosetting epoxy foams from epoxidized soybean oil and rosin with enhanced properties*. 2019. **139**: p. 111540.

334. Siefker, D., et al., *1,1,3,3-Tetramethylguanidine-Mediated Zwitterionic Ring-Opening Polymerization of Sarcosine-Derived N-Thiocarboxyanhydride toward Well-Defined Polysarcosine*. *Macromolecules*, 2022. **55**(7): p. 2509-2516.
335. Pilawka, R., et al., *High-performance isocyanate-epoxy materials*. 2014. **43**(6): p. 332-340.
336. Piñeiro-García, A., et al., *New insights in the chemical functionalization of graphene oxide by thiol-ene Michael addition reaction*. 2021. **26**: p. 100230.
337. Ahmad, T., et al., *Phytochemicals in *Daucus carota* and their health benefits*. 2019. **8**(9): p. 424.
338. Perotto, G., et al., *Bioplastics from vegetable waste via an eco-friendly water-based process*. 2018. **20**(4): p. 894-902.
339. Atabani, A., et al., *Non-edible vegetable oils: a critical evaluation of oil extraction, fatty acid compositions, biodiesel production, characteristics, engine performance and emissions production*. 2013. **18**: p. 211-245.
340. Yahya, H.M., K.E.J.T.I.J.F.M. Amori, and M. ENGINEERING, *EVALUATION OF THERMAL INSULATION PERFORMANCE OF PERLITE EXPANDED PARTICLES*. 2021. **21**(3): p. 183-196.
341. Ağbulut, Ü.J.J.o.T.E., *MATHEMATICAL CALCULATION AND EXPERIMENTAL INVESTIGATION OF EXPANDED PERLITE BASED HEAT INSULATION MATERIALS' THERMAL CONDUCTIVITY VALUES*. 2018. **4**(5): p. 2274-2286.
342. Mort, R., et al., *Biobased foams for thermal insulation: Material selection, processing, modelling, and performance*. 2021. **11**(8): p. 4375-4394.
343. Gong, P., et al., *Environmentally friendly polylactic acid-based thermal insulation foams blown with supercritical CO₂*. 2018. **57**(15): p. 5464-5471.
344. Tran, T.N., et al., *Starch-based bio-elastomers functionalized with red beetroot natural antioxidant*. 2017. **216**: p. 324-333.
345. Ceseracciu, L., et al., *Robust and biodegradable elastomers based on corn starch and polydimethylsiloxane (PDMS)*. 2015. **7**(6): p. 3742-3753.
346. Dilkes-Hoffman, L.S., et al., *The rate of biodegradation of PHA bioplastics in the marine environment: A meta-study*. 2019. **142**: p. 15-24.
347. Rheinberger, T., et al., *RNA-inspired and accelerated degradation of polylactide in seawater*. 2021. **143**(40): p. 16673-16681.
348. Altuna, F., et al., *Syntactic foams from copolymers based on epoxidized soybean oil*. 2010. **41**(9): p. 1238-1244.
349. Martino, C., *Biodegradable materials: current research and applications in the food packaging sector in Europe and Colombia*. 2022.
350. Vidil, T., A.J.M.C. Llevot, and Physics, *Fully Biobased Vitrimers: Future Direction toward Sustainable Cross-Linked Polymers*. 2022. **223**(13): p. 2100494.
351. Liu, X., et al., *Self-healing, reprocessable, degradable, thermadap shape memory multifunctional polymers based on dynamic imine bonds and their application in nondestructively recyclable carbon fiber composites*. 2023. **454**: p. 139992.
352. Sangaletti, D., et al., *Biobased boronic ester vitrimer resin from epoxidized linseed oil for recyclable carbon fiber composites*. 2023. **198**: p. 107205.
353. Santiago, D., et al., *Recyclable and reprocessable epoxy vitrimer adhesives*. 2023. **5**(3): p. 2006-2015.
354. Spallanzani, G., et al., *Self-Healing, Recyclable, Biodegradable, Electrically Conductive Vitrimer Coating for Soft Robotics*. 2023: p. 2300220.
355. Zych, A., et al., *Super tough polylactic acid plasticized with epoxidized soybean oil methyl ester for flexible food packaging*. 2021. **3**(10): p. 5087-5095.
356. Bayer, F.L. and J. Jetten, *Safety assessment of refillable and recycled plastics packaging for food use*, in *Present Knowledge in Food Safety*. 2023, Elsevier. p. 240-259.

357. Geng, H., et al., *Vanillin-based polyschiff vitrimers: reprocessability and chemical recyclability*. 2018. **6**(11): p. 15463-15470.
358. Liu, M., et al., *Room temperature-curable, easily degradable, and highly malleable and recyclable vanillin-based vitrimers with catalyst-free bond exchange*. 2022. **115**: p. 107740.
359. Li, P., et al., *Fully bio-based thermosetting polyimine vitrimers with excellent adhesion, rapid self-healing, multi-recyclability and antibacterial ability*. 2023. **204**: p. 117288.
360. Zhang, Y., E. Yukiko, and I.J.R.S. Tadahisa, *Bio-based vitrimers from divanillic acid and epoxidized soybean oil*. 2023. **1**(3): p. 543-553.
361. Zhao, X.-L., et al., *Sustainable epoxy vitrimers from epoxidized soybean oil and vanillin*. 2020. **8**(39): p. 15020-15029.
362. Gracia-Fernández, C., et al., *Comparative study of the dynamic glass transition temperature by DMA and TMDSC*. 2010. **29**(8): p. 1002-1006.
363. Awalekar, Y.J., et al., *Investigation of peel resistance of adhesives materials: a review*. 2018. **10**: p. 19.
364. Lange, J., Y.J.P.T. Wyser, and S.A.I. Journal, *Recent innovations in barrier technologies for plastic packaging—a review*. 2003. **16**(4): p. 149-158.